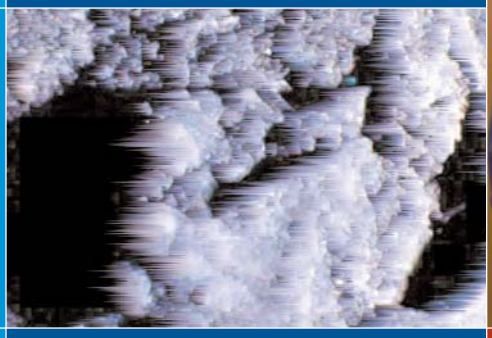

NALCO

People you trust, delivering results.

Corrosion in the Petroleum Industry

NALCO

People you trust, delivering results.

TABLE OF CONTENTS

LIST OF ILLUSTRATIONS

ILLUSTRATIONS

NALCO

People you trust, delivering results.

LIST OF ILLUSTRATIONS (CONTINUED)

LIST OF ILLUSTRATIONS (CONTINUED)

LIST OF ILLUSTRATIONS (CONTINUED)

LIST OF ILLUSTRATIONS (CONTINUED)

I. CARBON DIOXIDE CORROSION CHARACTERISTICS "SWEET CORROSION"

Form of Corrosion

Uniform — $FeCO_3$ film
Pits — Round to oval shape
Sharp edges
Round bottoms
Smooth sides and bottoms

Corrosion Products

Iron carbonate ($FeCO_3$), siderite
Iron oxide (Fe_3O_4, magnetite
Color — tan, green, brown to black

Corrosion Reactions

$$CO_2 + H_2O \rightarrow H_2CO_3$$
$$H_2CO_3 + Fe \rightarrow FeCO_3 + 2H^+ + 2e^-$$
$$3Fe + 4H_2O \rightarrow Fe_3O_4 + 8H^+ + 8e^-$$

Unique Forms of Corrosion

Wormhole attack
Ringworm corrosion
Heat-affected corrosion
Mesa attack
Rain drop

Treatment

Drilling — pH control with caustic soda
Producing wells — Corrosion inhibitors
Flowlines — Continuous corrosion inhibitor injection

CARBON DIOXIDE CORROSION

Carbon dioxide (CO_2) is absorbed in brines and can cause severe corrosive attack of steel. The corrosion rates of CO_2 can theoretically be from 1,000 to 10,000 mils per year, if not stopped by corrosion products or inhibitors. Uniform corrosion takes the form of hills and valleys with very little area that is not attacked (Figure I-1).

Figure I-1: Uniform Corrosion

An example of uniform CO_2 corrosion from tubing is shown in Figure I-2.

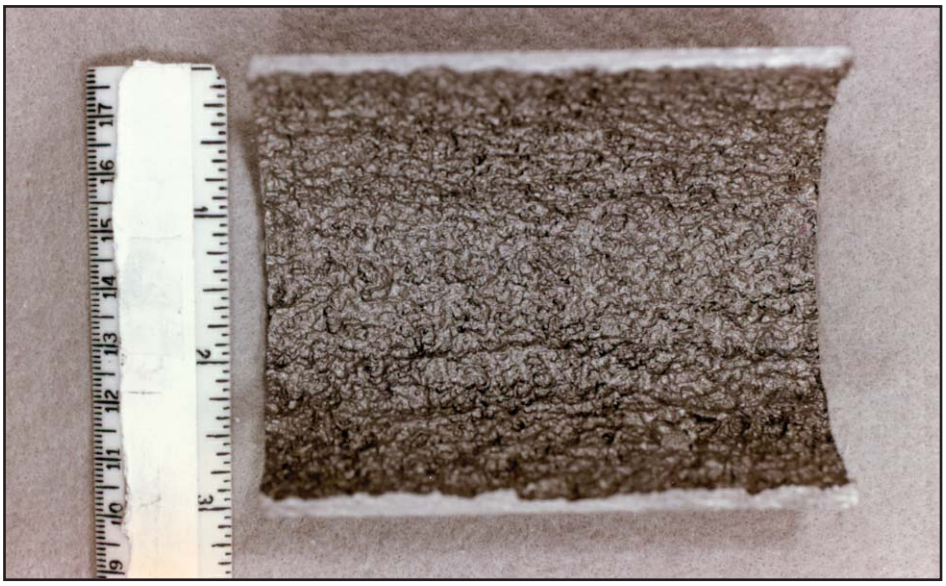

Figure I-2: Uniform Corrosion in Tubing

Another form of CO_2 corrosion takes the form of numerous pits (Figure I-3).

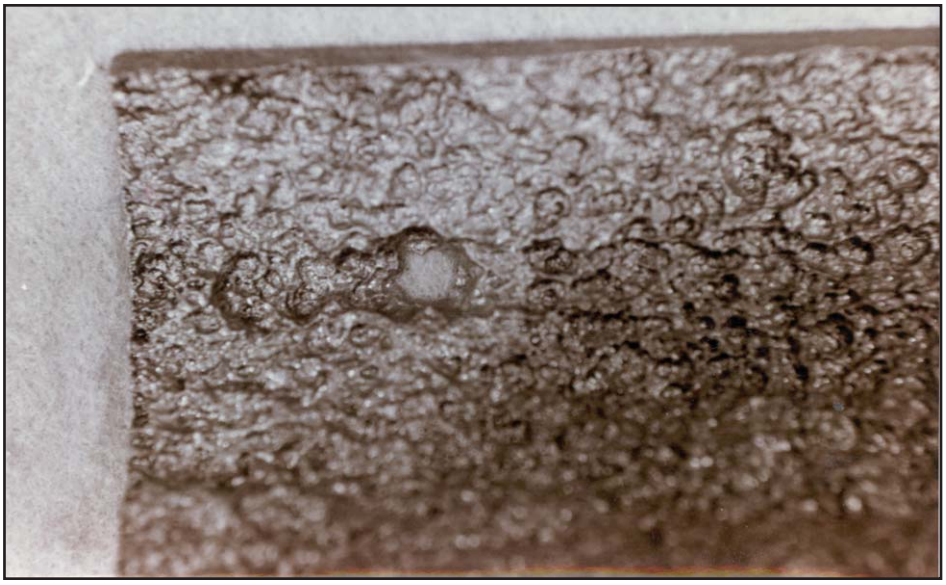

Figure I-3: Uniform Corrosion with Numerous Pits

Figure I-4 and Figure I-5 show additional examples of uniform corrosion, leaving a distinctive hill and valley texture.

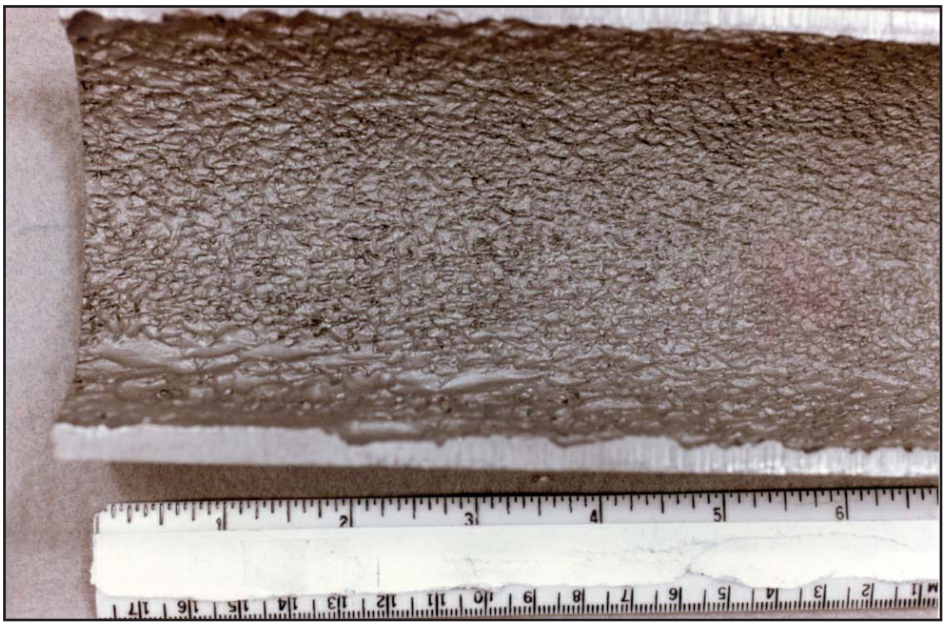

Figure I-4: Uniform Corrosion Showing Hills and Valleys

Figure I-5: Uniform Corrosion Showing Hills and Valleys

Another form of CO_2 attack has been observed on exposed faces of high-pressure wells, taking the form of an intricate honeycomb (Figure I-6 and Figure I-7).

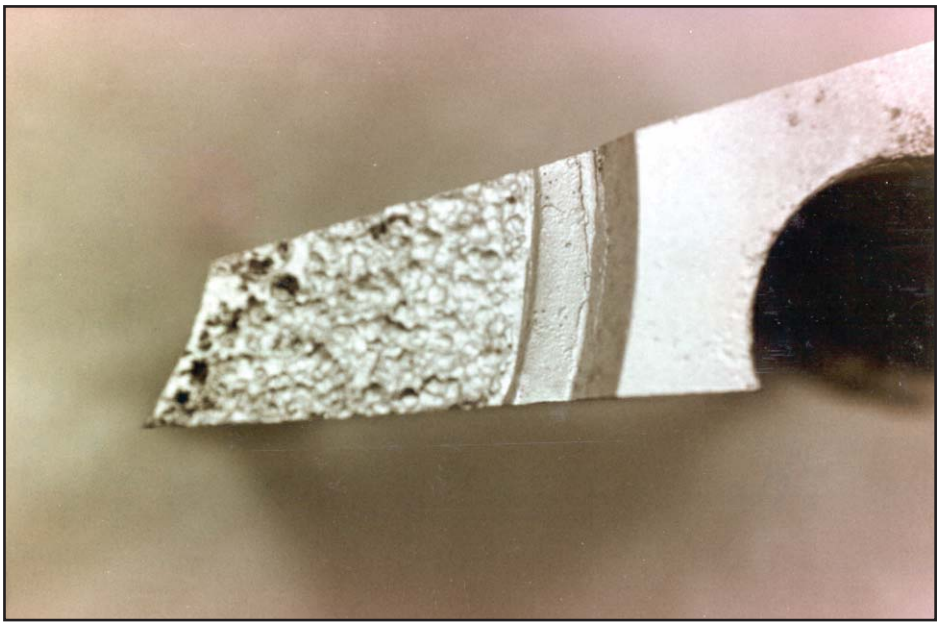

Figure I-6: CO_2 Attack — Honeycomb Pattern

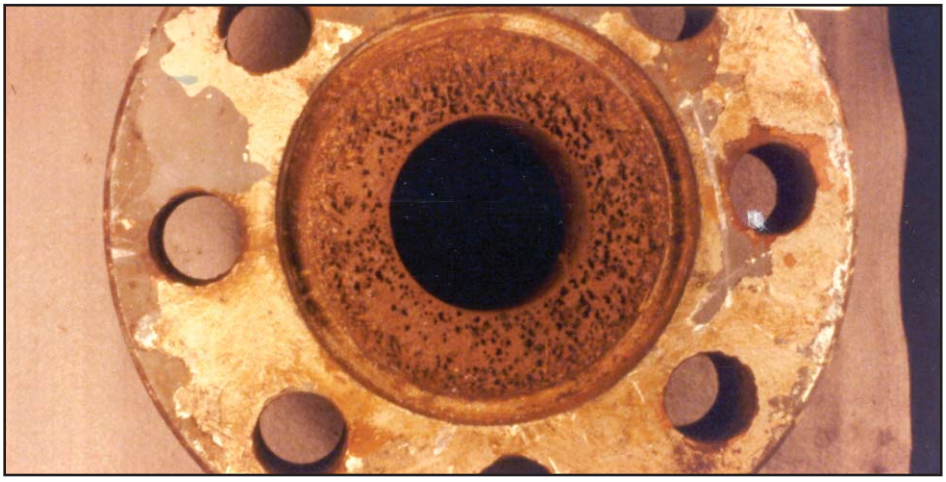

Figure I-7: CO_2 Attack — Honeycomb Pattern

Another example of honeycomb attack can be seen on a choke body (Figure I-8).

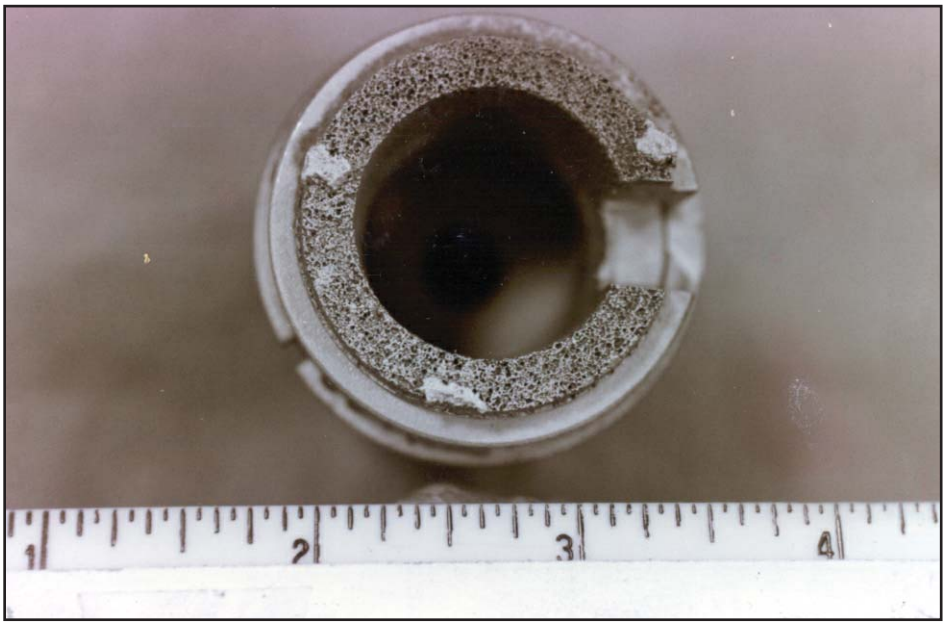

Figure I-8: Honeycomb Attack in a Choke Body

CO_2 dissolved in brine forms carbonic acid, and carbonic acid is extremely corrosive to steel, with horrendous corrosion rates. However, the carbonic acid corrosion by-product, iron carbonate ($FeCO_3$), usually forms protective films. $FeCO_3$ is relatively insoluble at downhole operating conditions. However, at breaks in the $FeCO_3$ film pits do develop. This pitting corrosion is extremely rapid and can cause failures. CO_2 pitting corrosion can be seen in Figure I-9.

Figure I-9: CO_2 Pitting Corrosion

A piece of downhole tubing that perforated within two years of operation is shown in Figure I-10 and Figure I-11.

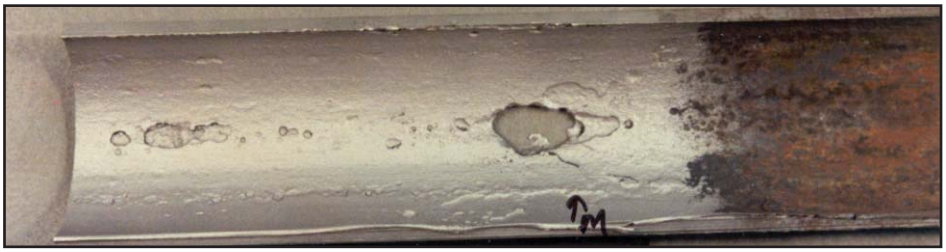

Figure I-10: Tubing Perforated by CO_2 Corrosion

Figure I-11: Tubing Perforated by CO_2 Corrosion

Another typical formation for CO_2 corrosion is called wormhole type of attack (Figure I-12).

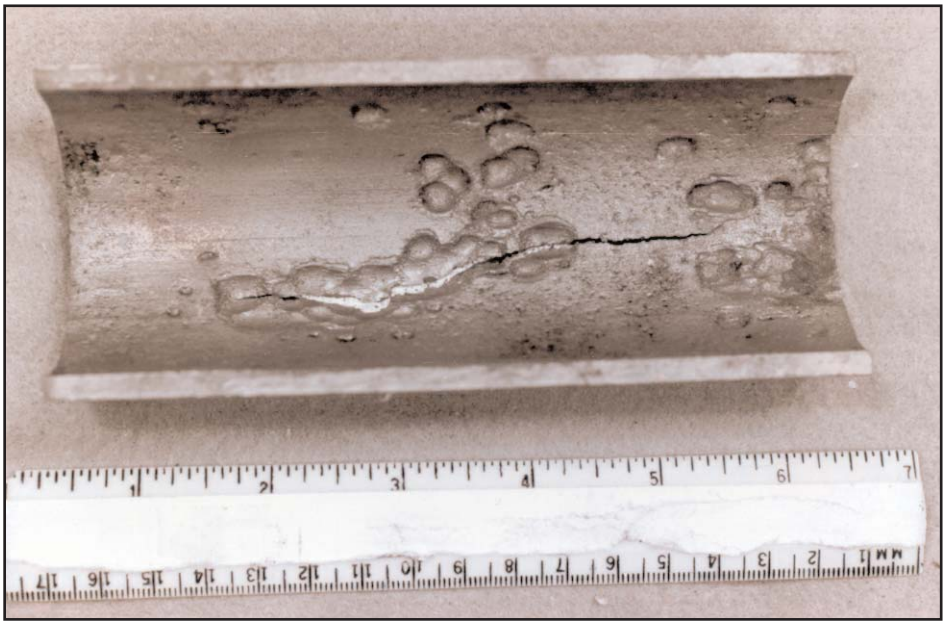

Figure I-12: Wormhole Attack

In the wormhole attack, individual CO_2 pits are interconnected and form a wormhole appearance, with segments very similar to the segmentation pattern on a worm. A sucker rod connector had a typical wormhole (Figure I-13).

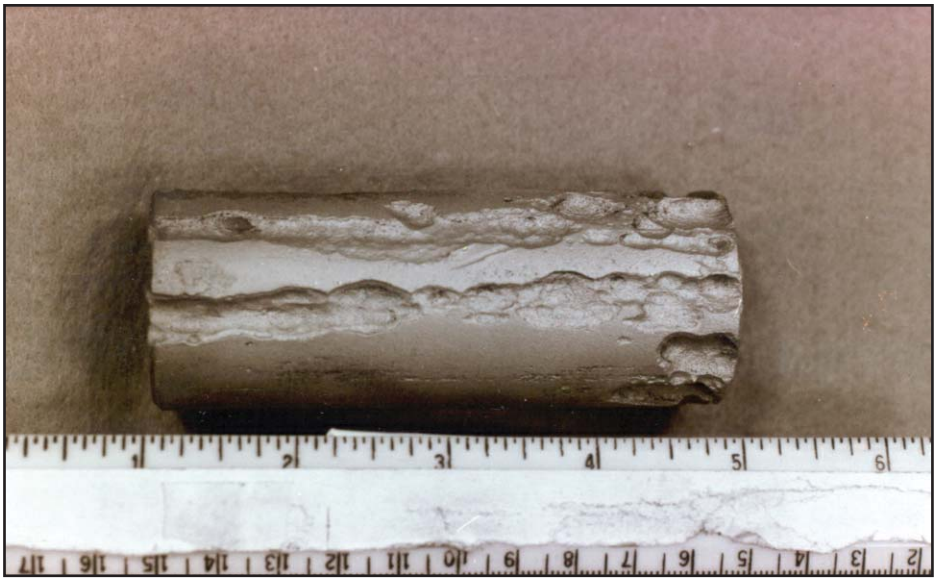

Figure I-13: Sucker Rod Connector with Wormhole

Tubing with wormhole attack can be seen in Figure I-14, with a close-up view in Figure I-15.

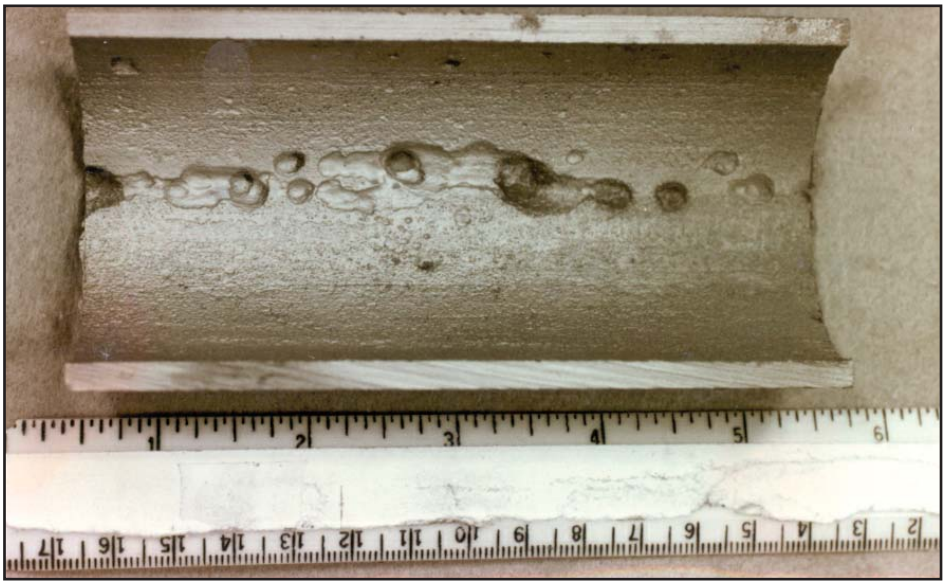

Figure I-14: Tubing with Wormhole Attack

Figure I-15: Close-up Tubing with Wormhole Attack

At times, the wormhole can take the form of a cluster of large pits (Figure I-16).

Figure I-16: Wormhole Effect — Cluster of Large Pits

Another form of corrosion observed in the oilpatch is named ringworm corrosion (Figure I-17).

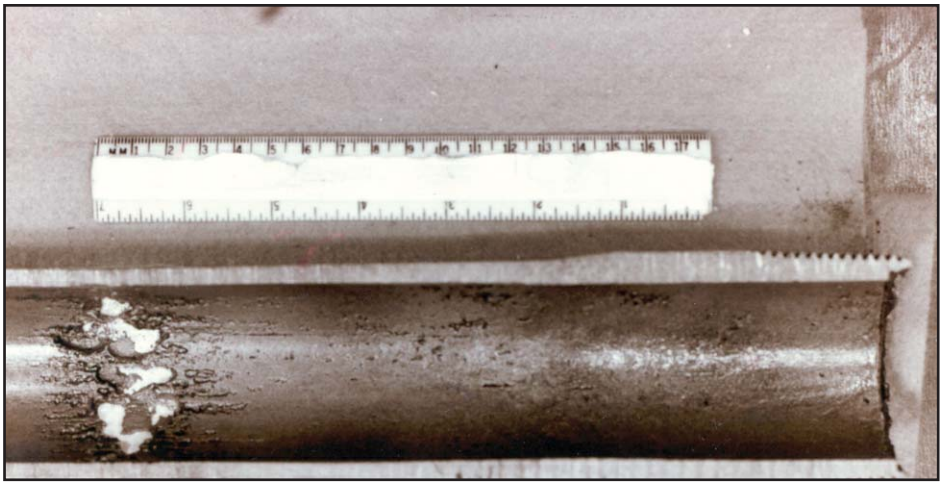

Figure I-17: Ringworm Corrosion

Ringworm corrosion is a metallurgical effect caused by the making of the upset. In fabricating the upset, a zone is created 4 to 6 inches from the upset shoulder, wherein carbon particles have been spheroidized. These spheroidal-shaped particles accelerate corrosion in mildly corrosive or even non-corrosive environments. This is a galvanic effect. If one observes numerous through-the-wall penetrations in tubing 4 to 6 inches from the upset shoulders such as in Figure I-18, ringworm corrosion is suspected.

Figure I-18: Suspected Ringworm Corrosion

Ringworm can cause tubing parting (Figure I-19).

Figure I-19: Parted Tubing by Ringworm Attack

Another example shows severe thinning at this point, with a smooth surface (Figure I-20).

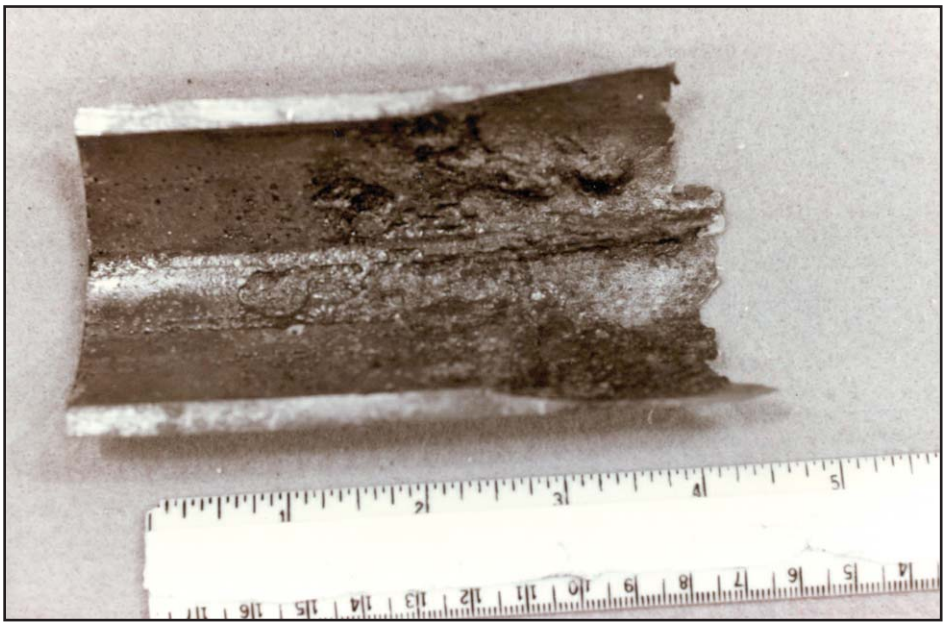

Figure I-20: Severe Thinning Caused by Ringworm Attack

The treatment for ringworm corrosion is to normalize the steel after making the upset. Normalizing redissolves the carbide particles eliminating the zone created by making the upset.

Another form of galvanically accelerated corrosion is called heat-affected zone corrosion (Figure I-21).

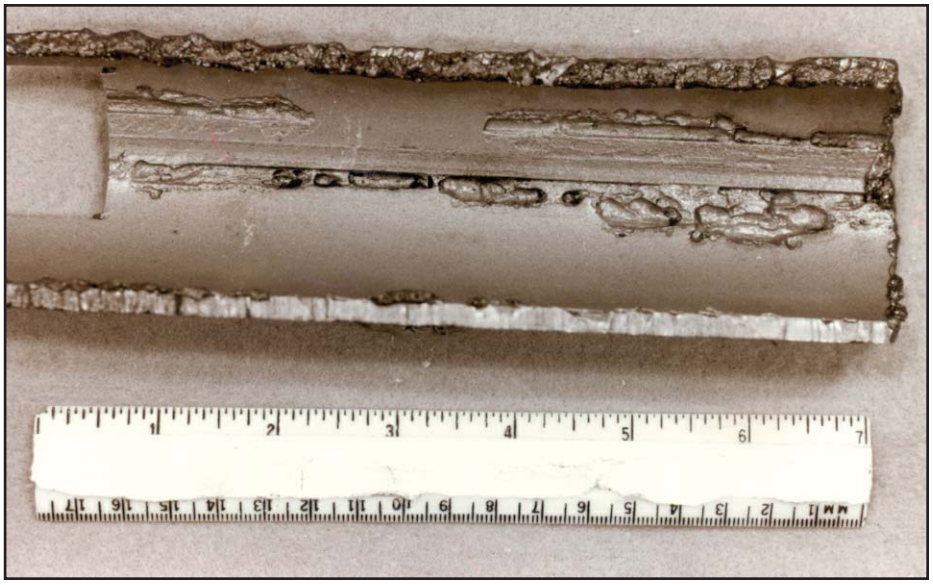

Figure I-21: Heat-affected Zone Corrosion

Heat-affected zone corrosion or HAZ attack is typified by deep corrosion along the weld seam. Figure I-22 shows a typical example and Figure I-23 illustrates a close-up view.

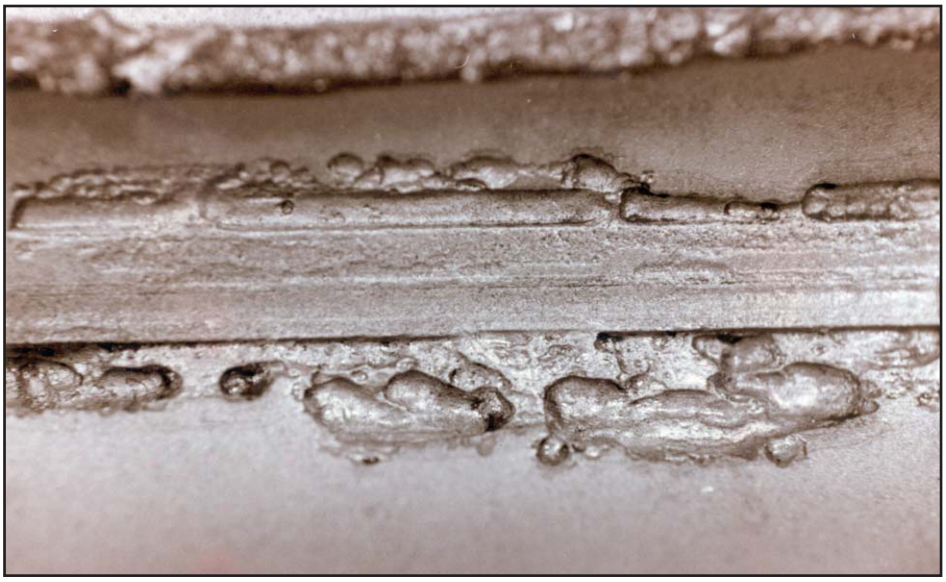

Figure I-22: HAZ as Typified by Deep Corrosion Along Weld Seam

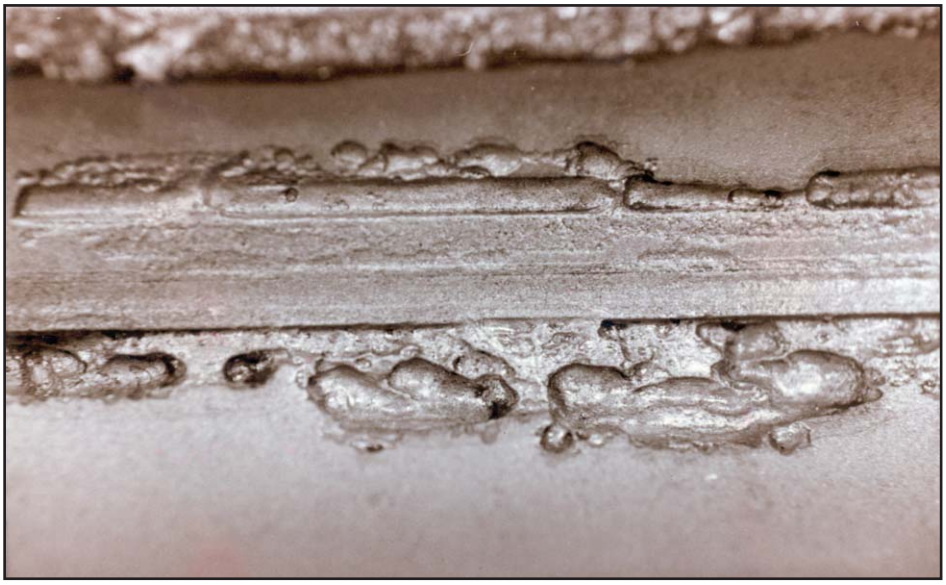

Figure I-23: Close-up of Figure I-22

The weld seam is relatively unharmed, although the zone right next to the weld is deeply corroded. This can be seen in a photomicrograph through the weld and heat-affected zone. The heat-affected zone is darker than the weld (Figure I-24).

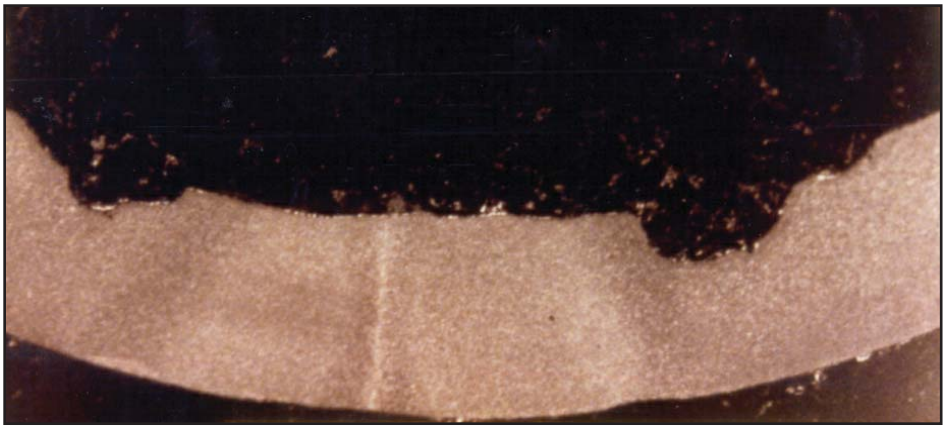

Figure I-24: Photomicrograph of HAZ Attack

The HAZ corrosion mechanism is similar to ringworm corrosion. During welding, a zone is created wherein carbon particles accumulate and precipitate to form nodules. These nodules in mildly corrosive environments form a galvanic cell. The weld itself can preferentially corrode at times (Figure I-25).

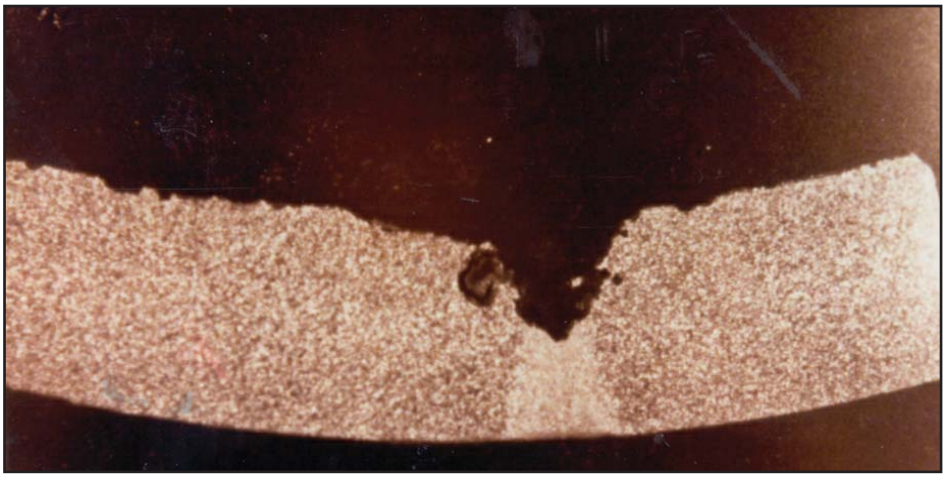

Figure I-25: Corroded Weld

Heat-affected zone corrosion is found in elbows, reducers, and flowline tees. These are typically field welds, where there are no means of negating the effect of welding by post weld heat treatments. The fix for heat-affected zone corrosion is to normalize the steel after welding, which can be done on tubing, but may not be possible on field welds.

Figure I-26: Corrosion Resulting from Rolled-in Inclusions

An unusual form of metallurgical attack on the outside of tubing is shown in Figure I-26 and I-27, and is attributed to rolled-in inclusions.

Figure I-27: Corrosion Resulting from Rolled-in Inclusions

Another form of CO_2 corrosion is called mesa attack. Mesa attack usually occurs where areas of metal that have a good protective coating exist and where other areas have no protective coating. In addition, mesa attack occurs in flowing environments (Figure I-28).

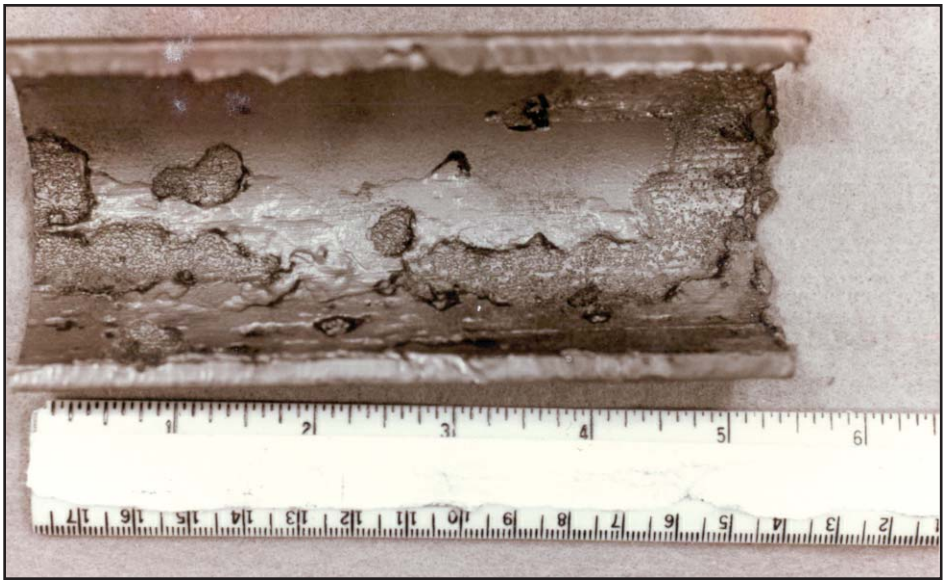

Figure I-28: Mesa Attack

Tubing that has undergone mesa attack can be seen in Figure I-29. Flat surfaces and deep gouges between the flat surfaces typify it (Figure I-30). Mesa corrosion can be controlled with inhibitor films to get greater protection on those surfaces where corrosion has occurred.

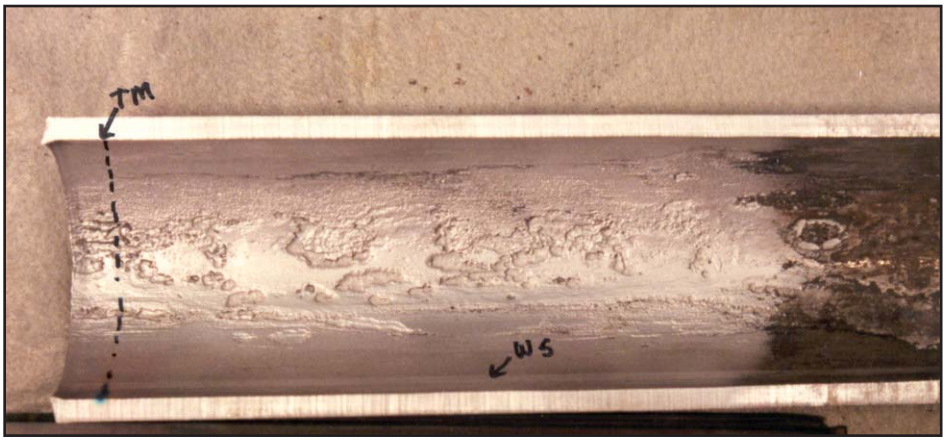

Figure I-29: Mesa Attack on Tubing

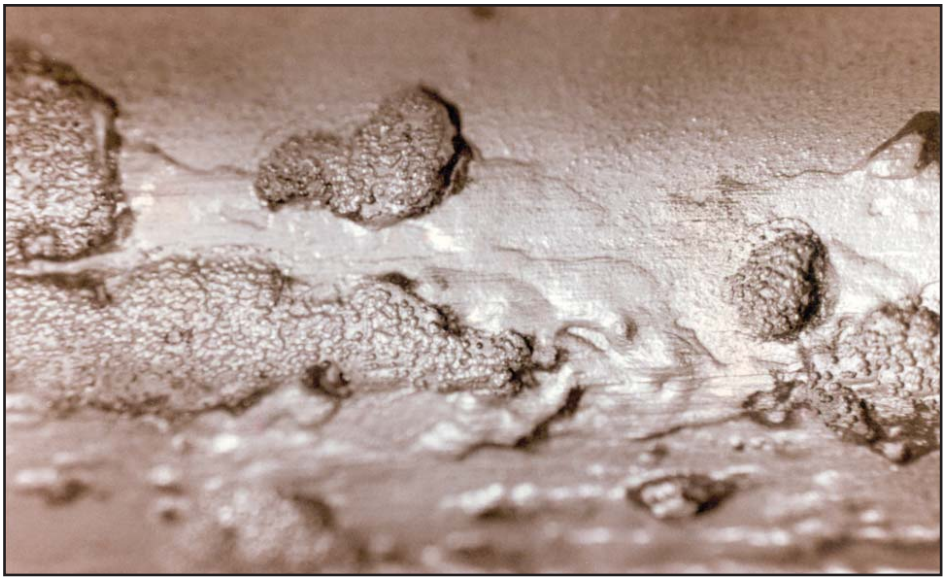

Figure I-30: Mesa Attack — Note Deep Gouges

Another form of CO_2 corrosion occurs in gas condensate wells, which do not produce a large amount of water. In these wells, a zone where water droplets, or water of condensation, will drop out. This phenomenon is labeled raindrop attack (Figure I-31).

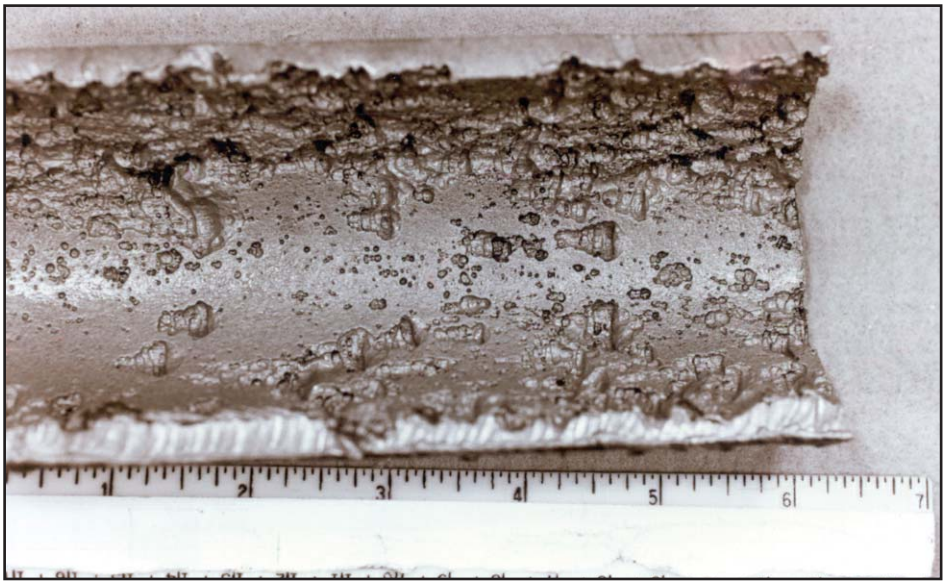

Figure I-31: Raindrop Attack

In this area, very deep pits occur with tails. These deep pits on tubing are shown in Figure I-32. This tubing was the second and third joint below the Christmas tree.

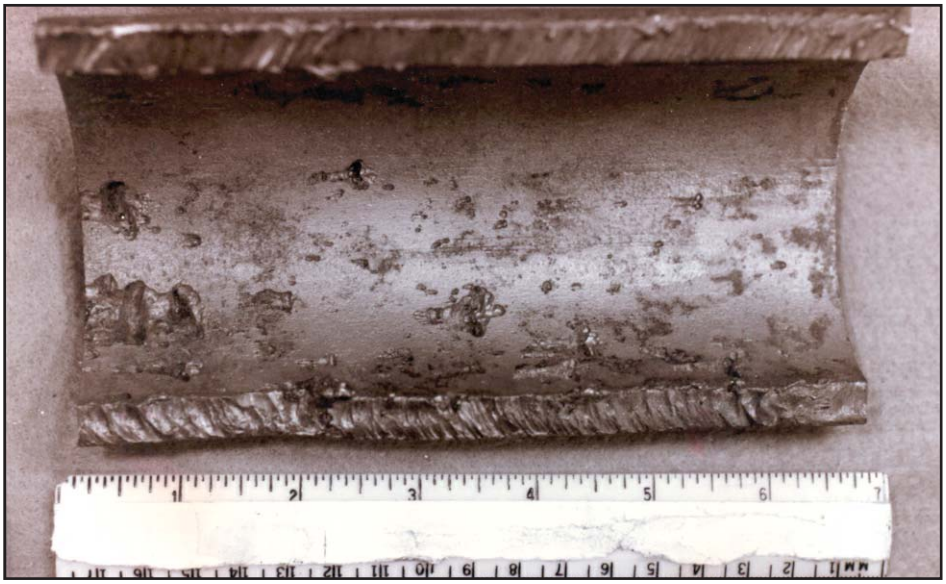

Figure I-32: Raindrop Attack — Deep Pits with Tails

A close-up view of the pit shows the typical tail. The tail is usually downstream of the flow, pointing opposite to the direction of flow. It is formed by the escaping or dripping of corrosion by-products out of the deep pit (Figure I-33).

Figure I-33: Close-up View of Pit

Other examples of the raindrop effect are shown in Figure I-34, Figure I-35, and Figure I-36. Use of corrosion inhibitor films might prevent the raindrop effect by preventing droplets from hanging up in the tubing. The most prevalent place for the raindrop effect has been relatively close to the Christmas tree head. However, the effect has also occurred at lower levels where the temperature is low enough to condense the moisture from the gas stream.

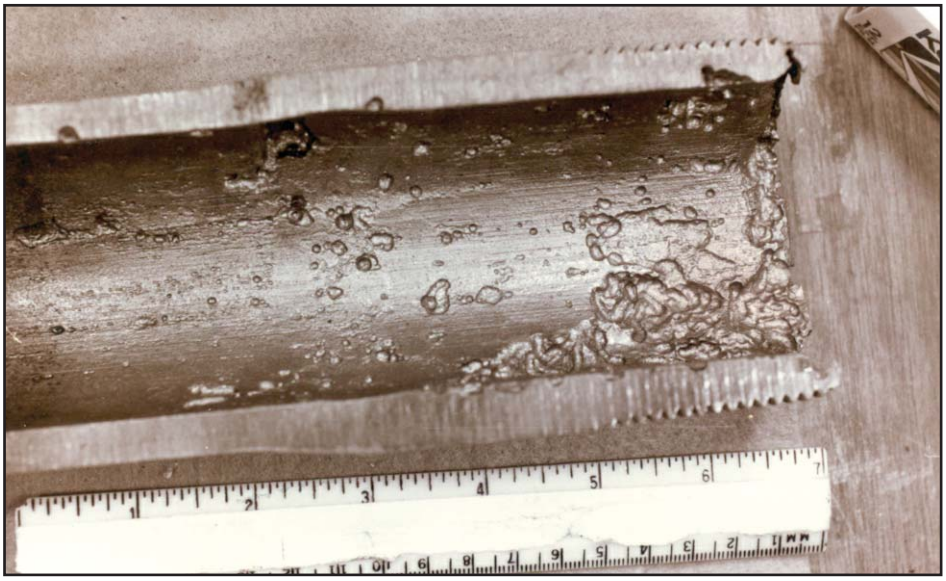

Figure I-34: Example of the Raindrop Effect

Figure I-35: Example of the Raindrop Effect

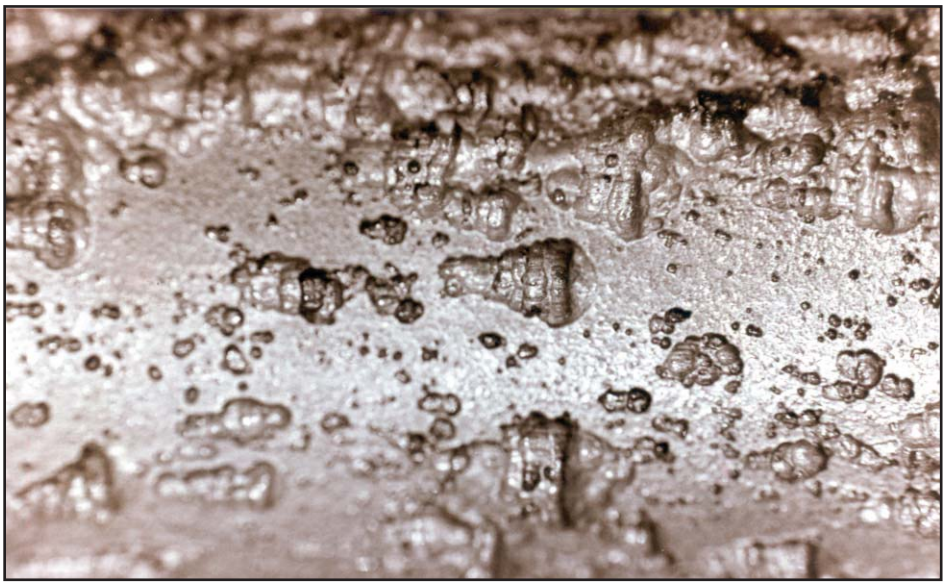

Figure I-36: Example of the Raindrop Effect

Another form of severe metal loss usually leading to rapid failures is flow-enhanced corrosion (Figure I-37).

Figure I-37: Flow-Enhanced Corrosion

Flow-enhanced corrosion was at one time called erosion-corrosion. Flow-enhanced corrosion usually occurs when a change of direction in the flow of fluids occurs, such as near an elbow. Typically, the mechanism follows a deposition of a protective $FeCO_3$ film with rubbing off the film by the flow of fluids, and sometimes solids. After the protective coating is abraded off, a new surface is exposed which then immediately starts to corrode. The corrosion product is a softer surface, which is then eroded away, and the process continues until a failure occurs. The following illustrates an elbow taken from a flowline (Figure I-38).

Figure I-38: Flow-Enhanced Corrosion in an Elbow

Figure I-39, a close-up view after cleaning, shows the severe metal loss. Figure I-40 shows the through-the-wall penetration.

Figure I-39: Close-up Showing Severe Metal Loss

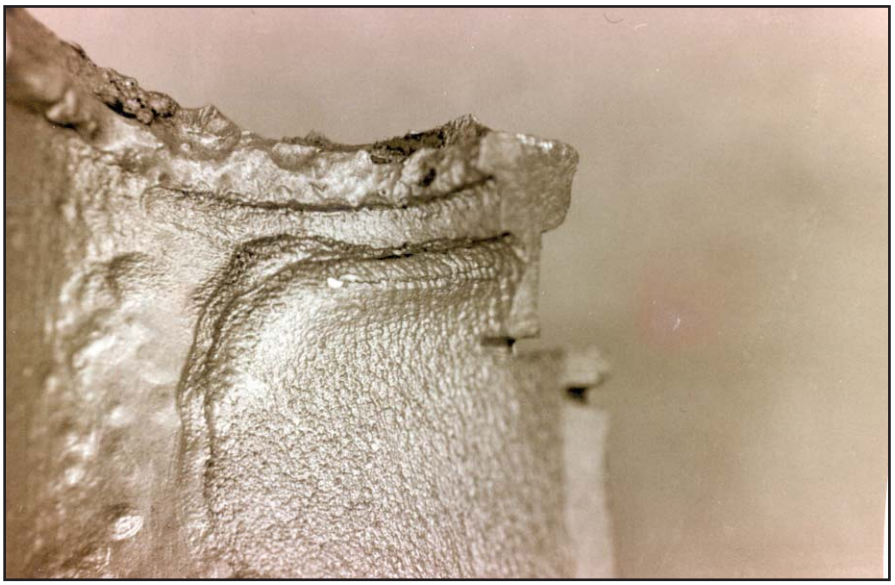

Figure I-40: Close-up Showing Penetration

In Figure I-41, this flowline has an unusual failure mode. It is a combination of flow-enhanced corrosion and heat-affected zone attack.

Figure I-41: Combination of Corrosion Mechanisms

After a 45° bend, severe metal loss was noted in the bend (Figure I-42). In addition, a clear demarcation can be found where the flow had ceased, and there was no further attack on the pipe.

Figure I-42: Severe Metal Loss in Bend

Another example of this flow-enhanced corrosion is located at the top of a U-bend, as seen in this flowline (Figure I-43).

Figure I-43: Flow-Enhanced Corrosion in U-bend

Another form of flow-enhanced corrosion is at nipple joints. Usually there is a gap when a threaded joint is made up, and at the gap, turbulence is generated and flow-enhanced corrosion can occur (Figure I-44 and Figure I-45).

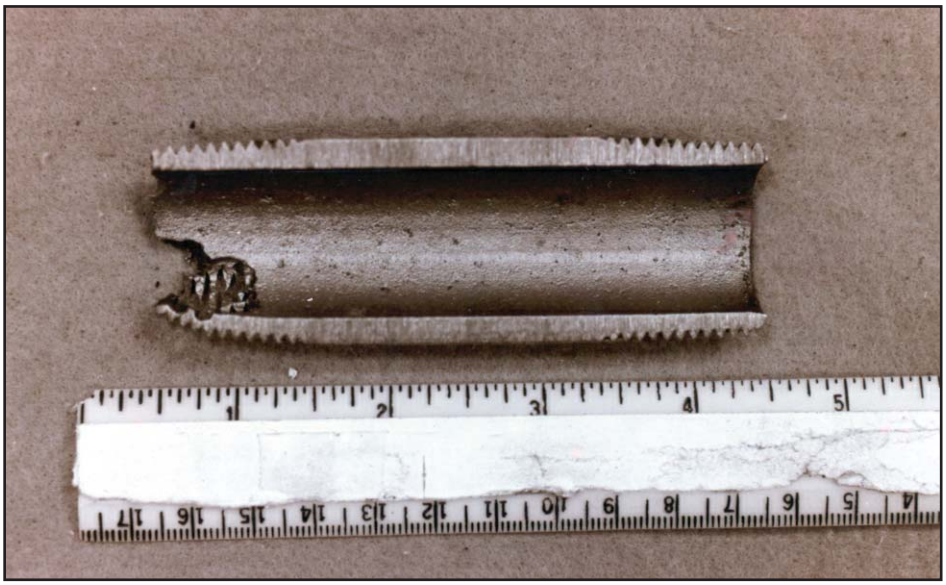

Figure I-44: Flow-Enhanced Corrosion at Nipple Joints

Figure I-45: Flow-Enhanced Corrosion at Nipple Joints

Sand erosion can also occur (Figure I-46). This erosion is typified by a smooth surface with a sand dune pattern.

Figure I-46: Sand Erosion

On coated tubing, wireline operations can sometimes cut the protective coating, resulting in corrosive attack where the breaks occur (Figure I-47 and Figure I-48). This attack is termed wireline attack.

Figure I-47: Wireline Attack

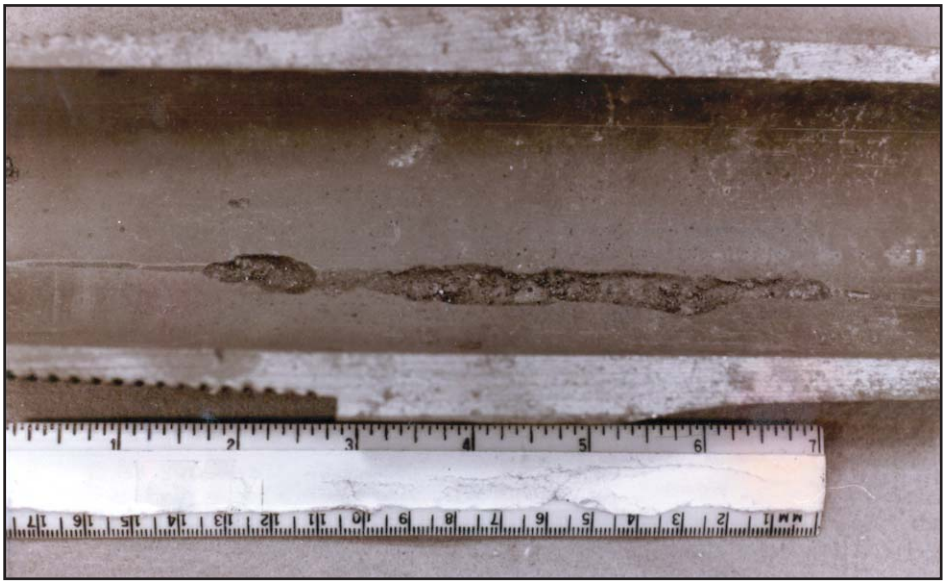

Figure I-48: Wireline Attack

Pores can sometimes cause an undercutting and pits in the base metal (Figure I-49).

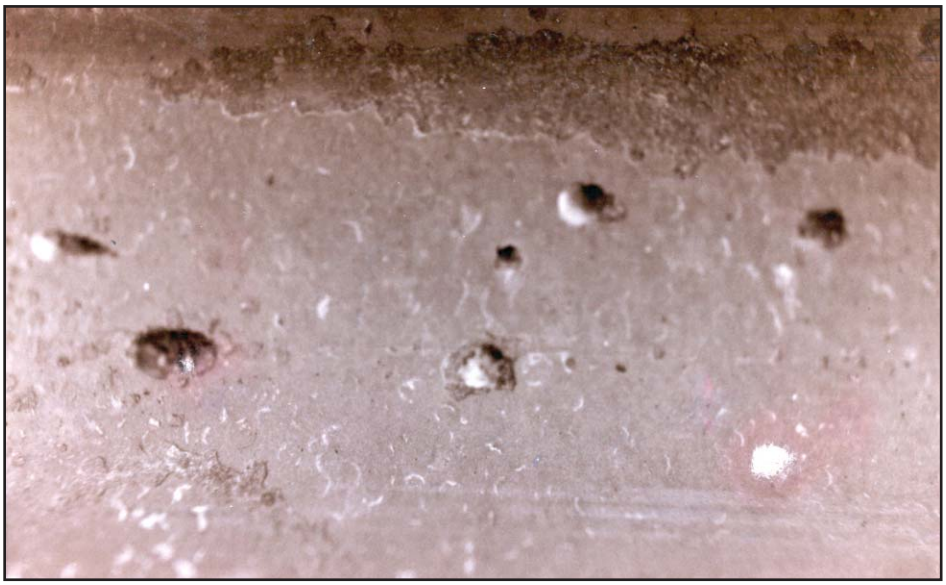

Figure I-49: A Pit Formed from a Pore in the Coating

Another form of attack is called crevice corrosion. Crevice corrosion usually occurs in metals with a good protective coating. However, at crevices, there are places where the protective coating does not get underneath, and severe localized corrosion can occur (Figure I-50 and Figure I-51).

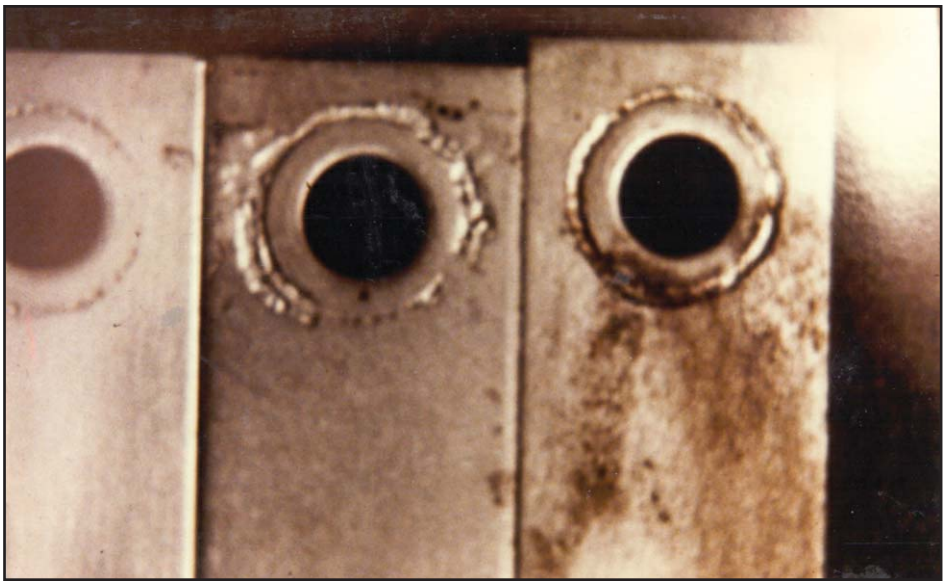

Figure I-50: Crevice Corrosion

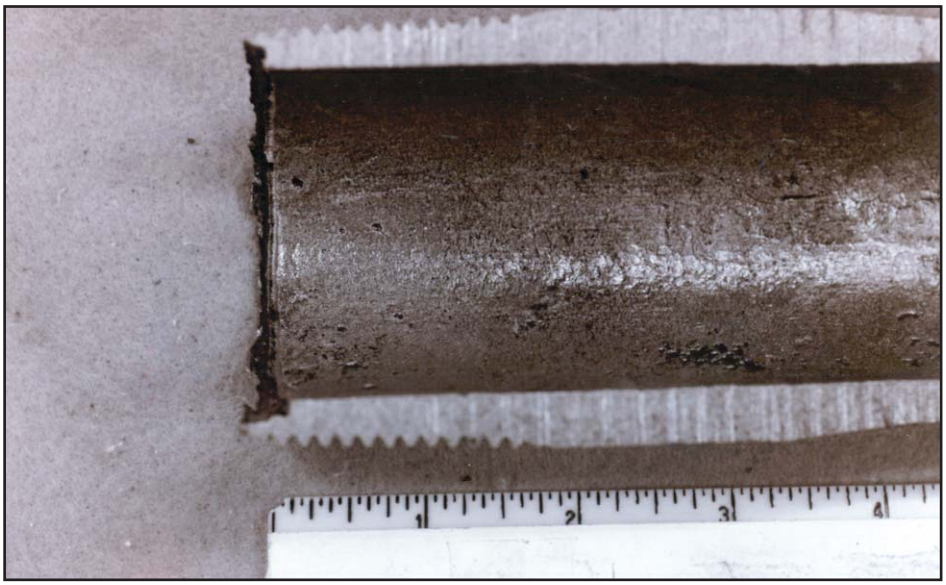

Figure I-51: Crevice Corrosion

Corrosion fatigue is a combination of corrosion and cyclic stresses (Figure I-52).

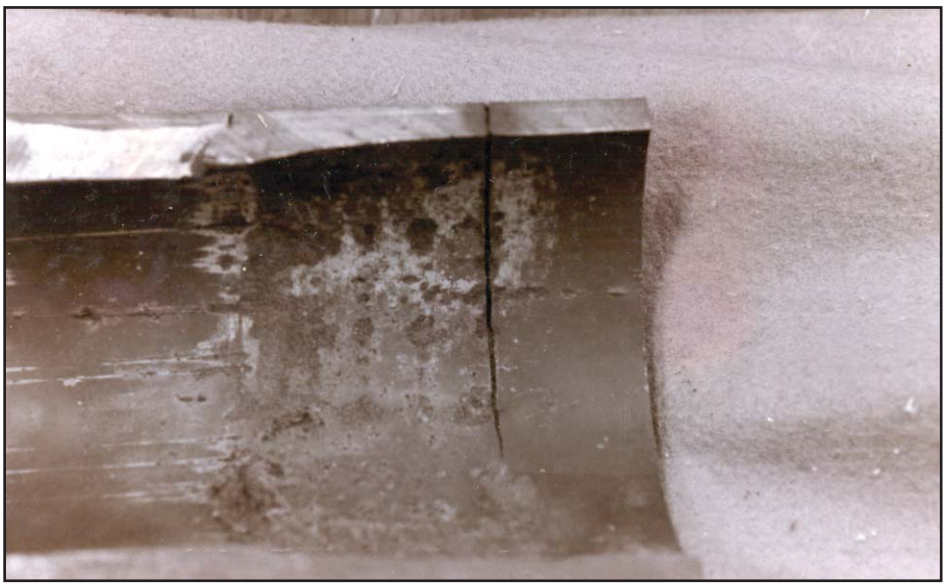

Figure I-52: Corrosion Fatigue in Drill Pipe

In the oilfield, the two places where corrosion fatigue is prevalent is in drill pipe and sucker rods. Both of these places are under severe cyclic stresses (Figure I-50 and Figure I-51).

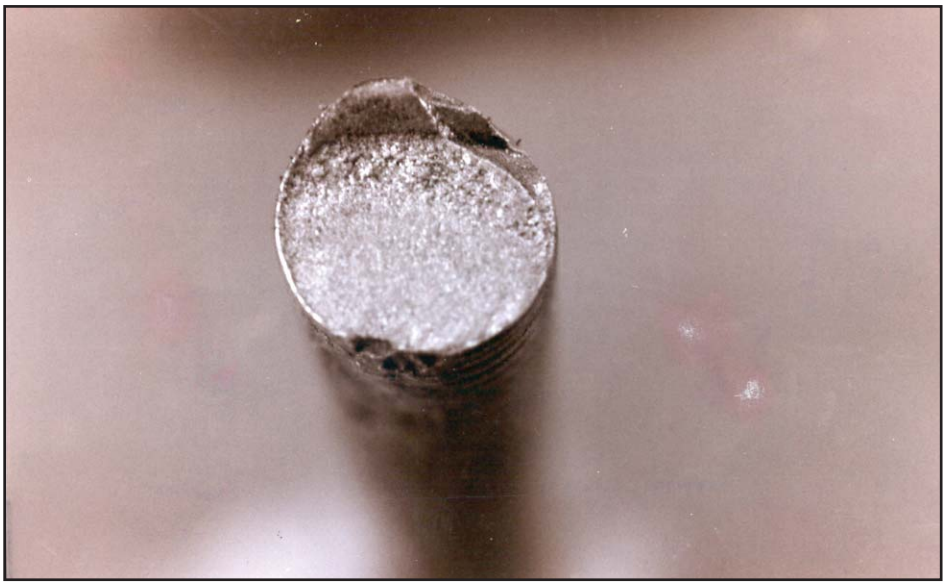

Figure I-53: Corrosion Fatigue in Sucker Rods

This failure has all the attributes of a corrosion fatigue failure, with an initiation point, a smooth half moon thumbnail, a crystalline area, and a lip break (Figure I-53).

Chart 1 demonstrates the relationship between grades to failure and applied stress. With corrosion, a safe operating stress does not exist.

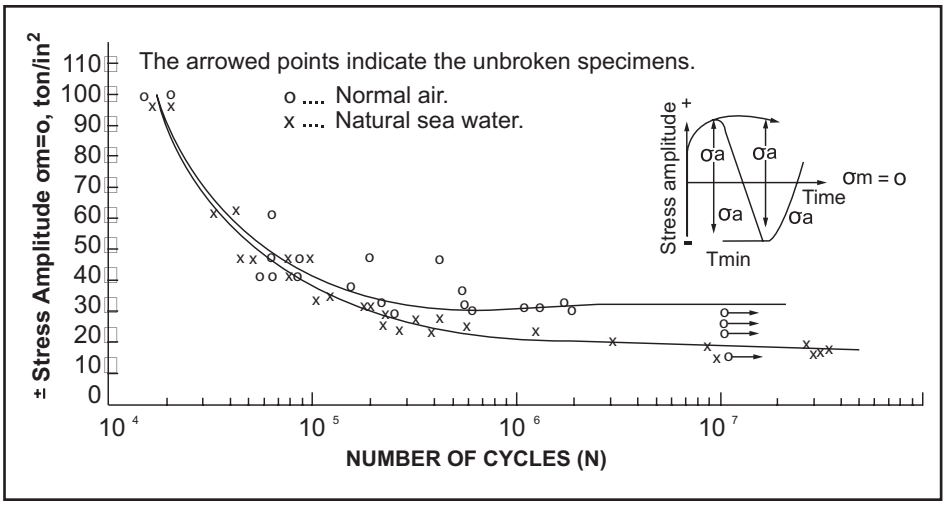

Chart 1

II. OXYGEN CORROSION CHARACTERISTICS

Forms of Attack

Uniform — With red rust deposit
Pits — Smooth bottoms
Smooth sides
Sloped edges
Width much greater than pit depth

Corrosion Products

Iron oxides	FeO(OH), geothite
	Fe_2O_3, hematite
	Fe_3O_4, magnetite
	FeO(OH), ferrous hydroxide

Corrosion Reactions

$2Fe + 3H_2O \rightarrow Fe_2O_3 + 6H^+$
$3Fe + 4H_2O \rightarrow Fe_3O_4 + 8H^+$
$Fe + 2H_2O \rightarrow FeO(OH) + 3H^+$

Unique Forms of Corrosion

Oxygen concentration cells
Tubercules

Treatment

Drilling — Oxygen scavengers
Producing wells — Corrosion inhibitors; elimination of oxygen sources, oxygen scavengers
Flowlines — Corrosion inhibitors; elimination of oxygen sources, oxygen scavengers

OXYGEN CORROSION

Oxygen is an extremely corrosive gas in produced brines, even more corrosive than CO_2. Oxygen corrosion (Figure II-1) usually results in iron oxide corrosion by-products, usually hematite, goethite, and magnetite.

Figure II-1: Oxygen Corrosion

Typically, the corrosive by-products are a reddish brown rust (Figure II-2).

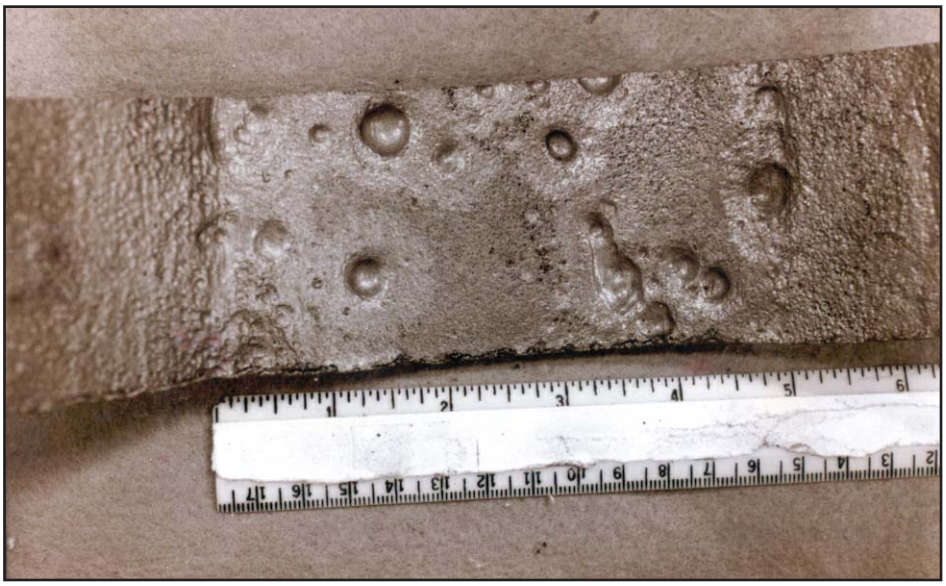

Figure II-2: Oxygen Corrosion in a Flowline

A close-up view shows the typical pits (Figure II-3).

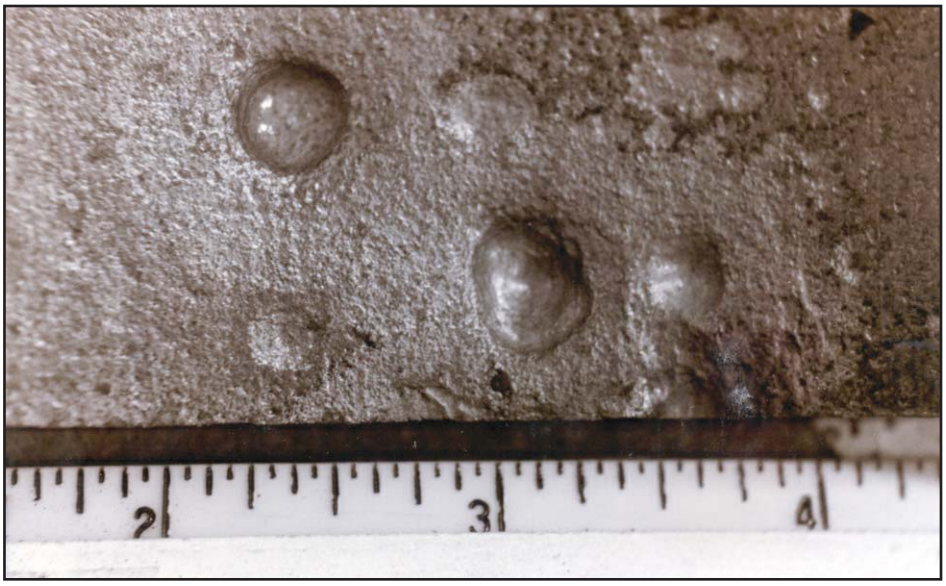

Figure II-3: Typical Pits

On cleaning, the shallow saucer-like pits are seen (Figure II-4).

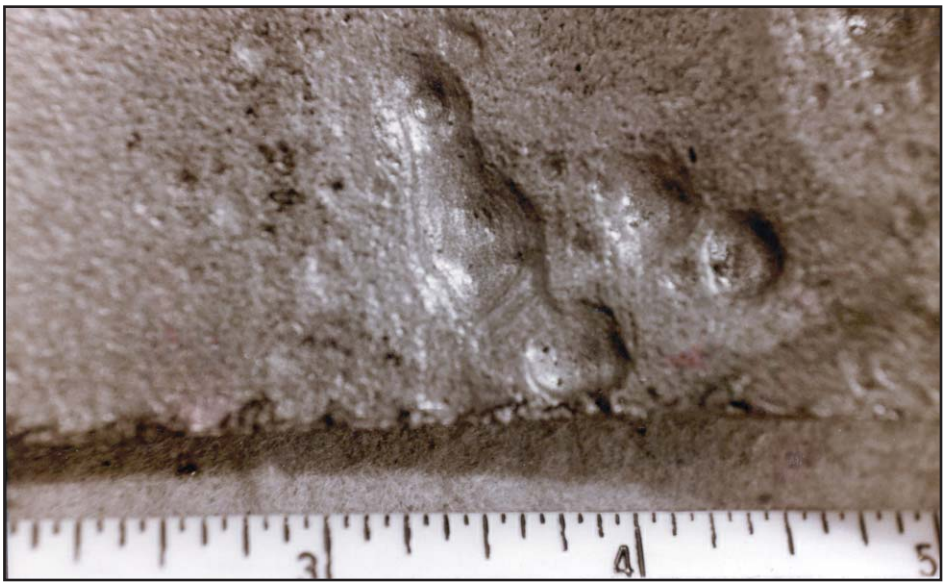

Figure II-4: Shallow Saucer-like Pits

Oxygen corrosion on sucker rods are large areas of metal loss (Figure II-5 and Figure II-6).

Figure II-5: Areas of Metal Loss on Sucker Rods

Figure II-6: Areas of Metal Loss on Sucker Rods

Typical rust-colored deposits taken from a water line in a mining operation are shown in Figure II-7.

Figure II-7: Typical Rust-colored Deposits

After cleaning, saucer-like deposits are seen (Figure II-8).

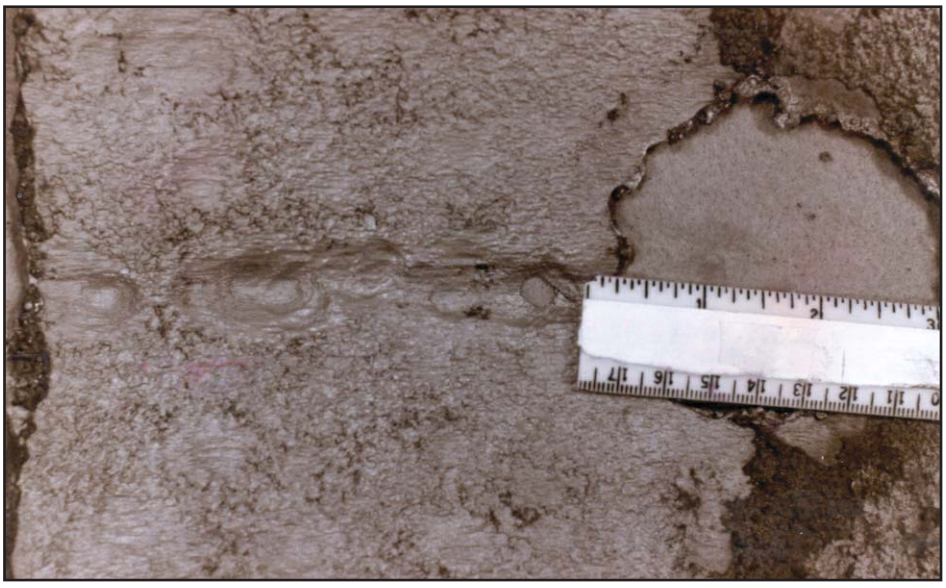

Figure II-8: Saucer-like Deposits and Pits

Another example of oxygen corrosion is in this 36" pipeline (Figure II-9).

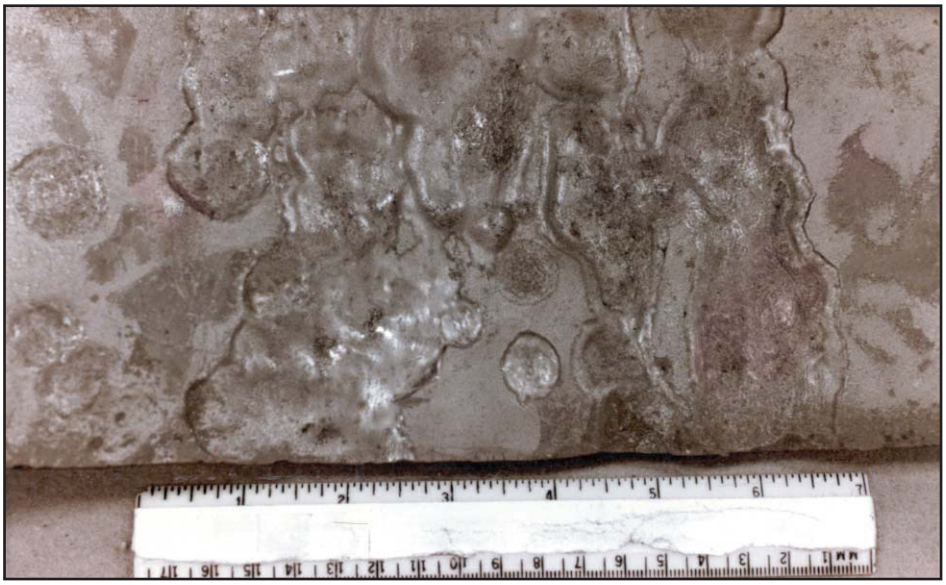

Figure II-9: Oxygen Corrosion in a 36" Pipeline

Oxygen is the most corrosive gas in the presence of water (see Chart 2). Although the maximum dissolved oxygen in the water is only 8 ppm, dissolved CO_2 can increase to 800 ppm and dissolved H_2S to 400 ppm.

Preventing the ingress of oxygen into the system can usually control oxygen corrosion. In addition, use of oxygen scavengers are notably effective in drilling operations where oxygen is a significant problem. Oxygen scavengers are also very effective in salt-water disposal systems where oxygen ingress can cause serious downhole and flowline corrosion failures.

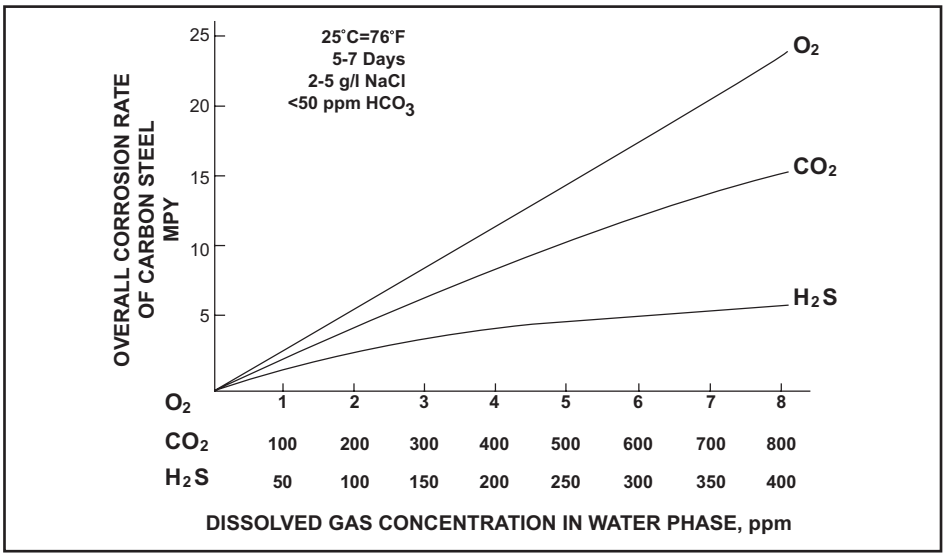

Chart 2

III. HYDROGEN SULFIDE CORROSION CHARACTERISTICS

Forms of Attack

Uniform — FeS_2 film
Pits — Conical shaped
Pit bottoms sharp
Edges etched and slightly sloped
Sides etched

Corrosion Products

Black, blue-black iron sulfide
$Fe_{1-x}S$ pyrite, greigite, mackinwaite
Kansite, iron oxide (Fe_3O_4), magnetite, sulfur (S)
Sulfur dioxide (SO_2)

Corrosion Reactions

$H_2S(g) + Fe + H_2O \rightarrow Fe_{1-x}S\ (Prec.) + 2H^+$
$Fe_{1-x}S + O_2 \rightarrow Fe_3O_4 + SO_2$

Unique Forms of Corrosion

Sulfide stress cracking
Hydrogen blistering
Hydrogen embrittlement
Stepwise cracking

Treatment

Drilling — High pH, Zn treatments
Production — Corrosion inhibitors
Flowlines — Corrosion inhibitors, hydrogen sulfide scavengers

HYDROGEN SULFIDE CORROSION

Hydrogen sulfide (H_2S) in produced brines generates hydrogen ions and HS ions. The hydrogen ions, being acidic, attack steel. H_2S corrosion is typified by pitting, which takes the form of shallow round depressions with etched bottoms (Figure III-1).

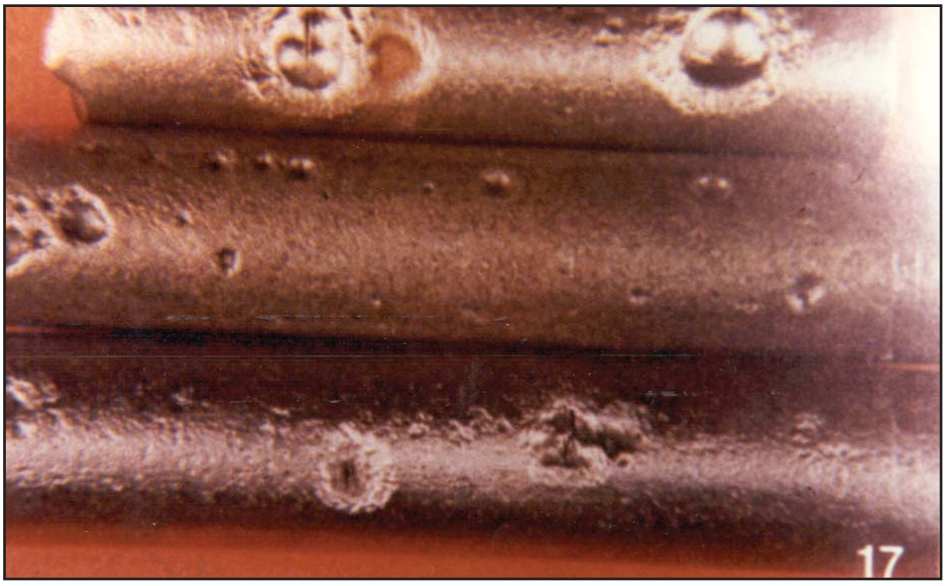

Figure III-1: Hydrogen Sulfide (H_2S) Corrosion

In addition, the sides of the pits are sloped. A quick test to detect H_2S corrosion is to test the fluids for H_2S. A few drops of hydrochloric acid with arsenious oxide on the surface deposits turns yellow if FeS_2 is present.

Some examples of the hydrogen sulfide attack are shown in Figure III-2.

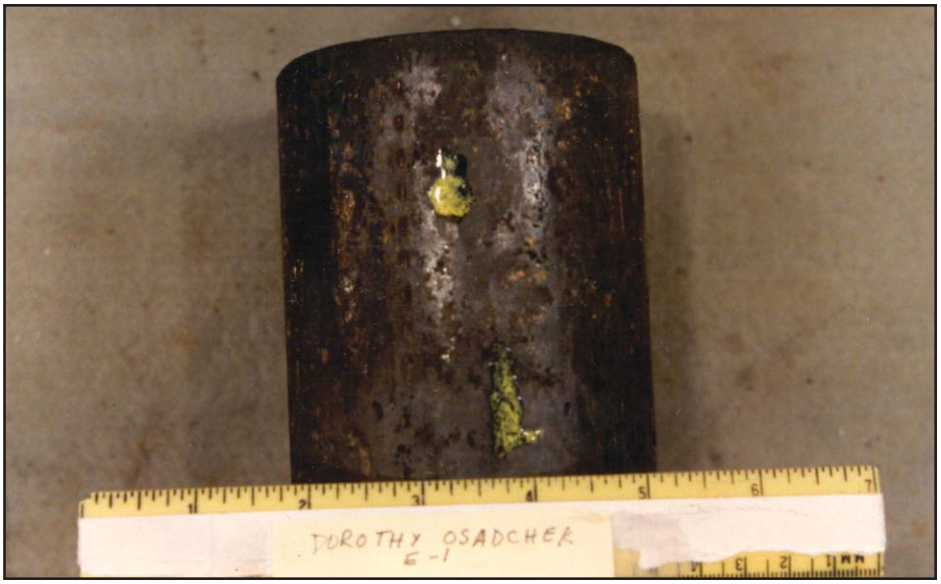

Figure III-2: Example of H_2S Attack

Also associated with H_2S attack are some crystals of FeS_2 (Figure III-3).

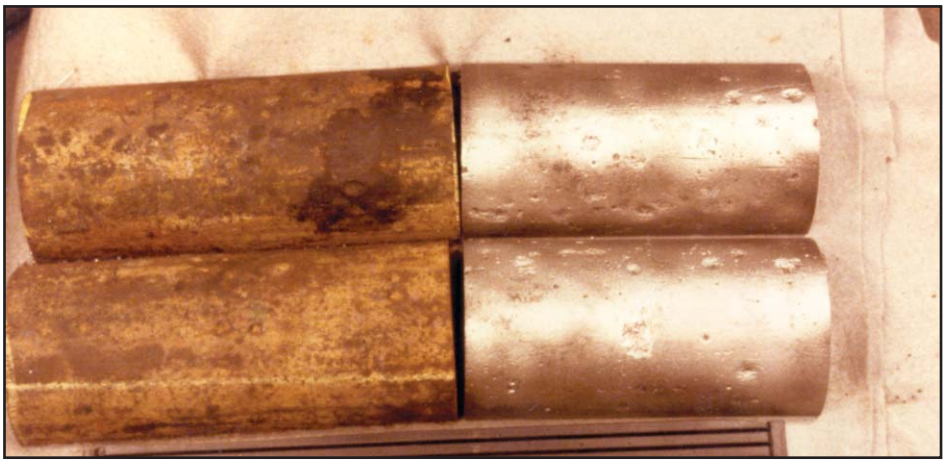

Figure III-3: FeS Crystals

H_2S attack on sucker rods can cause breaks because of corrosion fatigue (Figure III-4 and Figure III-5).

Figure III-4: H_2S Attack on Sucker Rods

Figure III-5: H_2S Attack on Sucker Rods Followed by Corrosion Fatigue Break

Sulfide stress cracking occurs when H_2S corrosion is accelerated by stresses (Figure III-6).

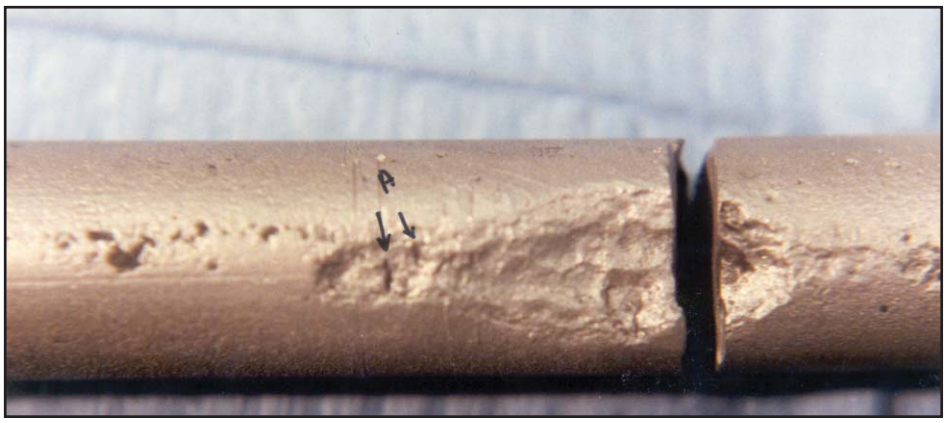

Figure III-6: Sulfide Stress Cracking

Alternating stresses can propagate notches, which are initiated by corrosion. An example of corrosion fatigue occurred in sucker rod connectors (Figure III-7).

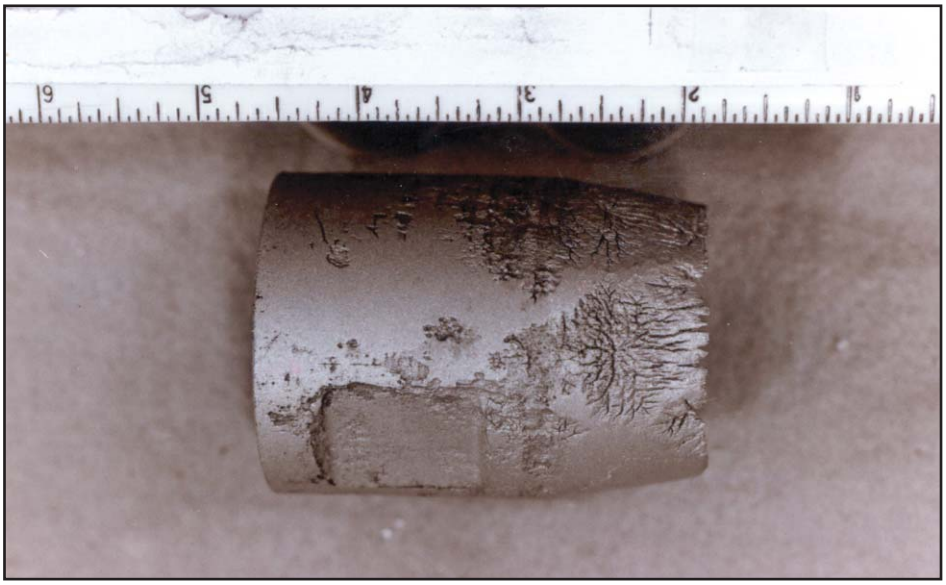

Figure III-7: Corrosion Fatigue in Sucker Rod Connectors

A cross-section shows how deep the cracking can propagate into the metal, with a very small opening (Figure III-8 and Figure III-9).

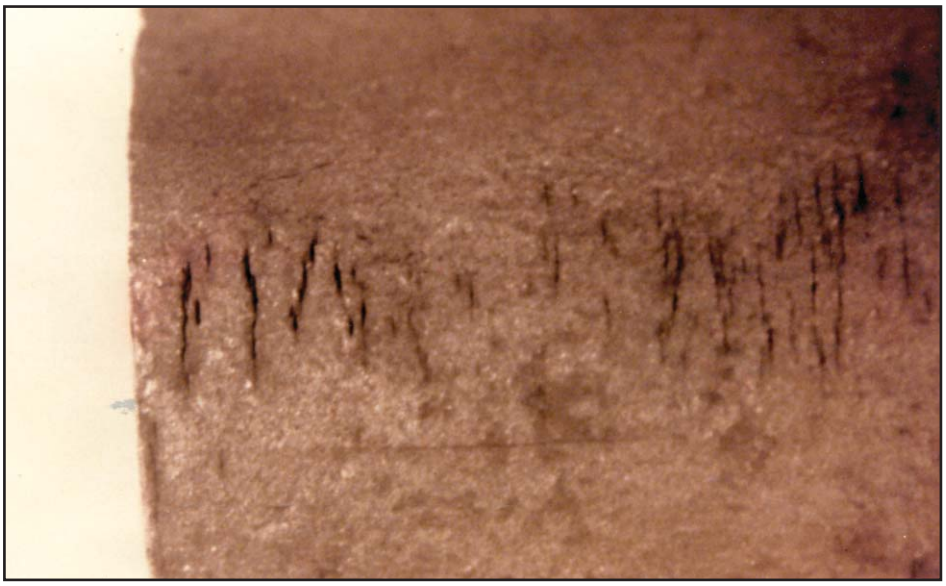

Figure III-8: Crack Propagation

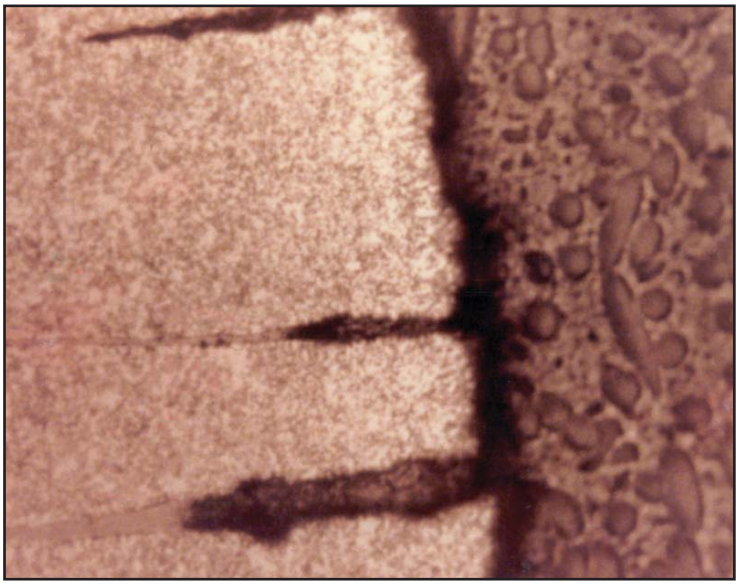

Figure III-9: Stress Cracks

An unusual instance of sulfide stress cracking occurred with H_2S in a kill string. During acidizing, the ends of the kill string cracked where the connectors were hardened. The field used brine, which contained H_2S, with the acid. The acid inhibitor was not effective, and all the joints cracked (Figure III-10).

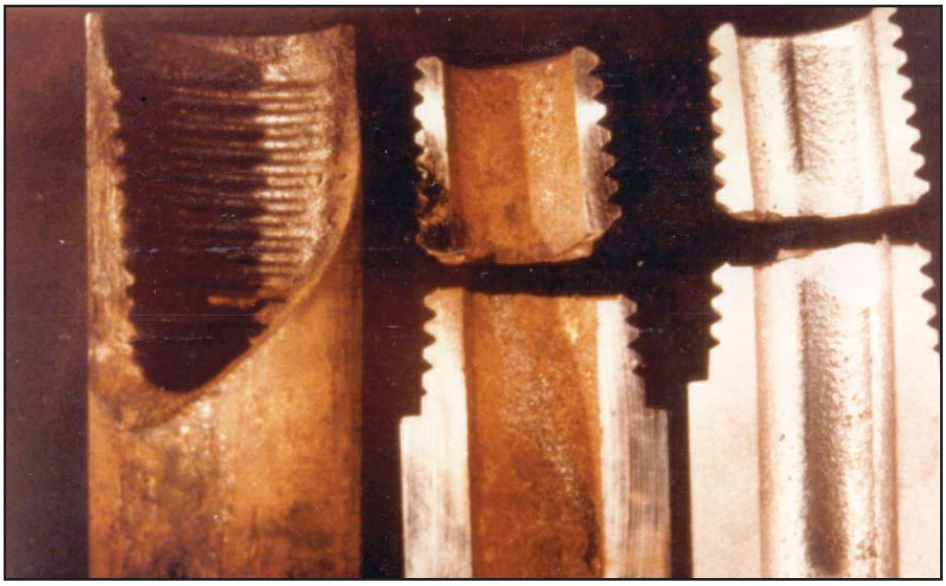

Figure III-10: A Failure Caused by Sulfide Stress Cracking of a Kill String

Drilling collars and the drilling operation are also subject to sulfide stress cracking. Drilling stresses can cause failures. Figure III-11 shows a failure of a casing collar attributed to H_2S stress cracking.

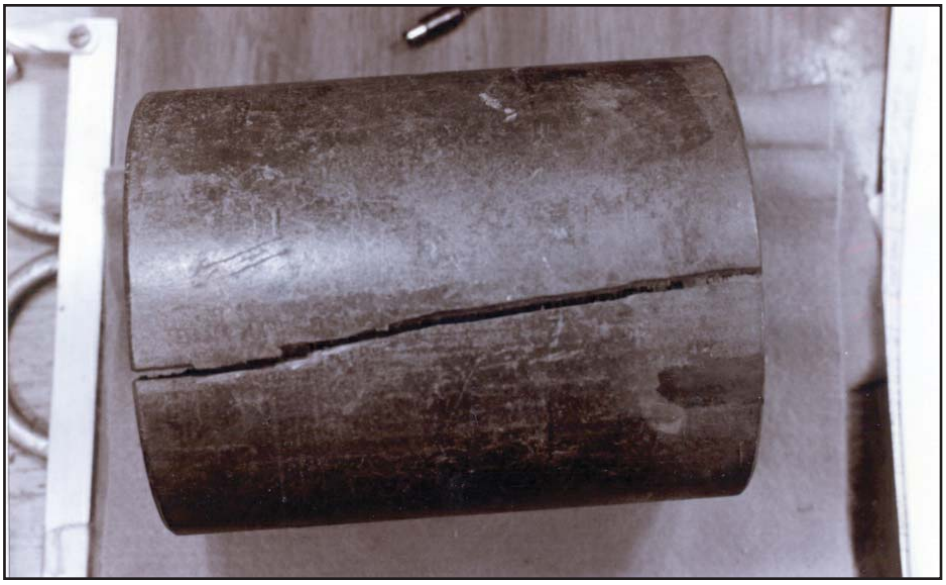

Figure III-11: Sulfide Stress Cracking of a Casing Collar

NACE document MR 01-75 defines the sulfide stress cracking region based on H_2S concentration and total line pressures (Chart 3).

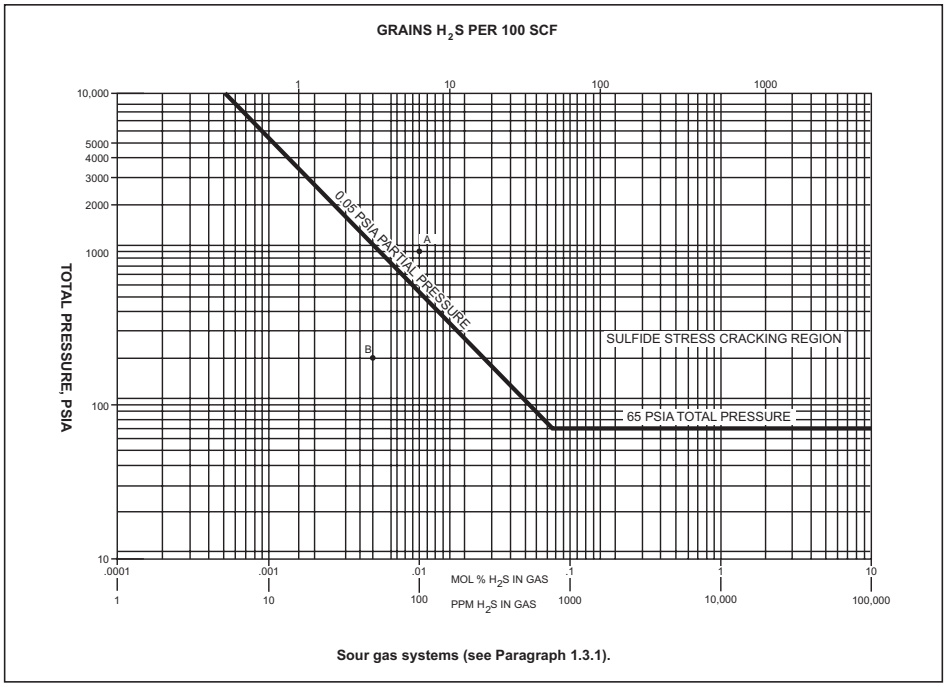

Chart 3: Sulfide Stress Cracking Region

Hydrogen, either from the corrosion process or during manufacture, can enter the metal and concentrate internally in high-stress areas, making the steel extremely brittle. Hydrogen embrittlement fractures are catastrophic because very little metal loss occurs before the break. Figure III-12 is an example of hydrogen embrittlement of a drill collar.

On high strength steels in acid environments a phenomenon called hydrogen embrittlement can occur. The mechanism is similar to sulfide stress cracking except H_2S may not be present.

Another occurrence of failures with high strength steel is hydrogen induced cracking (HIC), also known as step-wise cracking. In low strength steels, HIC can occur in wet, sour environments. Figure III-12 shows a cross-section of a pressure vessel plate with cracking initiated at an inclusion site. A related type of failure is stress-oriented hydrogen induced cracking (SOHIC). SOHIC occurs in tanks around welded outlets in corrosive service when the welds are highly stressed.

Figure III-12: Hydrogen Embrittlement

Austenic stainless steels such as SS 304 and SS 316 are susceptible to chloride stress cracking in hot aqueous chloride-containing environments. An SS 304 flowline handling a chloride-containing brine cracked at the highly stressed threaded areas (Figure III-13).

Figure III-13: Chloride Stress Corrosion in Stainless Steel

Stress corrosion cracking has three main avenues of control, namely mechanical, metallurgical, and environmental (Chart 4).

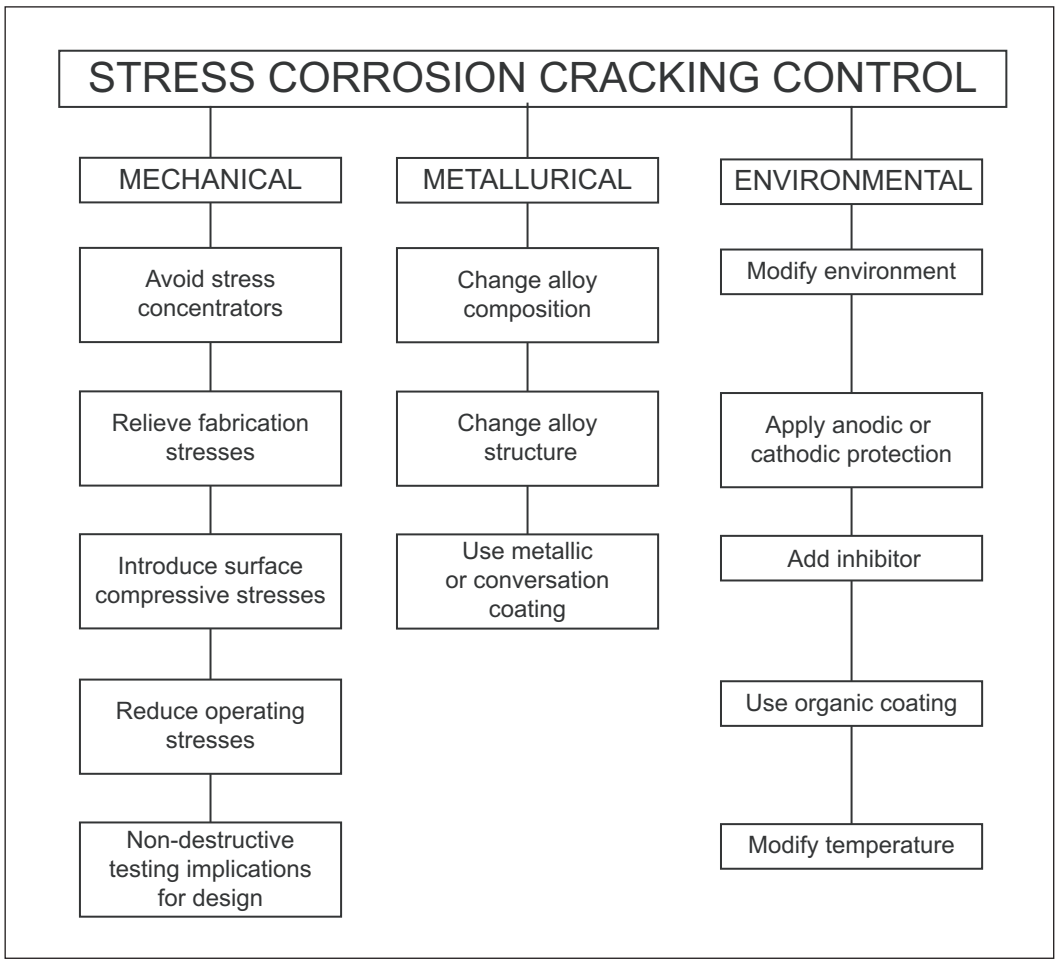

Chart 4: Approaches to Stress Corrosion Control

IV. MICROORGANISM INFLUENCED CORROSION CHARACTERISTICS

Forms of Attack

Pits — Irregular shaped
Sloped edges
Satiny bottom
Etched sides
Terraced sides

Corrosion Products

Iron sulfides, Sulfate reducing bacteria (SRB)
Slime
Growths of bacteria

Corrosion Mechanisms

Cathodic depolarization
Cathodic FeS_2
Concentration cells
Sour corrosion

Unique Forms of MIC

Stainless steel pitting
Slime
Plugging

Treatment

Drilling — Biocides
Production — Biocides, chlorine dioxide
Flowlines — Biocides, chlorine dioxide
Cost considerations — Continuous vs. batch
EPA
Biostat vs. biocide

MICROORGANISM INFLUENCED CORROSION

Another facet of corrosion is microorganism influenced corrosion (MIC) (Figure IV-1).

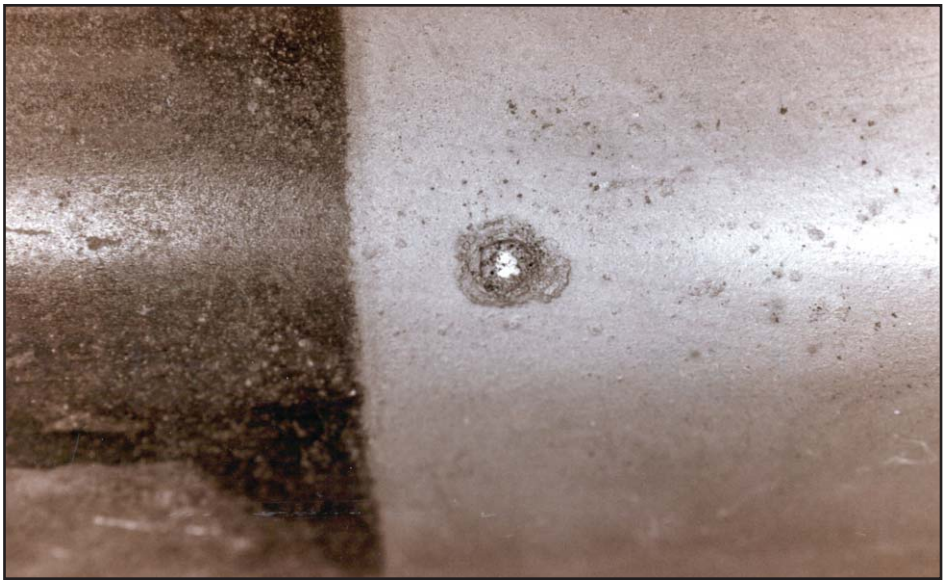

Figure IV-1: Microorganism Influenced Corrosion

MIC occurs under bacterial growths and the exact mechanism is still open to discussion. In some cases, the bacteria produce acids, which cause the corrosion. In other cases with SRB, H_2S is produced, which can cause H_2S corrosion. With CO_2, some typical CO_2 attacking can occur because of the breakdown of the film by the bacteria. Bacterial attack is usually characterized by rounded pits with etched sides, edges, and bottoms (Figure IV-2 and Figure IV-3).

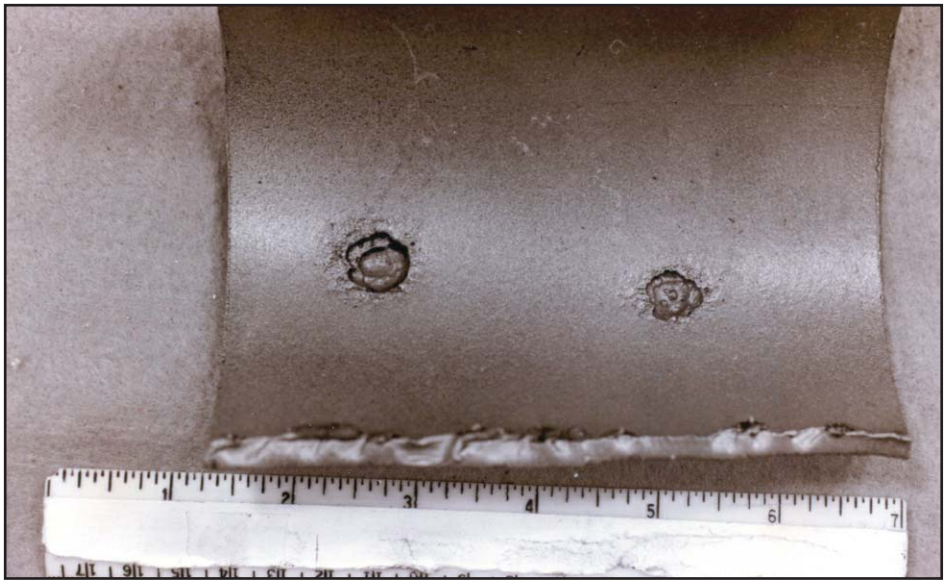

Figure IV-2: Bacterial Attack Characteristics

Figure IV-3: Bacterial Attack Characteristics

At times, the pits have a terraced effect (Figure IV-4 and Figure IV-5).

Figure IV-4: The Terraced Effect

Figure IV-5: Another Example of the Terraced Effect

One of the quick tests that can be run for SRB is the pipe cleaner test. Examples with positive results for the pipe cleaner test are shown in Figure IV-6 and Figure IV-7.

Figure IV-6: Pipe Cleaner Test Example

Figure IV-7: Pipe Cleaner Test Examples

Other examples of MIC attack in conjunction with CO_2 are shown in Figure IV-8.

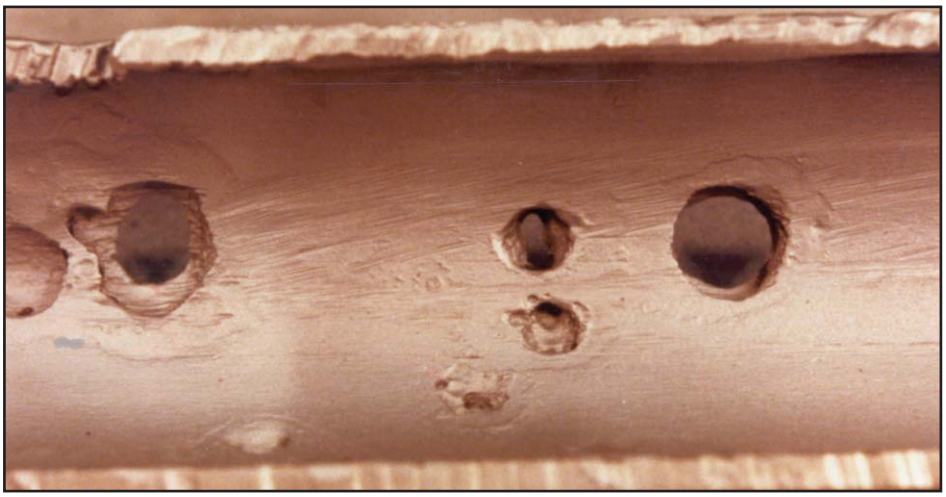

Figure IV-8: MIC Attack in Conjunction with CO_2 Attack

In most cases, MIC attack occurs at the bottom of the line where water accumulates. However, MIC has also been detected in the 3 o'clock to 9 o'clock position, where there was a possible water and oil interface (Figure IV-9 and Figure IV-10).

Figure IV-9: MIC Detected in the 3 o'clock Position

Figure IV-10: MIC Detected in the 9 o'clock Position

One of the failures had detectable black growths, which tested positive for SRB, and had corrosion pits beneath the growth (Figure IV-11).

Figure IV-11: Detectable Black Growth

OBTAINING AND ENUMERATING A SAMPLE OF SESSILE BACTERIA

1. Obtain the surface containing sessile bacteria and carry out the following procedure as quickly as possible (Note 1).

2. Using a scalpel that has been sterilized by soaking in ethyl or isopropyl alcohol, thoroughly scrape the surface (Note 2).

3. Place the scraping into a half-ounce bottle that contains 1 gm of glass beads (diameter = 2 mm) and 10 ml of sterilized field water or other appropriate fluid (Note 3) and is equipped with a tight screw cap (Note 4).

4. Vigorously shake the contents 500 times.

5. Using 1-ml volumes out of the half-ounce bottle, make serial dilutions into the appropriate media as described in your Nalco Microbiology Guide.

6. Report results in counts/cm^2.

Notes:

1. Speed is necessary to minimize exposure of the sample to air. Using many different surfaces is possible including pipe walls, pits on a pipe wall, studs from Robbins devices, and corrosion coupons.

2. Minimize the handling of the sample as much as possible. Samples should be held with pre-sterilized forceps, if possible. Scrape 0.5 to 2.0 cm^2 of the surface.

3. If sterilized field water is not available, or is impractical, a sterilized solution of similar salinity with pH of 7.0 can be substituted. Following are the ingredients for this formulation:

K_2HPO_4	6.06 g
KH_2PO_4	0.4 g
Cysteine HCl	0.5 g
Tween 80	1.0 ml
NaCl	30 gm or 80 gm (1)
Water	Add up to 1,000 ml by volume

(1) Use the strength that more closely approximates the total brine strength of the field. Sterilized sealed half-ounce bottles containing this formulation and glass beads can be obtained from several commercial sources.

4. If the surface to be scraped is small enough (such as a stud formulation from a Robbins device or biofilm probe), the scraped area may be put into the half-ounce bottle after scraping.

5. By measuring the amount of surface area that was scraped and observing the number of vials in the serial dilution that indicate growth, the number of bacteria per unit of surface area can be determined.

V. HYDROCHLORIC ACID (STRONG ACID) CORROSION CHARACTERISTICS

Corrosion Examples from Refining Industry

Each example of hydrochloric acid (low pH — strong acid) corrosion can actually represent several different mechanisms contributing to the total corrosion attack. The following represents general examples from the refining industry.

Form of Corrosion

Uniform acid etching
Localized — Round bottom pits caused by partial water wetting
Under deposit — Salts such as ammonium chloride

Corrosion Products

Black iron sulfide, (FeS)
Iron chloride (Fe Cl_2)

Corrosion Reactions

$2H_2O + 2HCl + Fe \leftrightarrow FeCl_2 + 2H_2O + H2\uparrow$
$FeCl_2 + H_2S \leftrightarrow FeS + 2HCl$

Unique Forms of Corrosion

Often referred to as orange peel look
Chloride stress corrosion of stainless steel

Treatment

Reduce chlorides — Desalting, caustic
Neutralize acid at dew point
Dilute acid and dissolve salts with wash water

Examples of Corrosion Locations

Crude units
Vacuum units
Straight-run distillation
Hydro-desulfurization (HDS)
Alkylation
NGL gas plants

HYDROCHLORIC ACID CORROSION — LOW pH AQUEOUS CORROSION

Acid attack is the largest corrosion challenge on a crude distillation unit. Most of the corrosion damage to a crude unit occurs in the first one or two exchanger sets in the crude unit overhead. Some crude units are also challenged by corrosion in the top of the crude tower or even in the overhead piping before the first exchangers. The corrosion is always due to low pH acids, but the physical and chemical mechanism can vary. Several descriptions describe the mechanisms, but these expressions are frequently misused.

This misuse has caused confusion in the industry, making it difficult to understand critical aspects of any corrosion control program. Following are the physical and chemical conditions that match these descriptions:

- **Shock Condensation Corrosion** — This corrosion is associated with strong acid, low pH corrosion in an area where the hot vapor stream is contacted with a cooled reflux stream or pumparound stream. Before the liquid and hot vapor reach thermal equilibrium, some of the metal surfaces are cooled enough to condense water. The location of this corrosion is usually one or two trays in the tower below the naphtha reflux or the top pumparound.

- **Under Deposit Corrosion —** This corrosion is associated with the deposition of ammonium, amine, or acidic iron chloride above the dew point of water. The area of attack often is in hot, dry exchangers or in the tower at temperatures from 20°F/11°C to 50°F/28°C above the estimated water dew point. In addition, any isolated area with limited access to vapor or liquid flow might have this type of corrosion.

- **Initial Condensation Corrosion** — With this corrosion, a high level of corrosion is associated with the first condensation of water as the overhead vapor is normally condensed in a crude overhead system. The area of attack is usually in the top exchanger(s) of a crude unit overhead.

HYDROCHLORIC ACID (LOW pH — STRONG ACID) CORROSION

Figure V-1 shows an example of hydrochloric acid and hydrogen sulfide corrosion. This sample of a carbon steel overhead line came from a horizontal section of the overhead system. The top half of the line had severe metal loss in the form of pitting and generalized corrosion. The bottom half of the line showed no corrosion.

Figure V-1: Hydrochloric Acid and Hydrogen Sulfide Corrosion

Closer inspection of the pits shows smooth depressions with gently sloping sidewalls and smooth bottoms (Figure V-2).

Figure V-2: Closer Inspection of the Pits

Possible causes of corrosion in these caps are hydrogen sulfide and ammonium chloride deposits (Figure V-3 and Figure V-4).

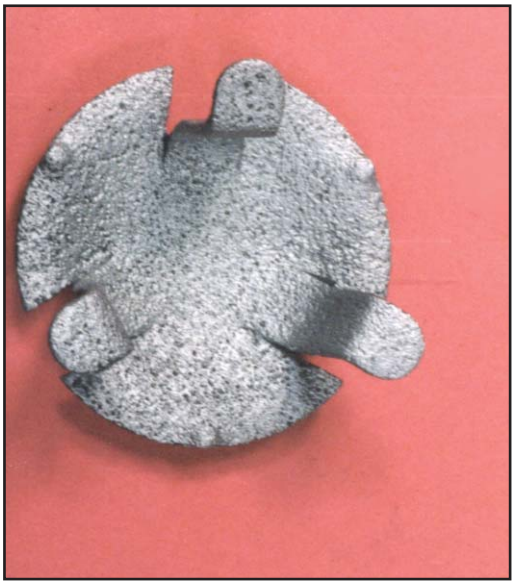

Figure V-3: 13 Cr Stainless Steel (UNS410) Bubble Cap Corrosion

Figure V-4: Close-up of Pitting Corrosion

Figure V-5 shows an example of ammonium chloride underdeposit corrosion.

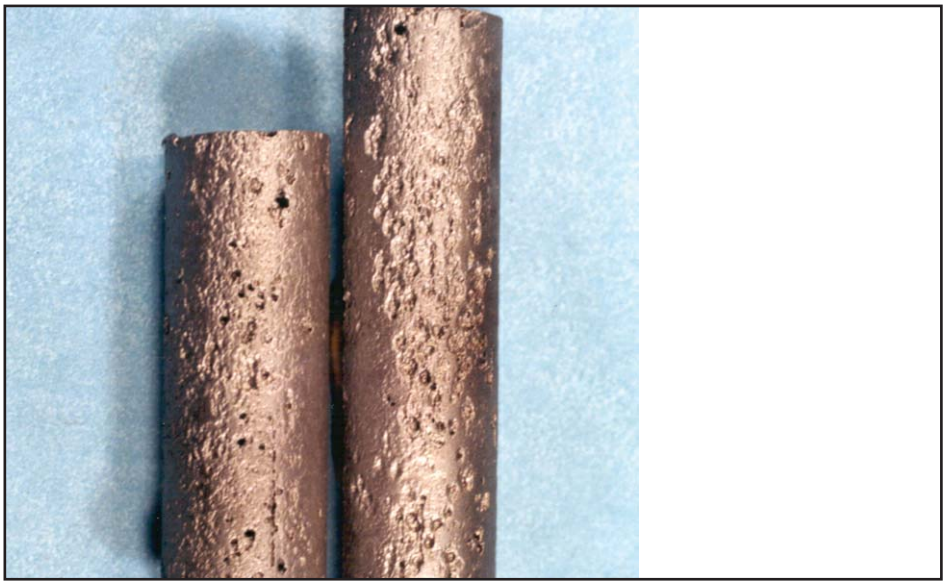

Figure V-5: Ammonium Chloride Corrosion on Carbon Steel Heat Exchanger Tubes

The pits with narrow openings and deep cavenous voids are typical of hydrochloric acid pitting (Figure V-6).

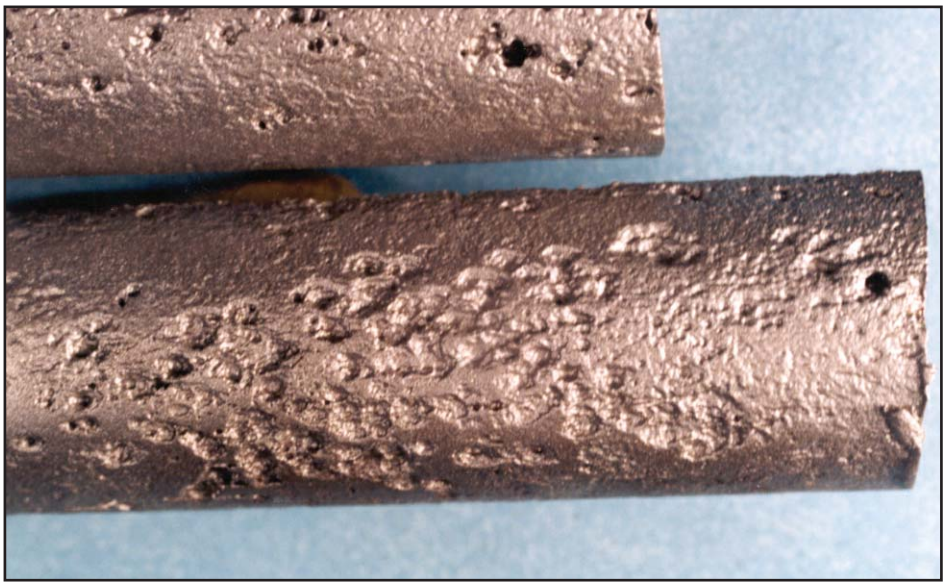

Figure V-6: Pits with Narrow Openings and Deep Cavernous Voids

NAPHTHENIC ACID CORROSION

Figure V-7 and Figure V-8 show SS410 (13Cr) tray cap parts that are severely deteriorated by ammonium chloride, and the hydrogen sulfide that formed the metal sulfides found on the surface after the alloy had been degraded.

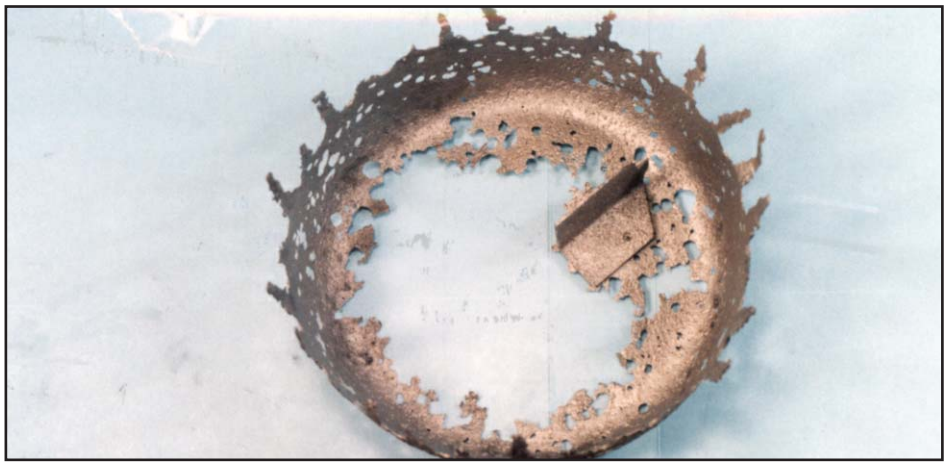

Figure V-7: Ammonium Chloride Corrosion on SS410 Trays

Figure V-8: Ammonium Chloride Corrosion on SS410 Trays

304L Stainless steel tray-stressed corrosion cracking failure. Corrosion was pitting attack attributed to hydrogen sulfides or chlorides.

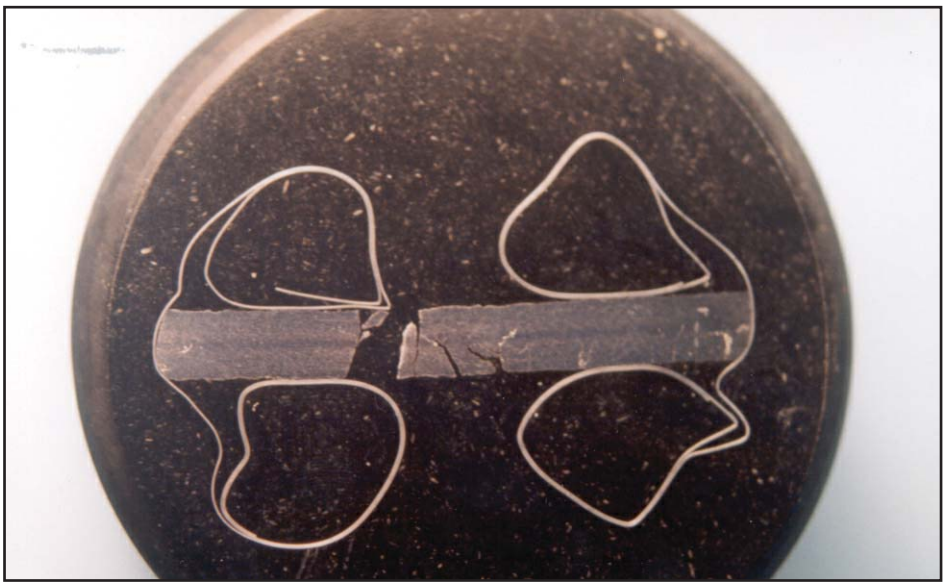

Figure V-9: 304L Stainless Steel Tray

Figure V-10: Stress Corrosion Cracking Failure

Figure V-11 and V-12 is an example of underdeposit corrosion by chlorides, sulfides, and ammonia.

Figure V-11: Carbon Steel Trays — HCl Corrosion

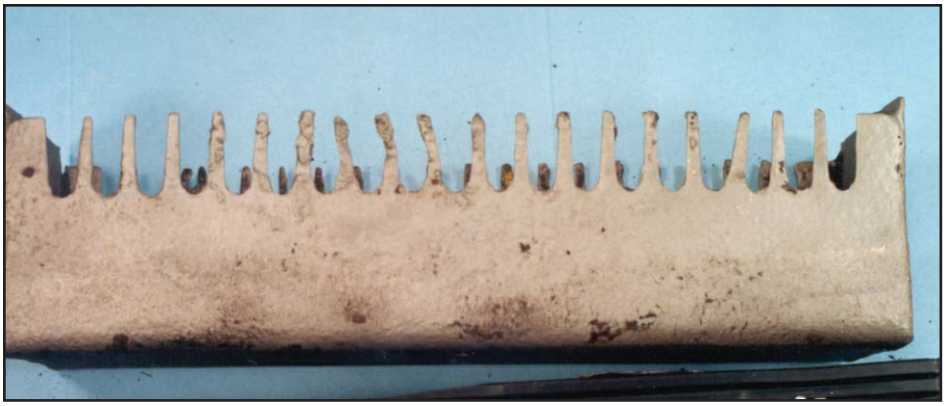

Figure V-12: Underdeposit Corrosion — Note the thinning cleaned surface

Figure V-13 shows a carbon steel upper tray with an orange peel corrosion pattern. Deposits indicate corrosion mechanisms could have been sulfidation, oxidation, or ammonium chloride.

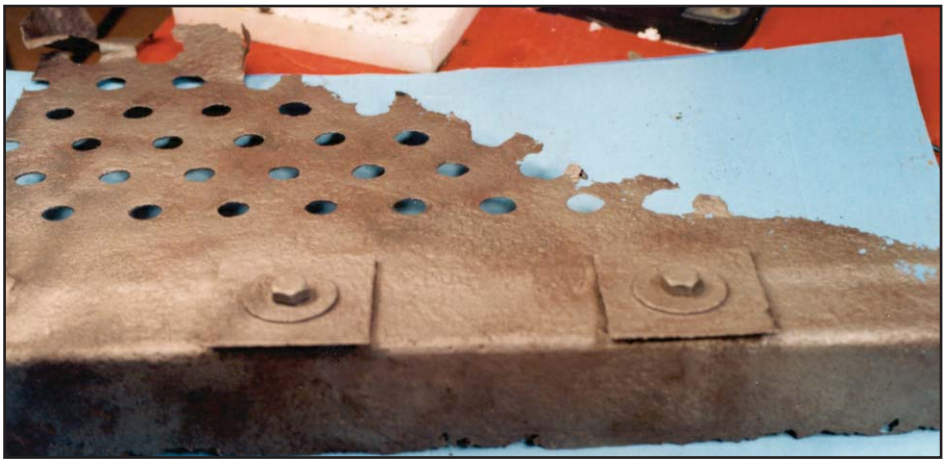

Figure V-13: Sulfidation/Oxidation or Ammonium Chloride

Figure V-14 shows an example of a carbon steel heat exchanger tube in pre-flash overhead with external underdeposit corrosion.

Figure V-14. Underdeposit Corrosion

In Figure V-15, pitting and gouging are most likely from acid penetration of fouled surface. Note the internal surface showed no corrosion.

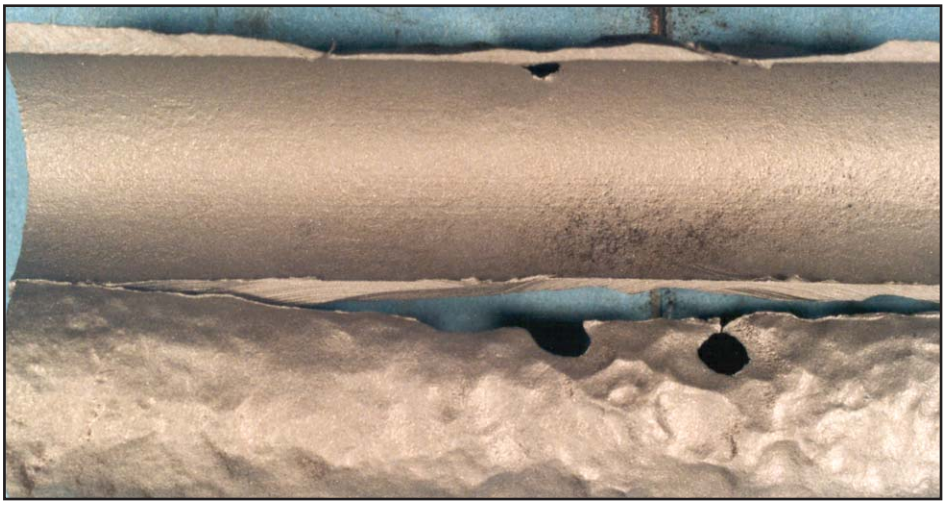

Figure V-15: Pitting and Gouging - External Surface

VI. NAPHTHENIC ACID CORROSION CHARACTERISTICS

Form of Corrosion

Can be pitting, gouging, or grooving

Corrosion Products

Iron naphthenates, possible iron sulfide

Corrosion Reactions

$Fe + 2R{=}COOH \rightarrow Fe(OOC\text{-}R)_2 + H_2$
$FeS + 2R\text{-}COOH \rightarrow Fe(OOC\text{-}R)_2 + H_2S$
$FeO + 2R\text{-}COOH \rightarrow Fe(OOC\text{-}R)_2 + H_2O$ (not as common)
$Fe(OOC\text{-}R)_2 + H_2S \rightarrow FeS + RCOOH$ (regenerated naphthenic acid)

Unique Forms of Corrosion

Usually found in areas of velocity or turbulence, and at vapor and liquid interface

Treatment

Improve metallurgy
Add high temperature stable chemical corrosion inhibitors specifically designed for protection against naphthenic acid

Examples of Corrosion Locations

Crude units
Vacuum units
Lube oil extraction units

NAPHTHENIC ACID CORROSION

Figure VI-1 shows an example of Naphthenic Acid attack on a 14Cr Tray.

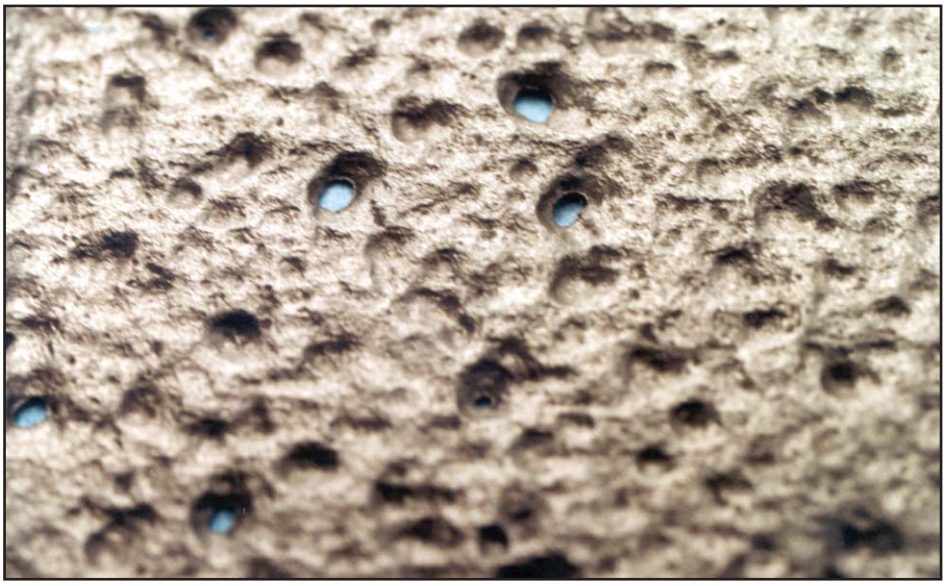

Figure VI-1: Naphthenic Acid attack on 14Cr Tray

Upgrade in metallurgy or corrosion inhibitor required to resist naphthenic acid corrosion (Figure VI-2).

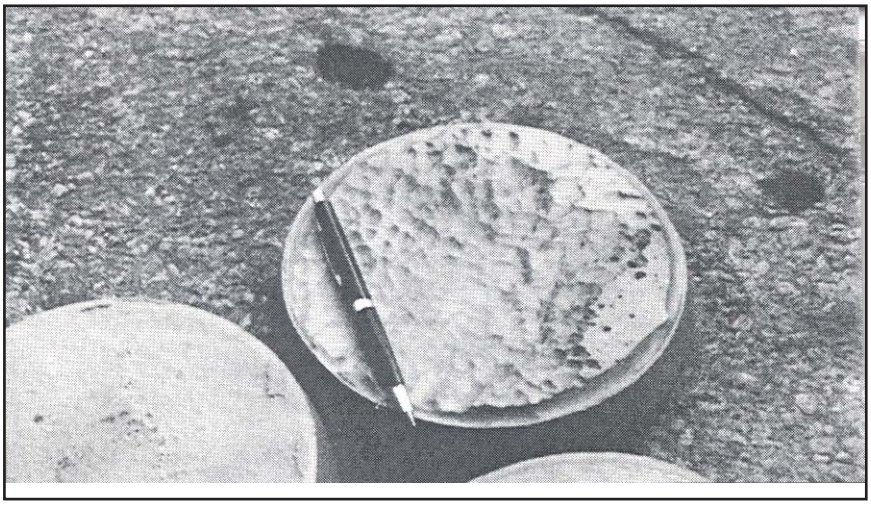

Figure VI-2: Typical Pitting From Naphthenic Acid Corrosion on Heater Plugs

VII. HIGH pH CORROSION CHARACTERISTICS

Primarily caused by H_2S
Can be accelerated by cyanides in some systems

Form of Corrosion

Pitting, blistering, and cracking

Corrosion Products

FeS

Corrosion Reactions

(High pH)
$2H_2S + 2NH_3 \leftrightarrow 2NH_4^+ + 2HS^-$ (bisulfide ion)

$2NH_4^+ + 2HS^- + Fe \leftrightarrow FeS\downarrow + H_2\uparrow + (NH_4)_2S$

$Fe + 2HS^- \rightarrow FeS\downarrow + S^{-2} + 2H^0$

$2H^0 \rightarrow H_2\uparrow$

$FeS + 6CN^- \rightarrow Fe(CN)^{-4}_6 + S^{-2}$ (if cyanide present)

Unique Forms of Corrosion

Sulfide Stress Cracking (SSC)
Sulfide Stress Corrosion Cracking (SSCC)
Hydrogen Induced Cracking (HIC)
Stress-Oriented Hydrogen-Induced Cracking (SOHIC)

Treatment

Dilute with water wash
Apply filming amines/corrosion inhibitors (filming amines — a specific type of the more generically used corrosion inhibitors)
Use polysulfide to remove cyanides when present
Apply metal passivation chemistry (amine units)

Examples of Corrosion Locations

FCC and FCC gas plants
Cokers
Sour water strippers
Hydrocrackers
Hydro-desulfurization (HDS)

Figure VII-1 and Figure VII-2 show an example of hydrogen sulfide attack on 90Cu-10Ni tubes leading to failure.

Figure VII-1: De-alloying Tubes — H_2S Corrosion 90-10 Cu:Ni Heat Exchanger Tubes

Figure VII-2: Close-up of De-alloying Tubes — H_2S Corrosion 90-10 Cu:Ni Heat Exchanger Tubes

VIII. MISCELLANEOUS EXAMPLES OF CORROSION

Erosion—Corrosion

Overhead line tee section
Overhead exchanger tubes
Amine unit

Storage Tank Corrosion

Crude Preheat Corrosion

Product Pipeline Corrosion

Aluminum Brass Stress Cracking

UAN Corrosion

Fuel Storage Tank Corrosion

MISCELLANEOUS EXAMPLES OF CORROSION

Figure VIII-1 shows an example of a carbon steel tee showing signs of erosion corrosion. The horseshoe-shaped pits indicate the direction of flow.

Figure VIII-1: Erosion Corrosion — Carbon Steel Tee

Figure VIII-2 shows a close-up of the pits after cleaning. Corrosion by-products in the pits suggest the corrosive agents were ammonium chloride and hydrogen sulfide.

Figure VIII-2: Close-up Pits after Cleaning

In this example of erosion-corrosion, fluids are channeled through the perforations in the diffuser plate, causing localized impingement sites. FeS film is continually eroded off, replaced, and eroded off again (Figure VIII-3).

Figure VIII-3: Erosion-Corrosion — Carbon Steel Overhead Exchanger Tubes

EROSION — CORROSION IN A DEA STRIPPER

Metal loss was confined to a DEA impingement zone. Corrosion was attributed to carbon dioxide in the DEA (Figure VIII-4).

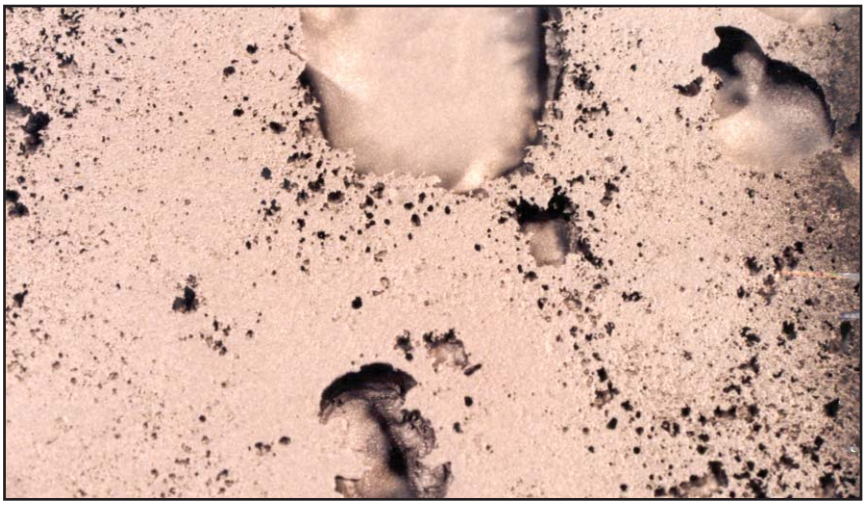

Figure VIII-4: Erosion-Corrosion — DEA Stripper Tower Wall

Figure VIII-5 shows the large areas that were eroded, leaving a smooth surface.

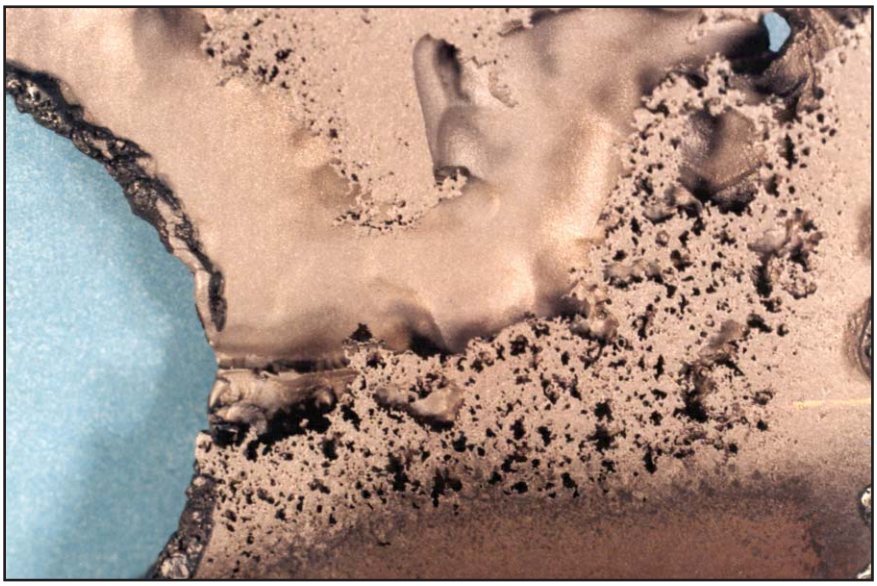

Figure VIII-5: Large Areas Eroded

CRUDE STORAGE TANK — CORROSION

SRB's and iron oxidizing bacteria attack carbon steel storage tank bottom floor (Figure VIII-6).

Figure VIII-6: Crude Storage Tank Failure Most Likely from Wet Oxygenated Soils

CRUDE PREHEAT CORROSION

Figure VIII-7 shows an example of a carbon steel exchanger tube from a crude pre-heat train (tubeside: crude oil, shell side: hot naphthas).

- Pits were round with smooth side walls and etched bottoms.
- Corrosion by-products were iron oxides, iron sulfides, and iron carbonates, suggesting 0_2, H_2S, and CO_2 as the corrosive species.
- Internal deposits contained calcium, magnesium, chlorine, sodium, and silicon — probably from water in the crude.

Figure VIII-7: Oxygen, H_2S, and CO_2 Corrosion

PRODUCT PIPELINE CORROSION

Underdeposit etching was attributed to sulfur containing species and oxygenated fuel in transported fuels (Figure VIII-8 and Figure VIII-9).

Figure VIII-8: Carbon Steel Product Pipeline Corrosion

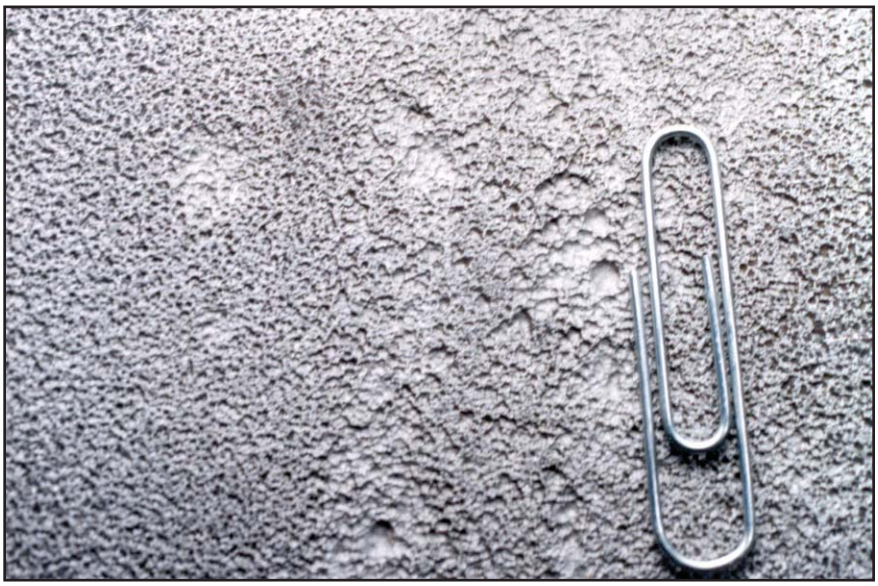

Figure VIII-9: Close-up of Carbon Steel Product Pipeline Corrosion

ALUMINUM BRASS STRESS CRACKING

Aluminum brass crude overhead heat exchanger tubes show signs of stress cracking (Figure VIII-10 and Figure VIII-11). There was no evidence of corrosion affecting the tubes. Therefore this was probably due to:

- Tubes overstressed during installation.
- Thermal stressing during hydrotest and operations.
- Operational stresses, such as water, hammering, and vibration.

Figure VIII-10: Aluminum Brass Stress Cracking

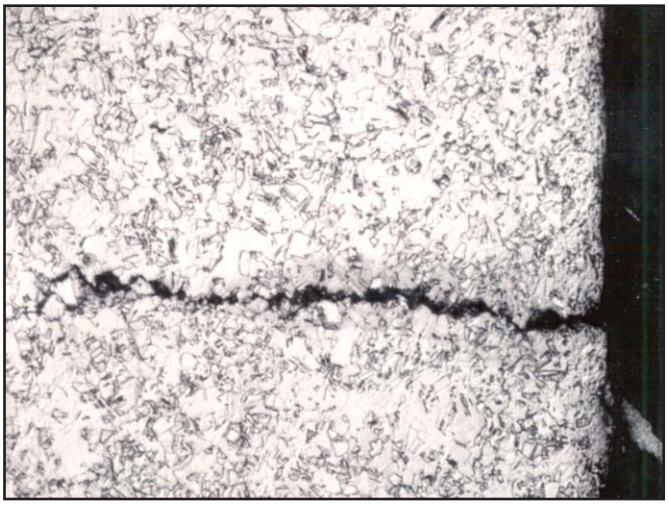

Figure VIII-11: Aluminum Brass Stress Cracking

UAN CORROSION

Figure VIII-12 and Figure VIII-13 shows an example of UAN corrosion. Note how the corrosion is more severe at the tank edges and along the plate boundaries.

Figure VIII-12: UAN Corrosion — Carbon Steel Storage Tank

Figure VIII-13: Close-up View of the Corrosion at a Plate Boundary

Figure VIII-14 shows an example of corrosion on a carbon steel storage tank bottom from concentrated UAN

Figure VIII-14: UAN Corrosion on Carbon Steel Storage Tanks

FUEL STORAGE TANK CORROSION

Figure VIII-15 and Figure VIII-16 shows an example of corrosion by pitting at the water layer in the bottom of diesel steel storage tanks. Possible mechanisms for pitting include microorganism influenced corrosion and/or galvanic corrosion due to sulfide inclusions in the steel.

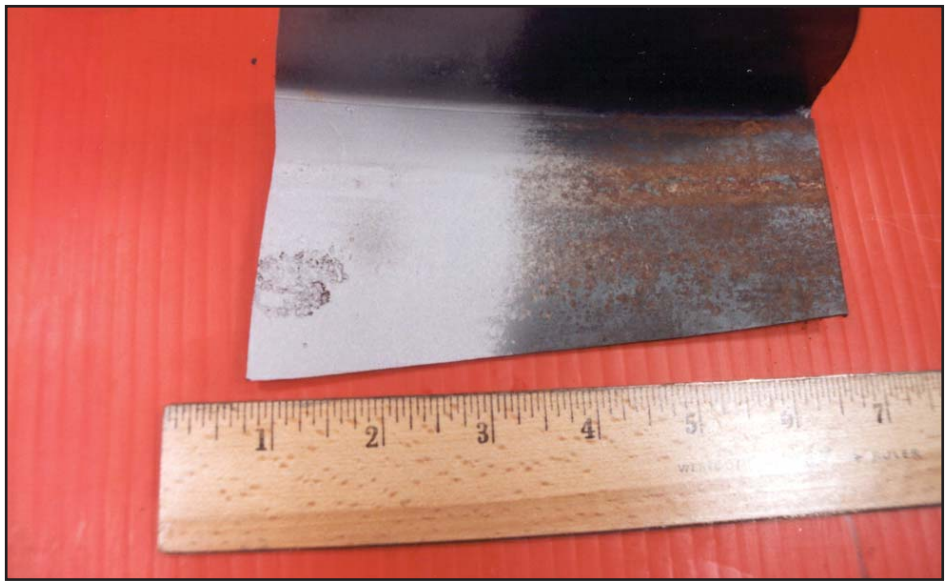

Figure VIII-15: Fuel Storage Tank Corrosion

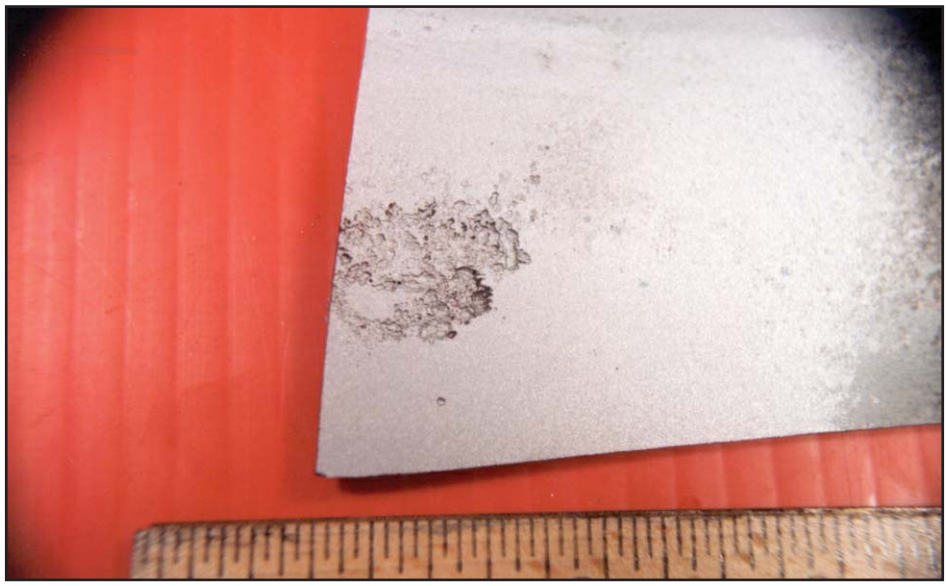

Figure VIII-16: Fuel Storage Tank Corrosion

Figure VIII-17 is a photomicrograph at 100X showing the cavernous pits, carbides, and manganese sulfide stringers.

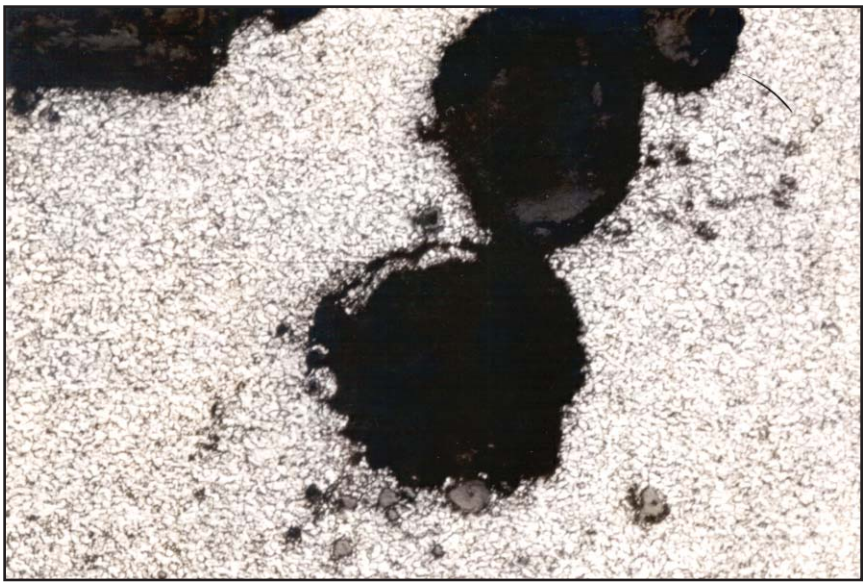

Figure VIII-17: Fuel Storage Tank Corrosion

Figure VIII-18 shows another section of the bottom of the fuel tank where corrosion had not occurred. Note the relative cleanliness as compared to figure VIII-17.

Figure VIII-18: Fuel Storage Tank Corrosion

IX. WATERSIDE FAILURES IN THE REFINING INDUSTRY

Steam Generating Systems

Steam generating systems include conventional fired boilers and boilers that generate steam from hot process streams such as transfer line exchangers. Several different failure mechanisms may occur on boiler tubing used in such systems. Case histories describing a few of the possible mechanisms are presented below. More detailed descriptions, and additional boiler system failure mechanisms, are presented in *The Nalco Guide to Boiler Failure Analysis*.

Case History #1 — Failure of a Steam Generator Tube Due to Caustic Corrosion

System — Waste heat steam generator (transfer line exchanger)
Specimen — Steam generator tube
Orientation — Vertical
Material — Carbon steel
Time in service — 4 years
System age — 20 years
Environment

Internal — Quenching gases
Temperature — 1,000°-1,500°F (538° - 816°C)
Pressure — 75 psi

External — Water and steam mixture
Temperature — 650°F (343°C)
Pressure — 1,500 psi
Chemical treatment — Phosphate/caustic

Deep, localized wastage occurred at the ends of several tubes at the bottom of a transfer line exchanger, causing two failures (Figure IX-1). Thick layers of deposits accumulated on the bottom tubesheet of this exchanger (Figures IX-2 and Figure IX-3). These deposits insulated the tubes and tubesheet, and prevented the rinsing away of caustic and other aggressive alkaline salts following steam generation. The alkaline salts concentrated to levels as high as the percent ranges to remove protective iron oxide layers and to attack the steel.

Figure IX-1: Localized Metal Loss at End of Tube that Contacted Bottom Tubesheet

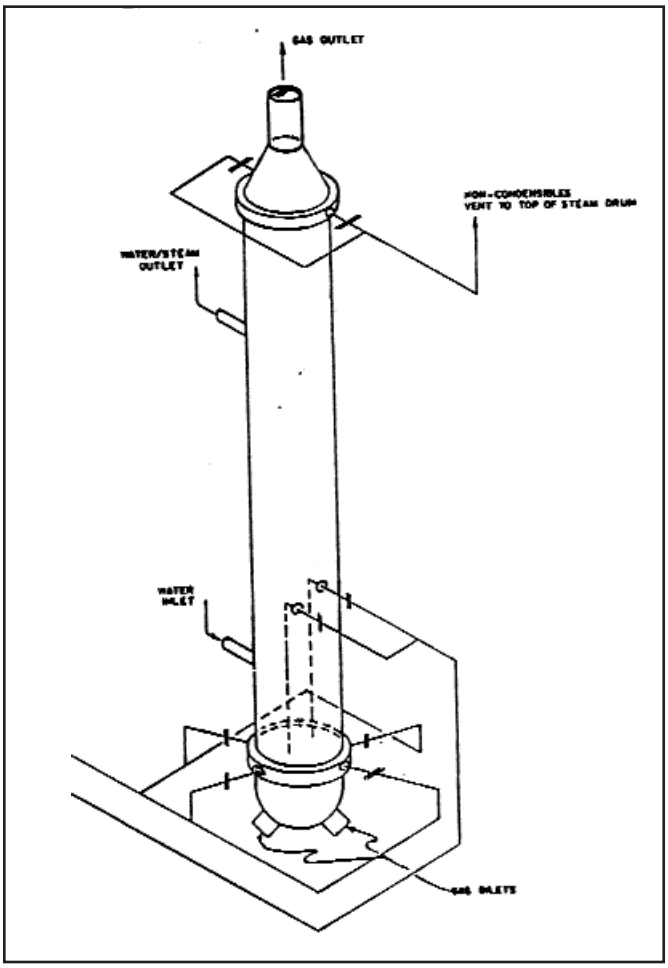

Figure IX-2: Transfer Line Exchanger

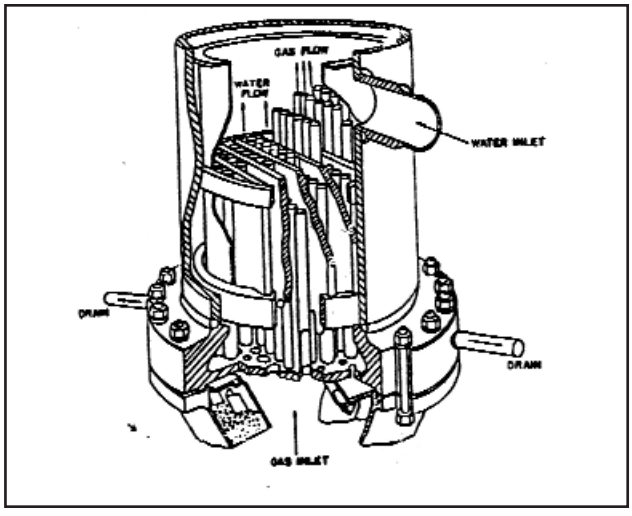

Figure IX-3: Tubesheet where Corrosion Occurred

Reactions

$4NaOH + Fe_3O_4 \rightarrow 2NaFeO_2 + Na_2FeO_2 + 2H_2O$

$Fe + 2NaOH \rightarrow Na_2FeO_2 + H_2$

Alkaline deposits, containing sodium, covered the surface in the corroded area (Figure IX-4). Metallographic analysis revealed the presence of magnetite needles and metallic copper on the corroded surface.

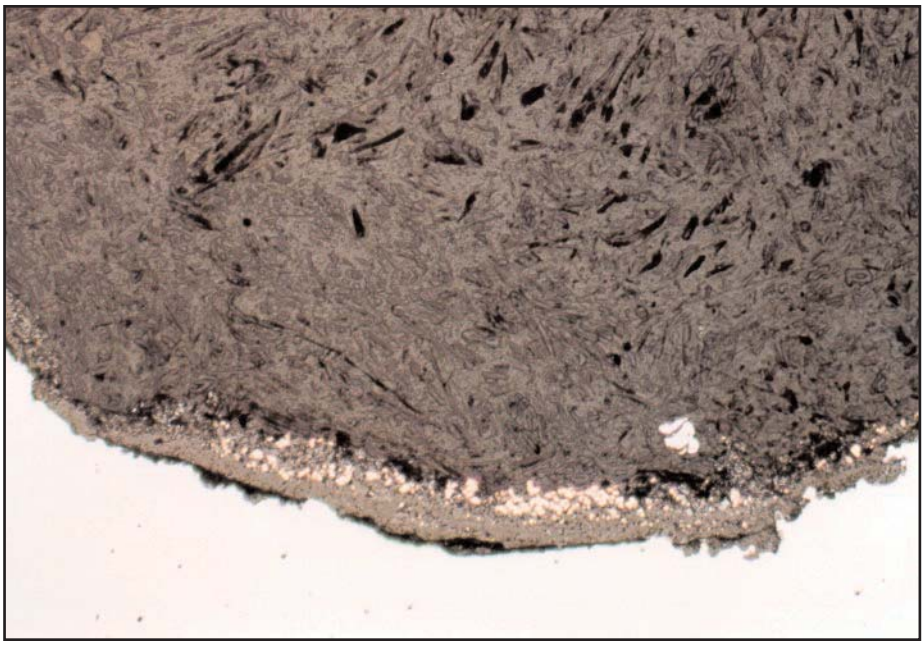

Figure IX-4: Corrosion Products in Wasted Area Containing Magnetite Needles and Metallic Copper Particles

Corrosion may also occur on tubes along the top tubesheet in vertical steam generators due to the formation and entrapment of a stable steam blanket. Water boils away to leave behind dissolved solids and a concentrated solution of caustic, alkaline, or even acidic salts.

Corrosion Control Measures

Clean and maintain clean tubesheet surfaces. Alter the design and operation of the exchanger to prevent the formation and entrapment of a steam blanket. Since no corrosion occurred away from the tube ends, boiler water chemistry and treatment was proper and did not contribute to the corrosion.

Case History #2 — Idle Time Oxygen Corrosion in a Power Boiler

System — Power generating boiler
Specimen — Riser tube
Orientation — Vertical
Material — Carbon steel
Time in service — 30 years
System age — 30 years
Environment

Internal —	Boiler water
	Pressure — 850 psi
	Chemical treatment — Polymer, organic oxygen scavenger
External —	Gas turbine exhaust with supplementary refinery or natural gas as needed
	Temperature — 2,500°F (1371°C) maximum furnace temperature
	Chemical treatment — None

A tube section was removed from the generating bank for surveillance. The internal surface of the section was generally covered with thin, uniform layers of black iron oxides and deposits (Figure IX-5). The uniform layers were interrupted in scattered sites by mounds or tubercles of black iron oxide (Figure IX-6). The presence of iron oxide tubercles indicated that oxygen corrosion occurred at the tubercle sites, resulting from exposure to waters containing excessive concentrations of dissolved oxygen. Removing the layers and tubercles revealed a mostly smooth, unattacked internal surface that was interrupted by moderately deep depressions where the tubercles were present (Figure IX-7).

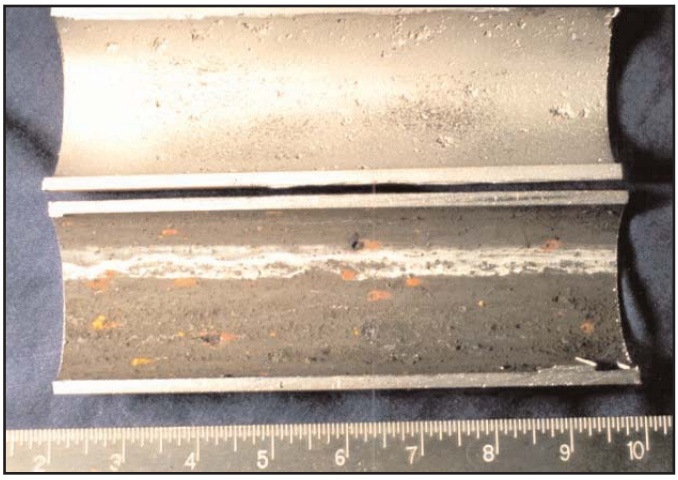

Figure IX-5: Bottom-half Section Showing Internal Surface Covered with Uniform Layer of Black Iron Oxide Interrupted by Scattered Iron Oxide Tubercles

Figure IX-6: Iron Oxide Tubercle with No Flow Orientation

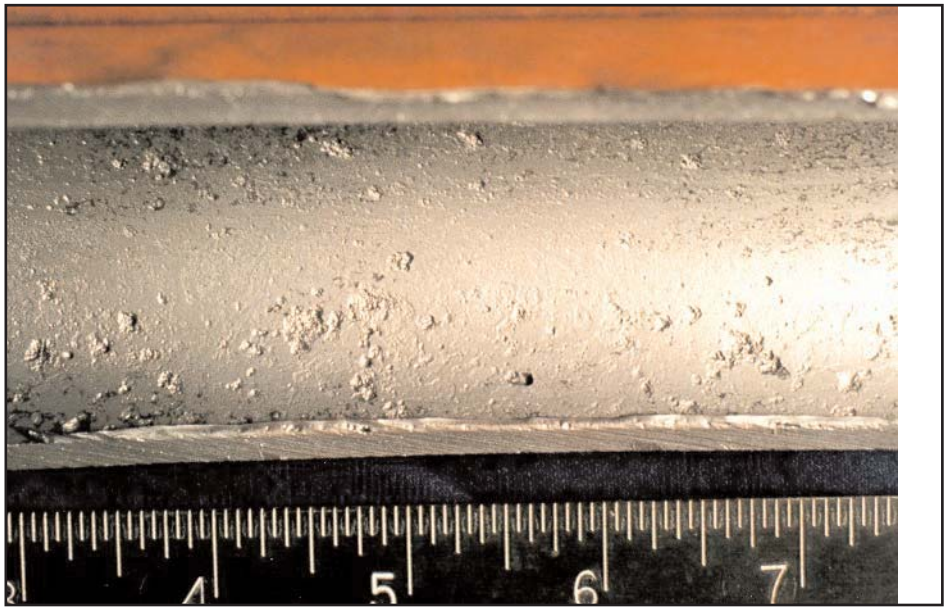

Figure IX-7: Depressions Formed at Tubercle Sites Revealed by Cleaning

The presence of black iron oxide in most areas indicated that oxygen concentration was low during boiler operation. In watertube boilers containing steam drums, it is extremely rare for significant oxygen corrosion to occur within the generating bank during boiler operation. Oxygen introduced to the drum in the feedwater tends to flash off with the steam in the drum. In addition, the scattered nature and small population of the tubercles indicated that oxygen corrosion did not occur during boiler operation. This evidence, and the lack of flow orientation of the tubercles, indicated that oxygen corrosion occurred during idle periods when water was present inside the tubes and was oxygenated by in-leaked air. Orange, brown or red are the colors of hematite, an iron oxide with a higher oxidation state than the black magnetite that normally forms on surfaces when boiler water contains the proper low dissolved oxygen concentration. Hematite formed during idle periods may be subsequently overlaid with or even reduced to a black magnetite during subsequent boiler operation.

In some cases, idle time oxygen corrosion may be identified by the pattern and nature of iron oxide formation. Figure IX-8 shows the internal surface of a horizontally-oriented economizer tube that experienced shallow metal loss within narrow strips along the bottom. During idle periods the boiler was drained and a shallow pool of water remained along the tube bottom. Air leaked into the boiler and oxygenated the residual water to cause oxygen corrosion that produced orange-brown iron oxide corrosion products.

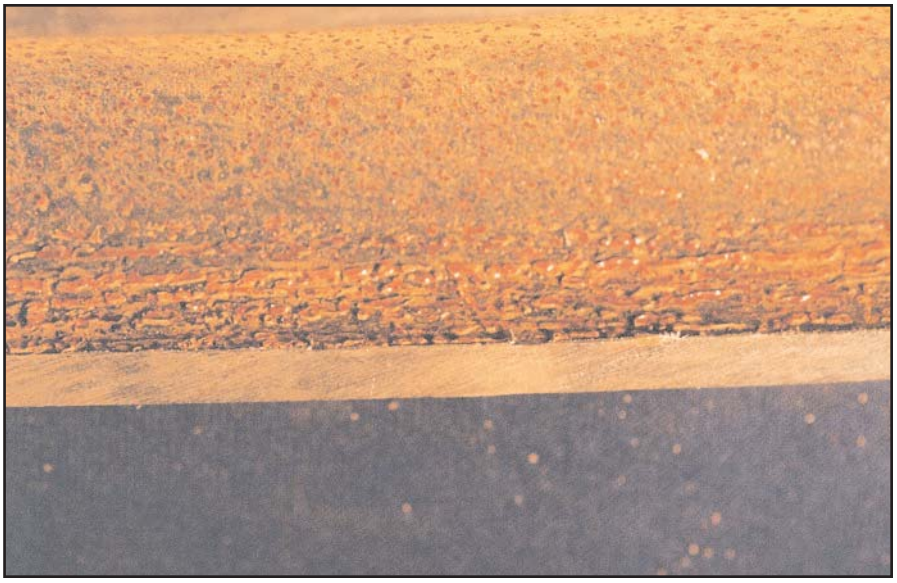

Figure IX-8: Localized Strip of Orange-brown Iron Oxide along bottom of Horizontal Tube

Reaction

$2Fe + H_2O + O_2 \blacklozenge Fe_2O_3$ (hematite) + 2H

Corrosion Control

Idle time oxygen corrosion may be controlled through use of proper lay-up practice. This may include inert gas (nitrogen) blanketing and the proper use of oxygen scavenging chemicals. Such chemicals may be fed to higher levels than used during boiler operation, and may require monitoring, replenishment and circulation. Oxygen corrosion during boiler operation requires proper feedwater deaeration and oxygen scavenging practice.

Case History #3 — Corrosion Fatigue Cracking of a Steam Generator Tube

System — Unspecified boiler
Specimen — Waterwall tube on the side wall, 10 tubes from the front burner
Orientation — Vertical
Material — Carbon steel
Time in service — 12 years
System age — 12 years
Environment

Internal —	Water and steam mixture
	Temperature — 500°F (260°C)
	Pressure — 600 psi
	Chemical treatment — Polymer/sulfite
External —	Unspecified fuel
	Temperature —1,300°- 1,475°F (704° - 802°C)

Multiple leaks occurred in tubes located near the received section of tubing. Regions containing families of moderately deep fissures were present on the hot side internal surface beneath thick deposit layers (Figures IX-9 and Figure IX-10). The fissures propagated transgranularly through the microstructure and were filled with dense oxide containing a centerline crack (Figure IX-11). These features indicated the fissures were caused by corrosion fatigue cracking.

Figure IX-9: Heavy Deposit Layers Covering Internal Surface of Boiler Tube

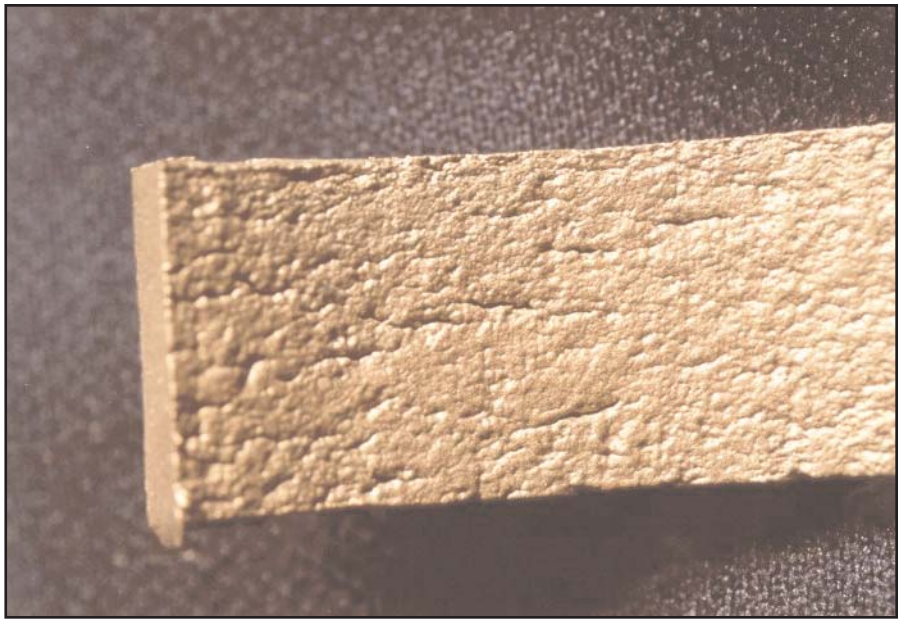

Figure IX-10: Numerous Transversely Oriented Fissures on Internal Surface

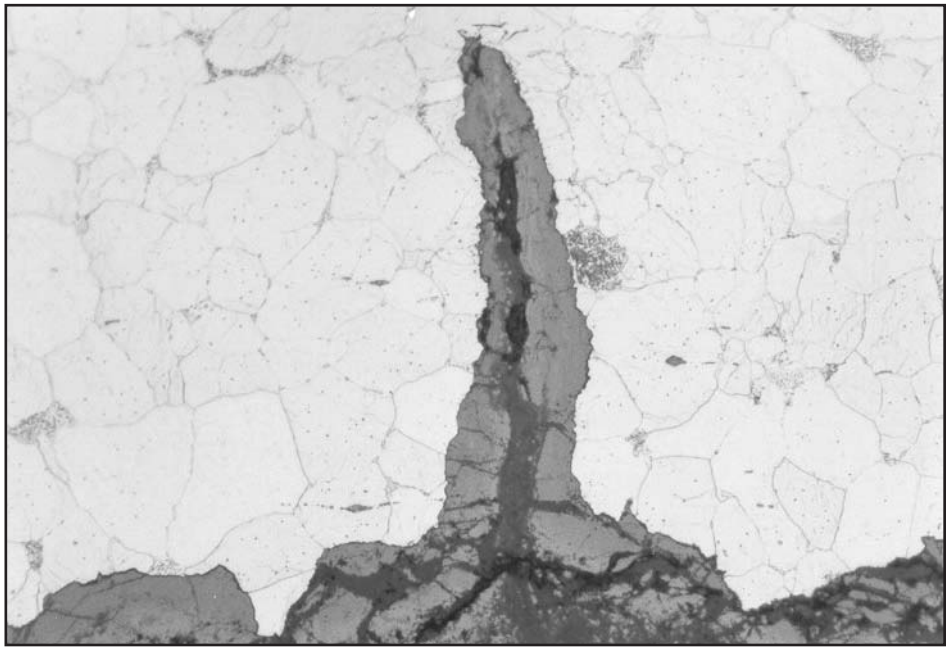

Figure IX-11: Fissure Caused by Corrosion Fatigue Cracking Filled with Dense Oxide Containing Centerline Crack

Corrosion fatigue cracking of boiler tubing results from the application of cyclic tensile stresses; the mechanism can be described as follows. Initially, the surfaces of the metal are covered with a thin layer of dense oxide (Figure IX-12a). Sufficient tensile stresses will result in fracture of the protective iron oxide layers covering the surfaces (Figure IX-12b). Where the oxide layer fractures, bare metal is exposed which immediately oxidizes (Figure IX-12c). Under subsequent stress cycles, oxide fracture and reformation occurs repeatedly at the same location to allow the cracks to grow (Figure IX-12d). No specific corrodents are required for corrosion fatigue to occur, as the protective iron oxide layer will form by reaction with water and/or steam. Although corrosion fatigue may be accelerated by oxygen corrosion, dissolved oxygen in the boiler water is not required for cracking to occur.

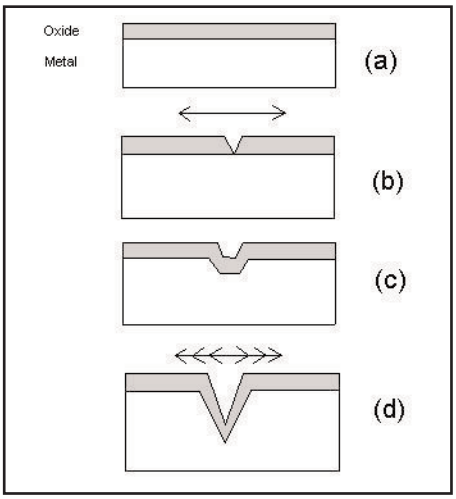

Figure IX-12: Illustration of the Mechanism of Corrosion Fatigue Cracking
(a) Normally Protective Oxide Layer on the Metal Surface
(b) Application of a Tensile Stress Cracks the Oxide Layer
(c) Exposed Metal at the Tip of the Crack Oxidizes
(d) Repeated, Cycling Tensile Stresses Cause the Fissure to Grow

Cyclic tensile stresses can result from a number of sources that include varying bending or tensile loads, vibrations, or temperature or pressure changes. The transverse orientation of the fissures indicated that cyclic bending stresses were responsible for cracking, as the fissures propagate in a direction perpendicular to the principle stresses. The fissures were only present on the internal surface, indicating that localized temperature changes related to the formation and collapse of a semi-stable steam blanket were likely responsible for cracking. Changing metal temperatures caused contraction and expansion of the tube metal, generating cyclic stresses. A small amount of sodium was identified in the internal surface deposits, indicating that evaporation to dryness occurred. The fissures were localized to an area slightly displaced from the hot side tube crown, likely the side facing toward the burner where heat input would be greatest.

Cyclic operation of boilers, including frequent start-ups and shut-downs or peaking service, can also result in corrosion fatigue cracking. Cycling changes in internal pressure of the system would tend to produce corrosion fatigue fissures having a longitudinal orientation if the resulting hoop stresses are sufficient to cause cracking.

Control Measures

The morphology of the fissures produced by corrosion fatigue cracking depends on numerous factors. Blunt, wedge-shaped cracks are generally associated with cyclic stresses of low frequency and/or stress level. Conversely, tight, narrow cracks are typically produced by cyclic stresses of high frequency and/or stress levels. A large number of fissures may also suggest high-level stresses. Crack arrest points, or nodes, present along the fissures indicate different periods of crack growth interrupted by corrosive attack.

Stresses may concentrate at locations of physical constraint and surface discontinuities, such as depressions and notches. The fissures were localized to shallow depressions caused by old oxygen corrosion that occurred during boiler idle time (Figure IX-13). These shallow depressions acted as stress concentrators, promoting nucleation sites for fissures.

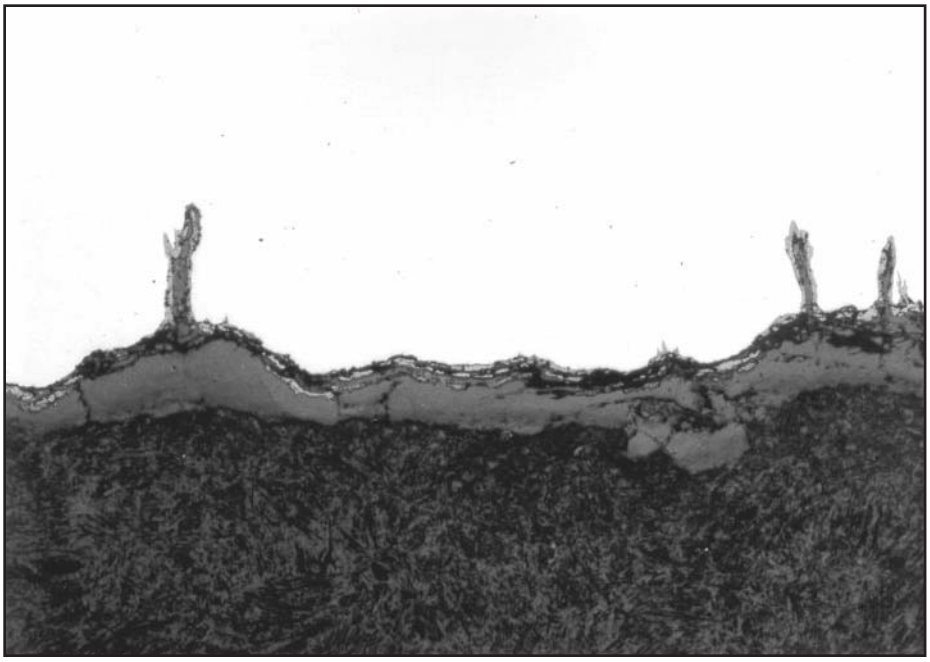

Figure IX-13: Numerous Fissures Initiating from Shallow Depressions Caused by Old Idle Time Oxygen Corrosion

Preventing the steam blanketing condition responsible for cracking would eliminate corrosion fatigue cracking. This may be accomplished by chemical cleaning to remove the insulating internal surface deposits and ensuring adequate coolant flow for the heat input. In general, eliminating or reducing corrosion fatigue cracking is accomplished by identifying and decreasing the cyclic stresses responsible for cracking.

Case History #4 — Failure of a Boiler Deaerator Due to Stress Corrosion Cracking

System — Deaerator
Specimen — Dome section from degasifier
Orientation — Horizontal
Material — 304L stainless steel
Time in service — 4 years
System age — 4 years
Environment

Internal — Wet steam, possible splashing of returned condensate
Temperature — 250°F (121°C)
Pressure — 14 psi
Chemical treatment — None to the deaerator and degasifier section

External — Ambient air, surface covered with insulation

Numerous fissures and cracks formed in the dome of the degasifier section of a deaerator, requiring replacement of the entire dome (Figure IX-14). The system was shut down for four weeks before failure, during which time the deaerator was kept hot with steam feed. No failures occurred when the unit was restarted. However, after four days of operation several cracks penetrated through the dome. The internal surface was also covered with substantial amounts of iron oxide corrosion products that formed in place. These corrosion products overlaid shallow depressions (Figure IX-15).

Figure IX-14: Cracks on Internal Surface Covered with Iron Oxide Corrosion Products

Figure IX-15: Iron Oxide Corrosion Products Removed to Reveal Depressions

Metallographic cross-sections revealed that the cracks were transgranular, highly branched and penetrated from the internal surface outward (Figure IX-16). This revealed that the fissures and cracks formed due to stress corrosion cracking.

Figure IX-16: Metallographic Cross-section Revealing Branched, Transgranular Cracks Penetrating Outward from Internal Surface

Stress corrosion cracking results from exposure of a particular alloy to specific corrodents. Stresses that are required to cause cracking may be applied, or may be residual stresses within the metal that are supplied by original metal forming operations and welding.

The possible corrodents that may have caused cracking in a deaerator include chloride, and caustic or other alkaline salts. Neither of these agents should have been present in the degasifier section. However, contamination of the steam, condensate or feedwater may have occurred, possibly on an intermittent basis. Corrodents may have concentrated to corrosive levels due to evaporation. No residue of either chloride or alkaline salts was found on the internal surface. This is not unusual, since such agents are very water soluble and would wash away after exposure when exposed to normal, noncontaminated water.

The most probable corrodent responsible for stress corrosion cracking was determined to be chloride for several reasons.

1) The threshold concentration of chloride necessary to cause cracking may be quite low at the normal operating temperatures of the deaerator. Cracking may occur at chloride concentration as low as 20 ppm at 200°F (93°C).

2) Caustic stress corrosion cracking rarely occurs at metal temperatures below 300°F (149°C) and generally requires concentrations of caustic in the percent levels. It is improbable that either condition was met in this system.

3) The presence of depressions and oxide corrosion products on the internal surface would have formed due to corrosion by chloride. Caustic would not tend to cause such corrosion.

Control of Stress Corrosion Cracking

Since chloride stress corrosion cracking may occur at even low concentrations at normal operating temperatures, it is recommended that deaerators and water-wetted components throughout boilers should not be constructed of austenitic stainless steels. Aside from this recommendation, chloride stress corrosion cracking may be prevented only by ensuring that no chloride gets into the deaerator, which will be very difficult and expensive to accomplish.

Case History #5 — Overheating in a Power Boiler
System — Power generating boiler
Specimen — Rear wall tube
Orientation — Vertical
Material — Carbon steel
Time in service — 26 years
System age — 26 years
Environment
Internal — Boiler water
Pressure — 1,200 psi
Chemical treatment — Equilibrium phosphate, organic oxygen scavenger
External — Natural gas fired
Temperature — 2,200°F (1204°C) maximum furnace temperature
Chemical Treatment — None

Two bulges formed within a localized area on the hot side of a boiler wall tube (Figure IX-17). The bulges occurred in a tube that was located near a burner. Internal deposition was light in all areas except at the bulges (Figure IX-18).

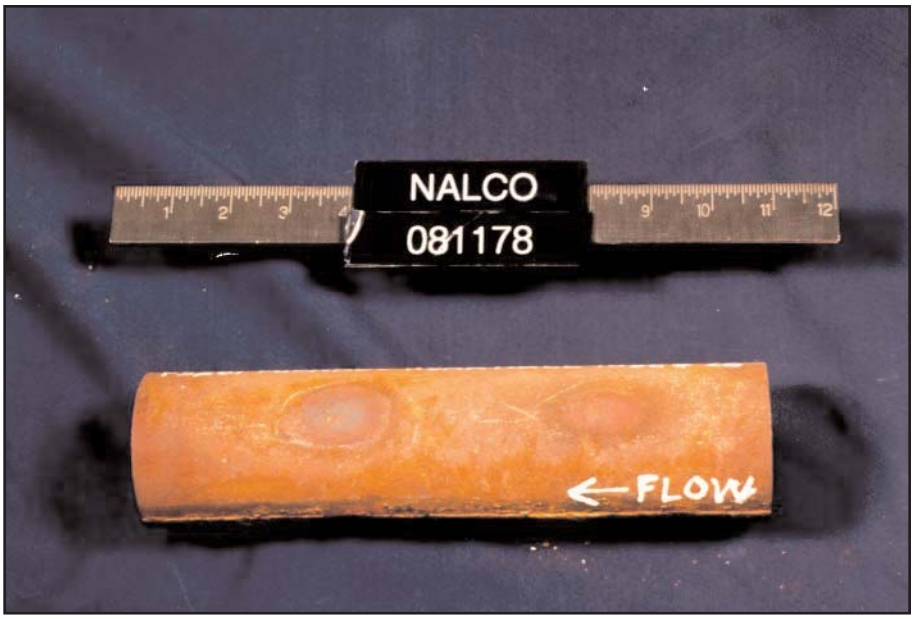

Figure IX-17: Localized Bulges on Hot Side of Wall Tube

Figure IX-18: Localized Deposition at Bulge Site

Metallographic analysis indicated that the original pearlite microstructure of the tube was maintained in all locations except the bulges (Figure IX-19). At the bulges, the microstructure changed to scattered spheroidal carbides in a ferrite matrix (Figure IX-20). Creep fissures also formed on the bulge external surfaces (Figure IX-21). Moderately thick layers of thermally-formed iron oxide built up on both internal and external surfaces at the bulges.

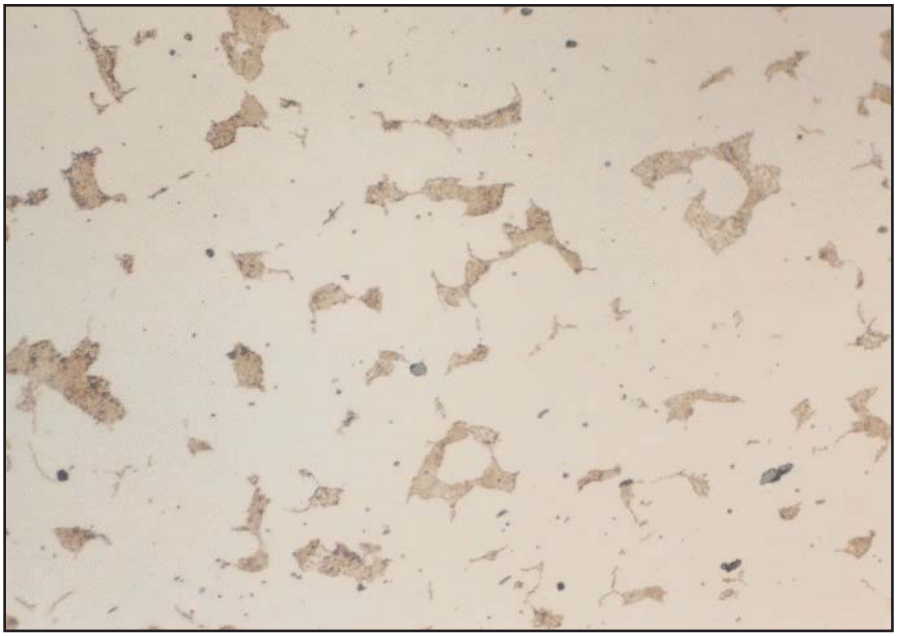

Figure IX-19: Microstructure of Tube in As-manufactured Condition in All Locations Except at Bulges Consisting of Colonies of Pearlite in Ferrite Matrix

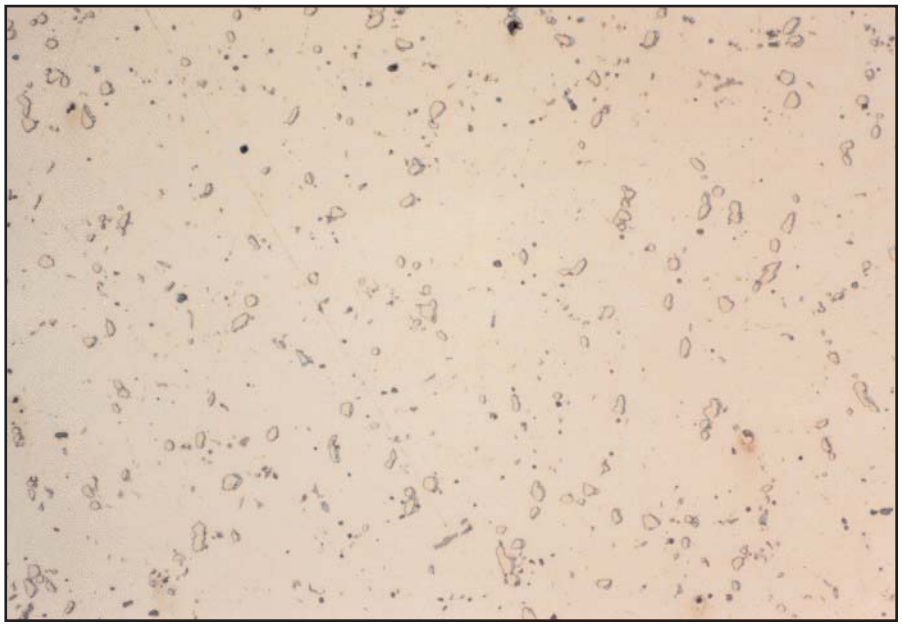

Figure IX-20: Microstructure at Bulges Consisting of Spheroidal Carbides in Ferrite Matrix

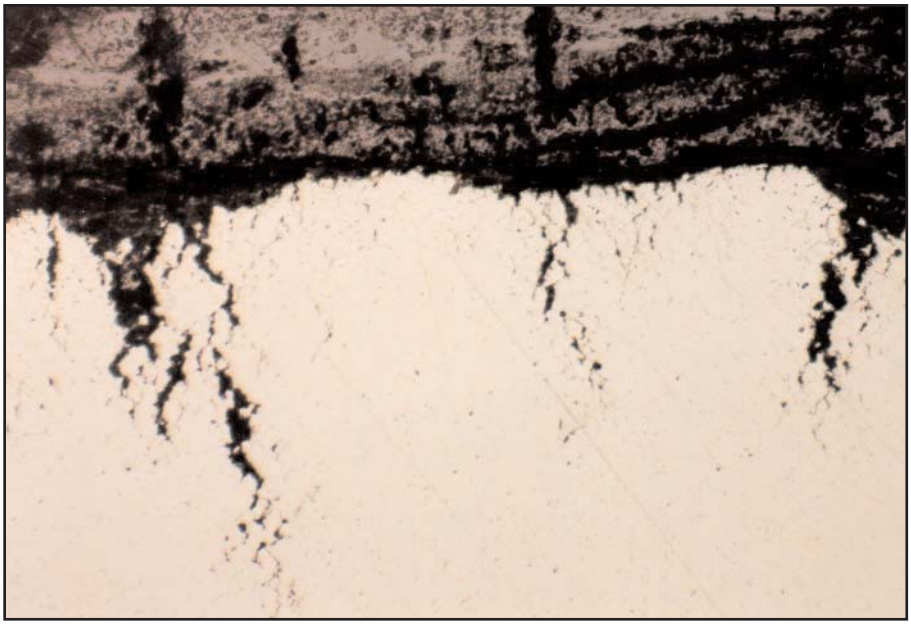

Figure IX-21: Intergranular Creep Fissures on External Surface at Bulge

All of the microstructural features at the bulges indicated that the tube wall at the bulge sites experienced mild, long-term overheating. Metal temperatures ranged from about 850° to 1,100°F (454° to 593°C) for a period ranging from several weeks to several months. Metals have decreased strength at high temperatures (Figure IX-22). Consequently, the tube wall bulged under stresses supplied by internal pressure. The localized nature of the bulging and internal deposition indicated that overheating was caused by excessive fireside heat input.

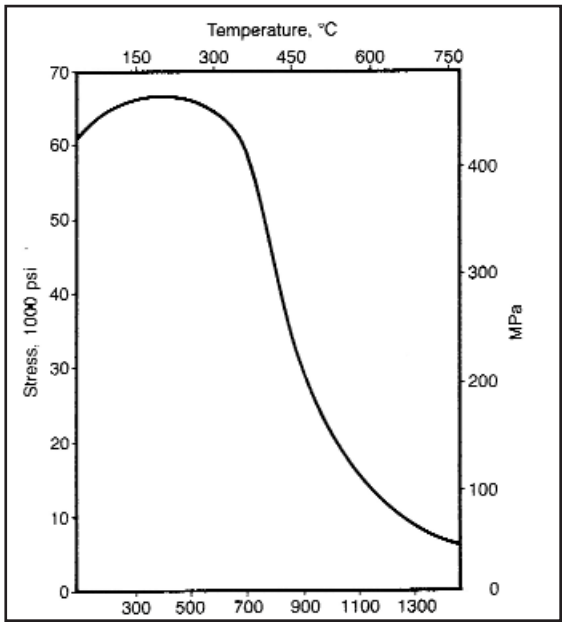

Figure IX-22: Metal Strength versus Temperature (Source: *The Nalco Guide to Boiler Failure Analysis*)

Control of Overheating

The most practical method of controlling overheating in this case would be through proper insulation of the external surfaces of the tubes in the location where the bulges formed. This may be provided by installing refractory or repairing damaged refractory at that location. If this cannot be accomplished, then excessive heat input should be prevented by decreasing firing rates and preventing localized channeling of hot gases to the zone of the bulged tube.

Overheating of boiler tubes may be caused by several different factors, including not only excessive heat input, but also internal fluid flow rate and deposition, possibly in combination. Therefore, the cause of any bulging or rupturing failure of a boiler tube should be diagnosed with a thorough metallographic examination.

Case History #6 — Failure of a CO Boiler Economizer Tube Due to Fireside Corrosion

System — Carbon monoxide boiler
Specimen — Economizer tube
Orientation — Horizontal
Material — Corten steel (carbon steel containing about 0.2% copper)
Time in service — 11 years
System age — 30 years
Environment

Internal — Boiler feedwater
Temperature — 275°F (135°C) inlet, 390°— 415°F (199° — 213°C) outlet
Pressure — 950 psi
Chemical Treatment — Chelant, polymer, sulfite

External — Carbon monoxide from fluid catalytic cracker, refinery gas, steam from soot-blowing
Temperature — 450°F (232°C)
Pressure — 5 — 8 psi
Chemical treatment — None

Numerous deep depressions formed on the external surfaces of several different economizer tubes (Figure IX-23). Thick layers and mounds of light-colored deposits covered the depressions and surfaces in the surrounding areas. Deep depressions were found beneath adherent deposits (Figure IX-24). These deposits tested acidic in a distilled water solution. Chemical analysis of the deposits revealed the presence of high concentrations of sulfate and volatile sulfur compounds. The presence of these deposits indicates that the fireside corrosion may have been caused in part by the condensation of sulfuric acid on the surfaces. When high sulfur content fuels are combusted, the sulfur is oxidized to sulfur trioxide, which combines with moisture in the furnace environment to form sulfuric acid.

Figure IX-23: External Surface Depressions and Acidic, Light-colored Deposits

Figure IX-24: Deposits Removed to Reveal Depressions

Reactions

$S + O_2 \rightarrow SO_2$

$SO_2 + O \rightarrow SO_3$, $SO_2 + {}^1/_2\, O_2 + \text{catalyst} \rightarrow SO_3$

$H_2O + SO_3 \rightarrow H_2SO_4$

$H_2SO_4 + Fe \rightarrow FeSO_4 + H_2$

The dewpoint of sulfuric acid varies as a function of moisture and sulfur trioxide concentration (Figure IX-25 and Figure IX-26). Significant amounts of moisture were supplied to the furnace environment by nearby soot-blowers that emitted steam to remove fireside deposits from boiler tubes. Typically, the operating temperature of the economizer was well above the sulfuric acid dewpoint at any water and sulfur trioxide concentration. Therefore, corrosion during boiler operation was improbable. However, acidic deposits remaining on surfaces during idle periods became hydrated by condensed water to form acids that caused corrosion.

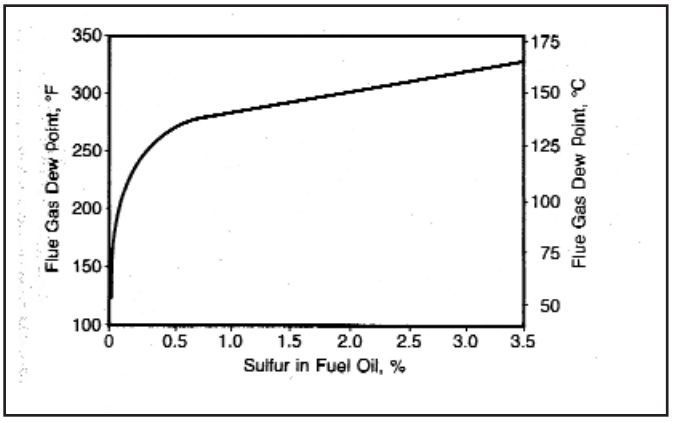

Figure IX-25: Sulfuric Acid Dewpoint as a Function of Fuel Sulfur Content (Source: *The Nalco Guide to Boiler Failure Analysis*)

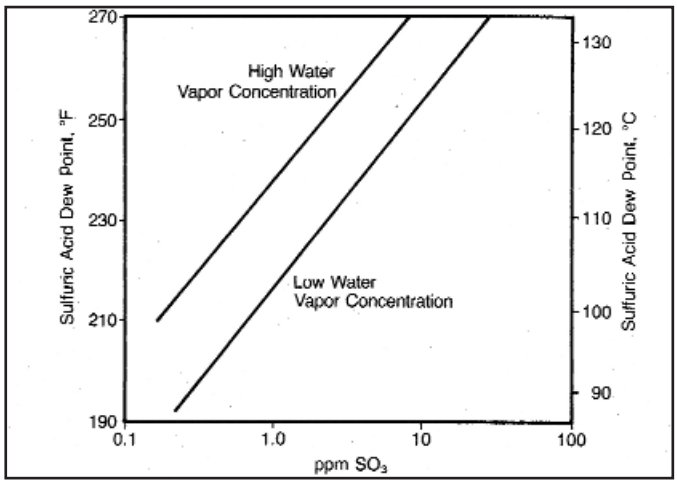

Figure IX-26: Sulfuric Acid Dewpoint as a Function of Water Vapor Concentration in Furnace Environment (Source: *The Nalco Guide to Boiler Failure Analysis*)

Corrosion Control Measures

If the fuel cannot be changed to one with a lower sulfur concentration, a few corrosion control measures may be effective.

Fireside acid corrosion during boiler operation may be controlled, if practical, by:

1) Maintaining metal temperatures above the sulfuric acid dewpoint.
2) Reducing moisture content (lower moisture content fuels and minimization of soot-blowing).
3) Altering firing practice, by combusting fuel with lower excess air.
4) Feeding fuel treatment additives.

Corrosion by acidic fireside deposits during idle periods may be controlled by:

1) Removing corrosive acidic fireside deposits with high pressure water sprays followed by rinsing with a neutralizing lime wash spray.
2) Maintaining a dry fireside environment with the aid of dessicants.

Corten steel, normally used to control atmospheric corrosion, was chosen to help control idle time corrosion. However, this alloy was inadequately resistant to the aggressive, acidic fireside deposits.

Cooling Water Systems

Cooling water systems include overhead condensers, surface condensers and a wide variety of process fluid heat exchangers. Several different corrosion and other failure mechanisms may occur on the watersides of heat exchanger tubing used in such systems. Some of these mechanisms are highlighted in the following case histories. More detailed descriptions, and additional cooling water system failure mechanisms are presented in The Nalco Guide to Cooling Water Systems Failure Analysis.

Case History #7 — Failure of a Heat Exchanger Tube Due to Stress Corrosion Cracking

System — Depentanizer
Specimen — Heat exchanger tube (externally finned)
Orientation — Horizontal
Material — Admiralty brass
Time in service — 10 years
System age — 40 years
Environment

Internal —	Cooling water
	Temperature - 85°-110°F (29° - 43°C)
	Pressure — 45 —70 psi
	Chemical treatment — Ortho/organic/polyphosphate, tolyltriazole, polyacrylate dispersant
External —	Crude unit light naphtha (C2 — C4)
	Temperature - 110°-120°F (43° — 49°C)
	Pressure — 45 psi

Approximately 200 heat exchanger tubes within the unit experienced sudden cracking failures (Figure IX-27). Metallographic analysis revealed the presence of deep, highly branched, intergranular cracks that penetrated from the internal, waterside surface (Figure IX-28). This mode of crack propagation is characteristic of stress corrosion cracking. Stress corrosion cracking of metals results from exposure to specific corrodents for the particular alloy while being subjected to applied and/or residual stresses. Residual stresses are supplied by original tube forming operations.

Figure IX-27: Wall of Admirality Brass Heat Exchanger Tube Penetrated by a Crack

Figure IX-28: Branched, Intergranular Crack and Fissures Penetrating from Internal Surface

The specific corrodents that most commonly cause stress corrosion cracking of admiralty brass are ammonia and hydrogen sulfide. These corrodents were considered as possible causes for the cracking. However, analysis of deposit and corrosion product layers that covered the internal surface revealed the presence of significant amounts of mercury compounds. Mercury causes rapid intergranular cracking of copper alloys in a manner similar to stress corrosion cracking, a mechanism referred to as liquid metal embrittlement. The rapidity of the failures and the intergranular propagation of the cracks more significantly implicate mercury as the corrodent. The presence of mercury is highly unusual in cooling water and could only have been introduced due to contamination. One possible source of mercury is from a pressure-measuring device.

Control Measures

Corrodents that may cause stress corrosion cracking of admiralty brass at low concentrations, such as mercury, should be eliminated from the environment. Other corrodents, such as ammonia and hydrogen sulfide, should be kept to low concentrations to avoid cracking. Reduction of stresses may control cracking to a less significant degree.

Case History #8 — Stress Corrosion Cracking of a Brass Heat Exchanger Tube

System — Propane condenser
Specimen — Exchanger tube from the first pass of the condenser
Orientation — Horizontal
Material — Inhibited admiralty brass
Time in service — Unknown
System age — Unknown
Environment

Internal — Cooling water
Temperature — 65°- 80°F (18° - 27°C)
Pressure — 35 psi
Chemical Treatment — Phosphonate/tolytriazole/chlorine, pH 8.0

External — Propane vapor
Temperature — 150°F (66°C)
Pressure — 135 psi

Numerous leaks occurred in the system over a short period of time. The received section contained a thick wall fracture on one end (Figure IX-29). Multiple crack initiation sites were present along the circumference. Numerous tight, transversely oriented cracks and fissures were present on the internal surface near the fractured end (Figure IX-30). Stratified deposit layers covered a smooth surface contour that showed no significant evidence of corrosion on the internal surface.

Figure IX-29: Brittle Fracture Edge Containing Multiple Crack Initiation Sites

Figure IX-30: Numerous Transversely Oriented Fissures near Fracture Edge

Metallographic cross sections revealed many tight, highly branched fissures indicative of Stress Corrosion Cracking (SCC) (Figure IX-31). The cracks propagated transgranularly into the tube microstructure (Figure IX-32). SCC of brass may be transgranular or intergranular. SCC of a susceptible alloy requires the simultaneous presence of sufficient tensile stress and a specific corrodent. The stress and corrodent interact synergistically to produce cracks on the surfaces exposed to the corrodent and propagate in response to the stress state. The transverse orientation of the cracks and multiple initiation sites along the circumference indicated that the tensile stresses responsible for cracking were uniaxial (longitudinally oriented). The tensile stresses required for cracking can be applied or residual. Residual stresses can be developed from fabrication and installation of the tubes.

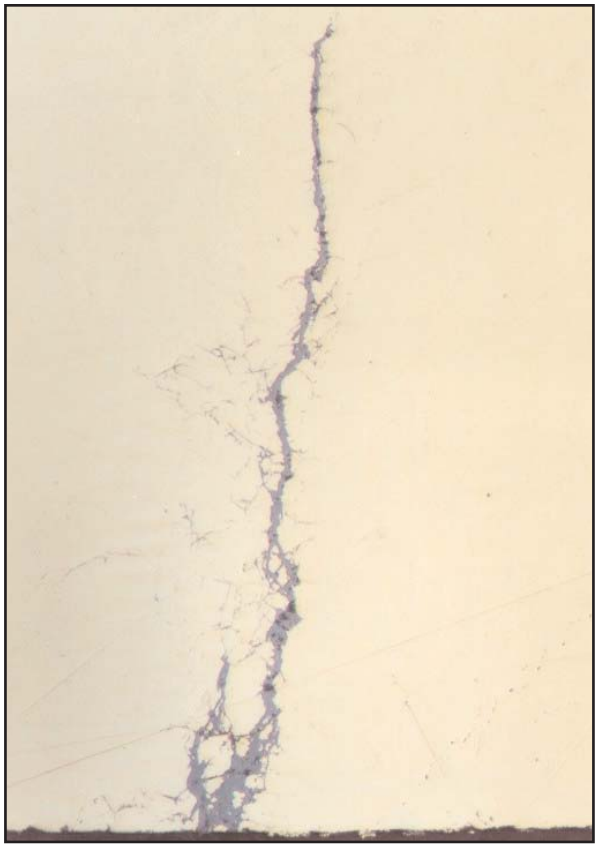

Figure IX-31: Tight Branched Fissure Caused by Stress Corrosion Cracking

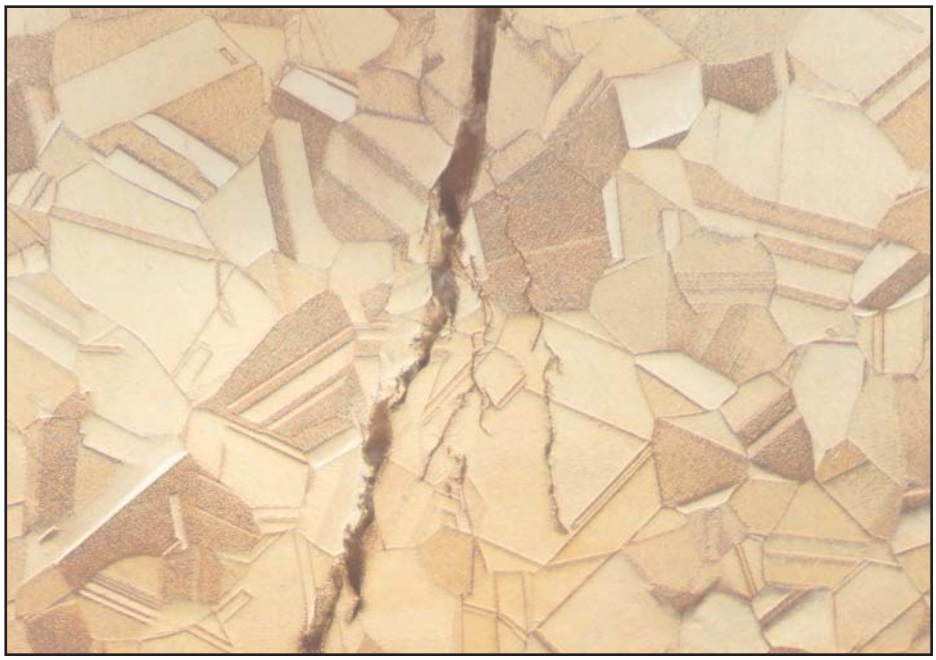

Figure IX-32: Transgranular Propagation Path of a Fissure

Stress corrosion cracking in copper alloys occurs most frequently in environments of aqueous solutions or moist atmospheres that contain ammonia or amines. Sulfur dioxide, hydrogen sulfide, nitrates and nitrites have also been shown to produce stress corrosion cracking in copper-base alloys. The fissures on the section initiated on the internal surface. It was reported that the cooling water was contaminated with amines for a period of time just prior to leaks developing in this condenser.

Control Measures

Stress corrosion cracking can be prevented by removing one of the requirements of cracking, (i.e., tensile stress, the corrodent or the susceptible alloy). In general, the propensity and severity of the cracking increases as stress levels rise. For many alloys, there is a threshold stress below which stress corrosion cracking will not occur (Figure IX-33). Threshold stress depends on many factors, including temperature, alloy composition and concentration of the corrodent. Reduction of the applied and/or residual stresses can reduce or eliminate cracking. Preventing contamination into the system of corrodents responsible for stress corrosion cracking will eliminate cracking. In addition, changing to a less susceptible material may also prevent cracking. Substitution of 70-30 cupronickel in place of admiralty or other copper-base alloys has been suggested as a preventative measure for stress corrosion cracking in refinery service.

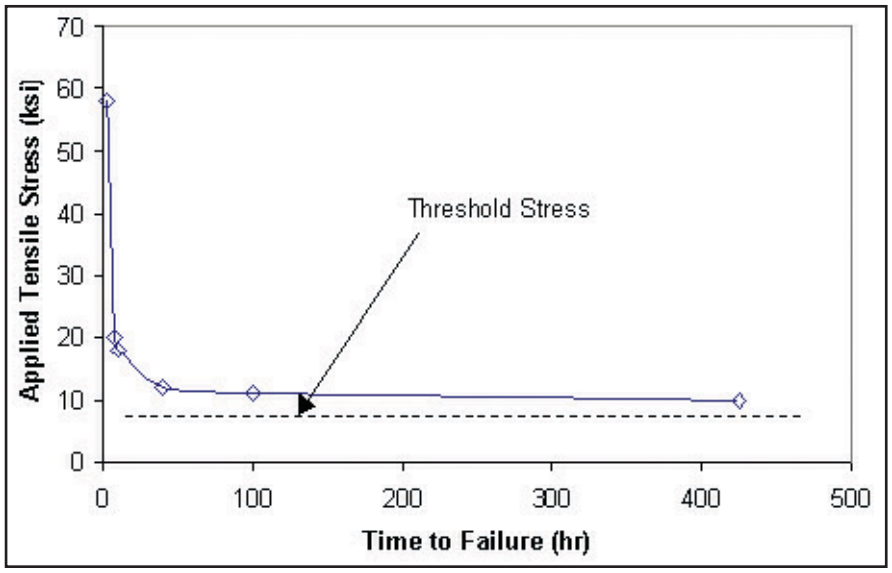

Figure IX-33: Increase in Time to Failure with Decreasing Stress and Threshold Stress Below Which Cracking Does Not Occur

Case History #9 — Failure of a Heat Exchanger Tube due to Dealloying and Corrosion Fatigue Cracking

System — Surface condenser
Specimen — Condenser tube
Orientation — Horizontal
Material — Admiralty brass
Time in service — 6 years
System age — 20 years
Environment

Internal — Cooling water (high chloride concentration, > 400 ppm)
Temperature — 100°- 118°F (38°- 48°C)
Pressure — 5 kgf
Chemical treatment — Organic phosphate, dispersant, bleach

External — Steam condensate from a boiler
Temperature — 130°- 140°F (55°- 60°C)
Pressure — Slight vacuum

A crack-like failure occurred in a surface condenser tube (Figure IX-34). Scattered depressions formed on the internal surface (Figure IX-35). Metallographic analysis revealed that the surfaces of the depressions were covered with layers of metallic copper, indicating that dezincification, a form of dealloying, occurred (Figure IX-36). Dezincification occurred beneath occlusive deposit layers due to the concentration of chloride from the water solution by an ion concentration cell mechanism. The corrosion caused zinc to be preferentially removed from the copper-zinc matrix of the alloy. This left behind a weak, porous mass of pure copper on the corroded surface.

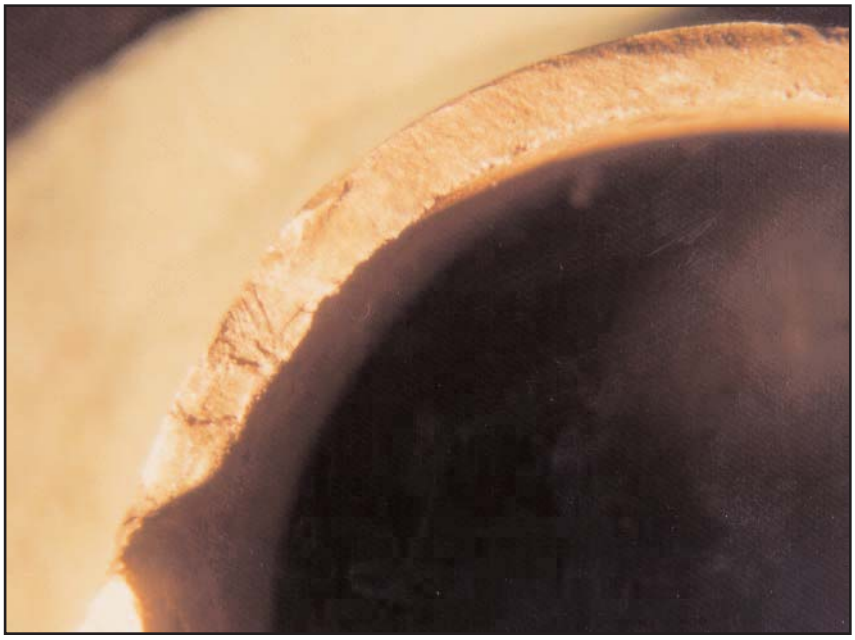

Figure IX-34: Cracking Failure

Figure IX-35: Internal Surface Depressions

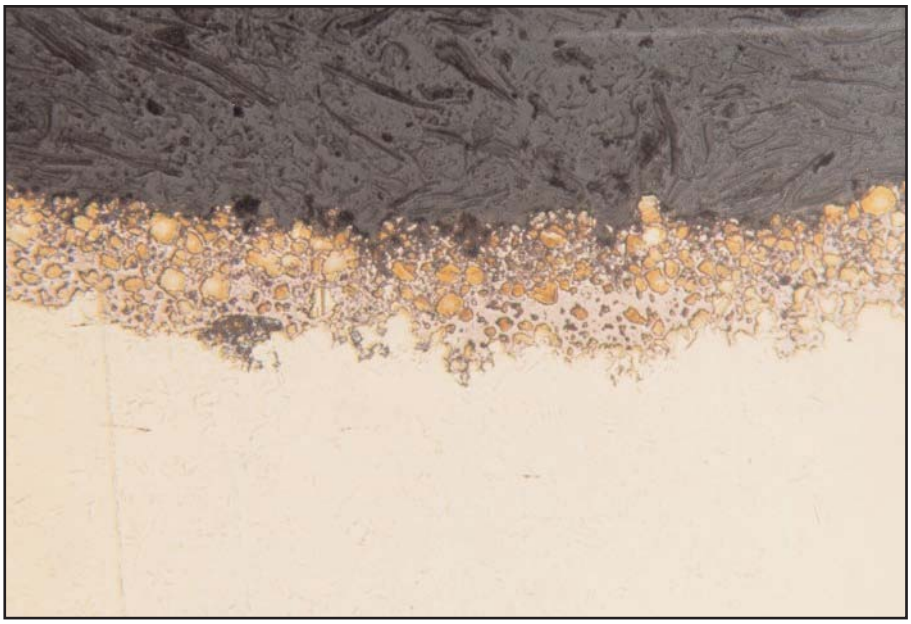

Figure IX-36: Metallic Copper Covering Surface, Indicating Dezincification

Failure occurred primarily due to corrosion fatigue cracking. The crack initiated at the base of one of these depressions, which served as a point of stress concentration (Figure IX-37). This cracking resulted from the application of cyclic tensile stresses. These stresses were supplied by cyclic bending, expansion and contraction, and vibration in service.

Figure IX-37: Corrosion Fatigue Fissures Penetrating from Base of Depression

Corrosion Control

Dezincification may be controlled by maintaining clean metal surfaces, and by avoiding low or stagnant flow. Exposure to acidic or alkaline waters, or high chloride waters, promotes dezincification. Therefore, the use of an alternate, more resistant alloy such as cupro-nickel may be considered.

Corrosion fatigue cracking may be controlled most effectively by minimizing the magnitude and frequency of the applied stresses.

Case History #10 — Failure of a Heat Exchanger Tube due to Microbiologically Influenced Corrosion
System — Lean amine cooler
Specimen — Heat exchanger tube
Orientation — Horizontal
Material — Carbon steel
Time in service — 2 1/2 years
System age — 7 years
Environment
Internal — Lean amine
Temperature — 140°F (60°C)
Pressure — 2,800 kPa
External — Cooling water
Temperature — 112°F (45°C)
Pressure — 650 kPa
Chemical treatment — Zinc phosphate, polymer, nonoxidizing biocide

Clusters of mutually intersecting, deep depressions formed in scattered spots on the external surfaces of several tubes in the exchanger (Figure IX-38). The depressions were hemispherical in shape. In some locations, the depressions mutually intersected (Figure IX-39). The depressions were lined with iron sulfide corrosion products (Figure IX-40). It was reported that a gooey slime layer covered the external surface when the bundle was removed. Bacterial counts on tube surfaces were 5 million CFU/ml total, with 8,000 CFU/ml of sulfate reducing bacteria.

Figure IX-38: Scattered, Deep External Surface Depressions

Figure IX-39: Clusters of Mutually-intersecting, Rounded Depressions

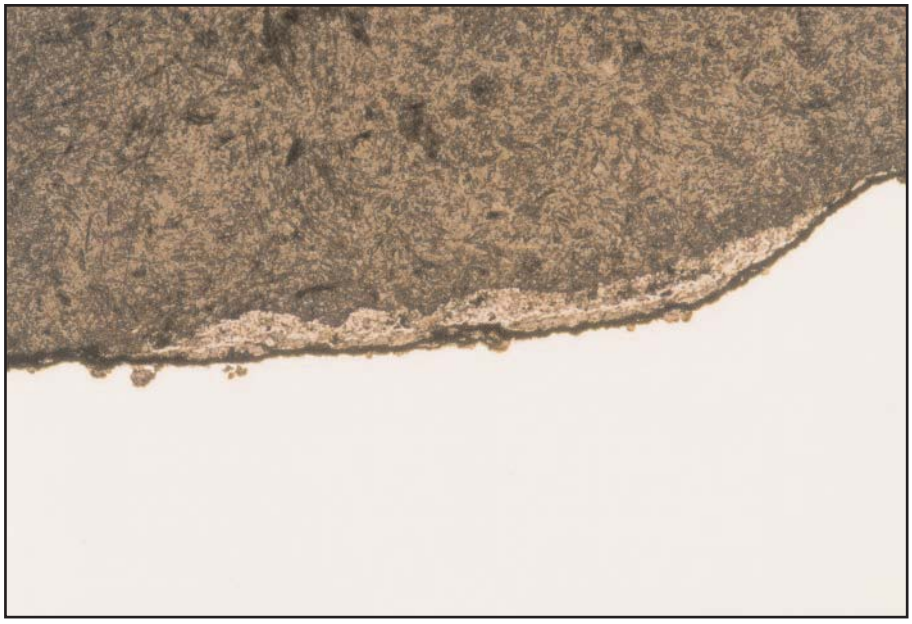

Figure IX-40: Metallographic Cross-section of Depression Covered with Corrosion Products Containing Sulfide

In any failure analysis investigation, all four factors listed below are required to positively confirm a case of microbiologically influenced corrosion. In this case, all four factors were identified to confirm that corrosion was caused by sulfate reducing bacteria.

1) The presence of microorganisms — Confirmed by high bacteria counts.
2) Unique corrosion morphology — Hemispherical depressions, some in clusters.
3) Specific corrosion products and deposits — Sulfide layers lining the depressions.
4) Compatible environmental conditions — Sulfate reducing bacteria are anaerobic.

Sulfate reducing bacteria reduce sulfate ions to sulfide in their biological process. One of the more popular proposed mechanisms to explain how these bacteria promote corrosion is through removal of hydrogen, which depolarizes the cathode in the corrosion cell. Sulfate reducing bacteria are anaerobic, so they live and grow beneath occlusive layers of deposits and slime. Slime also promotes the growth of anaerobic bacteria by depleting oxygen.

Corrosion Control

Microbiologically influenced corrosion may be controlled through use of adequate concentrations of proper biocides that are fed in a proper manner. Low (< 3 ft/s) or stagnant (<1 ft/s) flow should be minimized or prevented. Clean metal surfaces should also be maintained. In this case history, flow rates were low, since cooling water flowed across the shell sides of the tubes. In addition, slug feed of biocide was inadequate for the system.

Case History # 11 — Failure of a Heat Exchanger Tube due to Concentration Cell Corrosion

System — Splitter bottoms cooler
Specimen — Heat exchanger tube
Orientation — Horizontal
Material — Carbon steel
Time in service — 2 years
System age — 25 years
Environment

Internal — Cooling water
Temperature — 75°F (24°C) in, 95°F (35°C) out
Chemical treatment — Organic phosphate, bleach

External — Heavy lean oil
Temperature — 317°F (158°C) in, 90°F (32°C) out
Pressure — 12 psi

The internal surface of a steel heat exchanger tube section was covered with thin layers of light-colored deposits that consisted primarily of calcium phosphate (Figure IX-41). These deposits overlaid layers and tubercles of brown iron oxide. Some of the tubercles were hollow and lined with material that was acidic and contained significant amounts of chloride and sulfur compounds. The hollow tubercles were broken away to reveal rough-surfaced, undercut depressions that were bare, or lined with very thin deposit and corrosion product layers. These surfaces could be cleaned to bare metal quickly with a concentrated hydrochloric acid solution (Figure IX-42). Metallographic cross-sections also revealed undercut depressions that were capped with hollow tubercles (Figure IX-43).

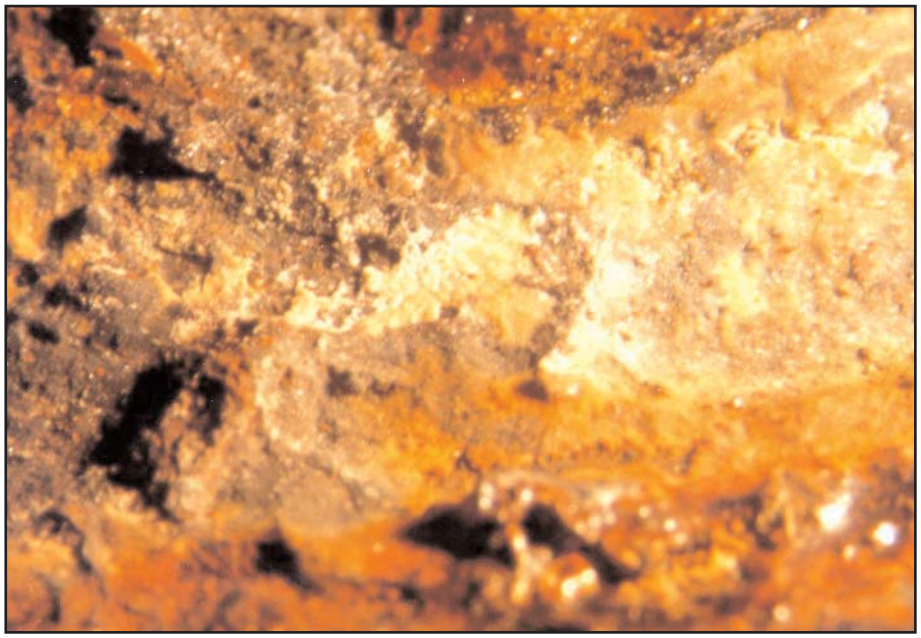

Figure IX-41: Iron Oxide Layers and Tubercles Overlaid with Water-formed Deposit Layers

Figure IX-42: Deposit and Corrosion Product Layers Removed to Reveal Rough-surfaced, Undercut Depressions

Figure IX-43: Metallographic Cross-section of Rough-surfaced, Undercut Depressions beneath Hollow Iron Oxide Tubercle

Initial corrosion was caused by the formation of differential oxygen concentration cells beneath occlusive deposit layers. A diagram of a differential oxygen concentration cell between contacting metal surfaces is shown in Figure IX-44. The water beneath an occlusive deposit or corrosion product layer or within a tight crevice between contacting metal surfaces becomes depleted in oxygen concentration. Consequently, the cathodic reaction in the corrosion cell could only occur where oxygen concentrations were higher, such as at breaks in the deposit layer, and on the outer surfaces of iron oxide layers and tubercles. The anodic reaction in the corrosion cell occurs within the oxygen depleted zone to produce metal dissolution. Metal ion leaks out of the oxygen depleted zone into the zone where oxygen concentration is high to produce iron oxide corrosion products. By this process, iron oxide tubercles form.

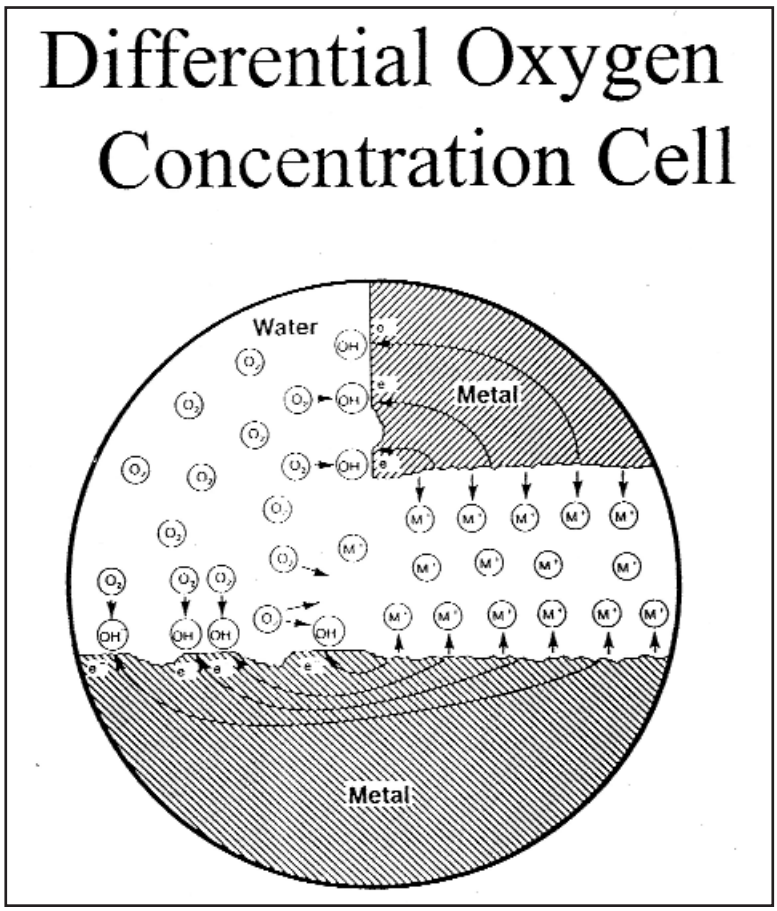

Figure IX-44:
(Source: *The Nalco Guide to Cooling Water Systems Failure Analysis*)

Reactions

Oxygen concentration cell

Anodic reaction $Fe \rightarrow Fe^{2+} + 2e^-$

Cathodic reaction $O_2 + 2H_2O + 4e^- \rightarrow 4OH^-$

Corrosion products formed $2\,Fe^{2+} + 4e^- + O_2 + 2H_2O \rightarrow 2Fe(OH)_2$

Ion concentration cells also may form beneath occlusive deposit and corrosion product layers, tubercles and between crevices (Figure IX-45). The positively charged metal ions within the occluded zones attract aggressive anions such as chloride, sulfate, and sulfide. Aggressive anion concentration may become several times that in the bulk water to produce locally acidic and highly corrosive environments. The acidic environments dissolve protective corrosion product layers and then the metal itself to produce rough-surfaced, undercut pits and depressions. Acid corrosion significantly accelerates metal loss. The reactions and corrosion products that may occur within an iron oxide tubercle are shown in Figure IX-46.

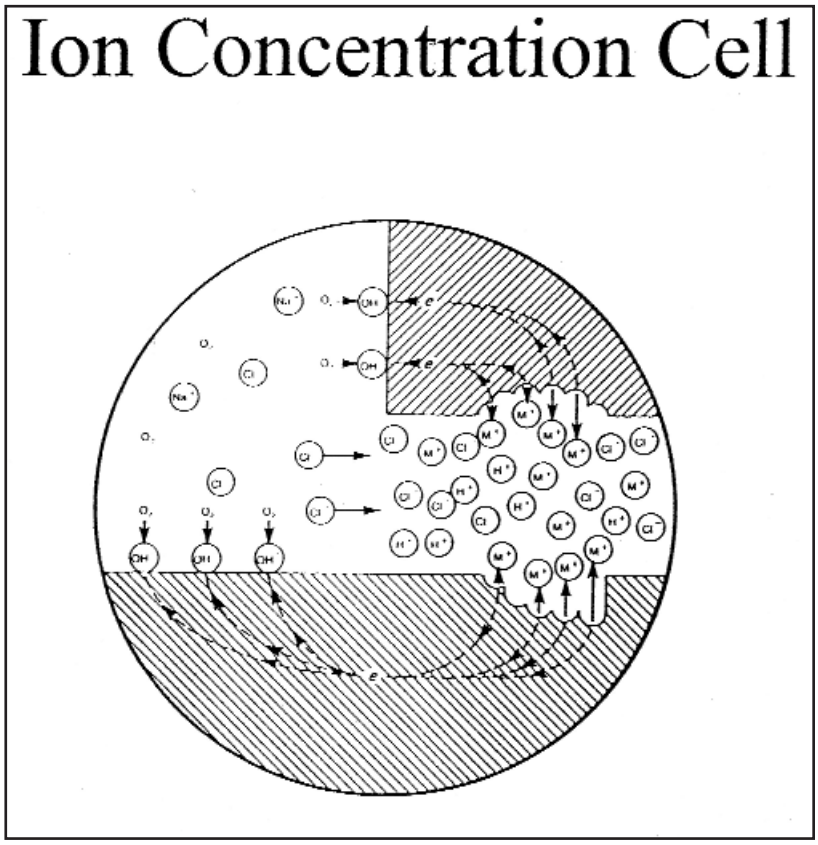

Figure IX-45:
(Source: *The Nalco Guide to Cooling Water Systems Failure Analysis*)

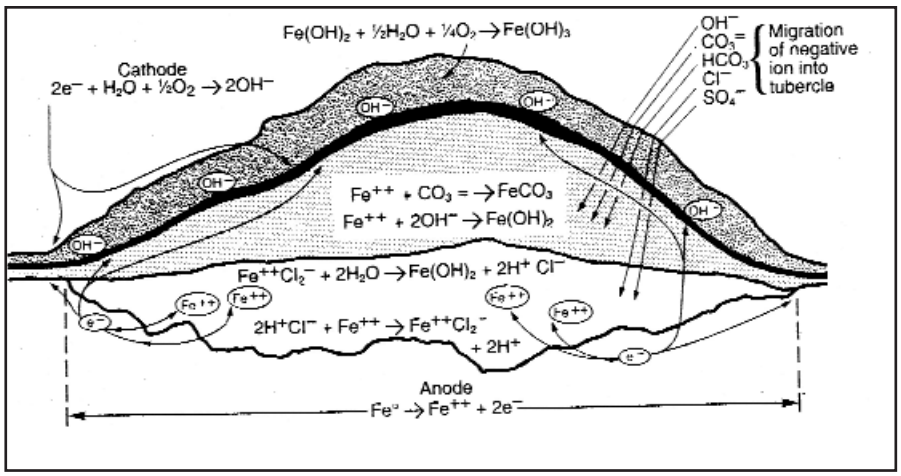

Figure IX-46: Tubercle
(Source: *The Nalco Guide to Cooling Water Systems Failure Analysis*)

Corrosion Control Measures

Concentration cell corrosion may be controlled by maintaining clean metal surfaces, both mechanically and through proper water treatment and corrosion inhibition. Corrosion may also be controlled by minimizing or eliminating low or stagnant flow, and by decreasing concentration of aggressive anions. If these measures cannot be taken, and/or if corrosion cannot be controlled, then the use of alternate materials of coatings may be considered.

ABOUT THE AUTHORS

William (Bill) Tillis
Consultant

William (Bill) Tillis has 46 years experience in the field of corrosion. Presently retired from Exxon, he is consulting with Nalco on oilfield and refinery failure analysis. He has worked for Curtis-Wright, Pennwalt, FMC Corp., General Electric, NL Industries, NL Treating Chemicals, and Exxon Chemicals. Bill has worked the past 23 years in oilfield corrosion inhibitor testing and failure analysis.

Bill received a BS degree in chemistry from Long Island University, and a MS in chemistry from Drexel University. He is a NACE certified corrosion specialist and an active member of both NACE and the American Society of Metals (ASM). Bill holds several U.S. patents and has authored numerous SPE and NACE papers.

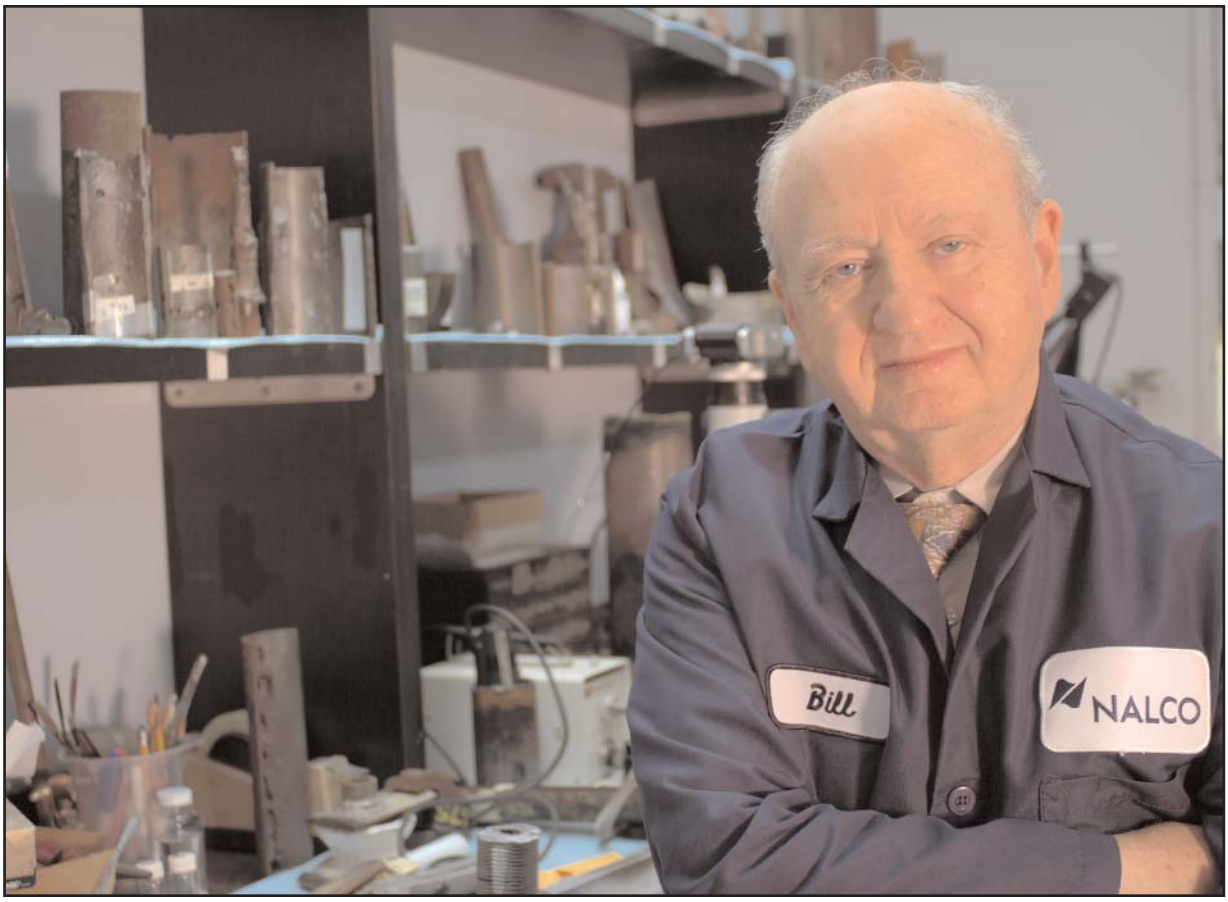

Bill Tillis

James (Jim) Dillon
Research Scientist

Jim has been a part of the Nalco metallurgy group for 20 years, serving as senior research metallurgist, staff scientist and his current position. He has conducted more than 3,000 failure analysis investigations on components from a variety of industrial systems, both in the laboratory and during on-site inspections. Jim has been involved in the consultation and education of customers as well as sales, marketing and research personnel concerning the identification and mitigation of corrosion and other failure mechanisms.

Jim received a BS degree in metallurgical engineering from the Illinois Institute of Technology. His professional associations include the American Society for Metals (ASM), National Association of Corrosion Engineers (NACE), Association of Iron and Steel Engineers (AISE), and American Iron and Steel Institute (AISI). Jim has authored numerous articles for NACE.

Paul Desch
Senior Research Metallurgist

Paul has been with Nalco for 6 years serving as a senior metallurgist and senior research metallurgist. Paul has extensive experience in boiler systems and cooling water systems, especially regarding material selection and failure modes associated with different materials. He currently serves as the lead contact for the company's compatibility testing program, which encompasses many aspects of product compatibility with metals, nonmetals and coatings.

Paul received a BS degree in 1988 and a PhD in 1996 from the Illinois Institute of Technology in Chicago. His professional associations include the American Society for Metals (ASM), National Association of Corrosion Engineers (NACE), and the Society of Plastics Engineers (SPE).

Paul Desch (Left) and Jim Dillon (Right)

NALCO

People you trust, delivering results.

Energy Services Division Worldwide Headquarters
P.O. Box 87, Sugar Land, Texas 77487-0087 U.S.A. +1 281 263 7000

SUBSIDIARIES AND AFFILIATES IN PRINCIPAL LOCATIONS AROUND THE WORLD

www.nalco.com

 Printed in USA 11/04 NE-66 DS/OFC